PROCEEDINGS

TECH LIBRARY KAFB, NM

0152345

GEORGE C. MARSHALL SPACE FLIGHT CENTER

SPACE TRANSPORTATION SYSTEM PROPULSION TECHNOLOGY CONFERENCE

APRIL 6 & 7, 1971

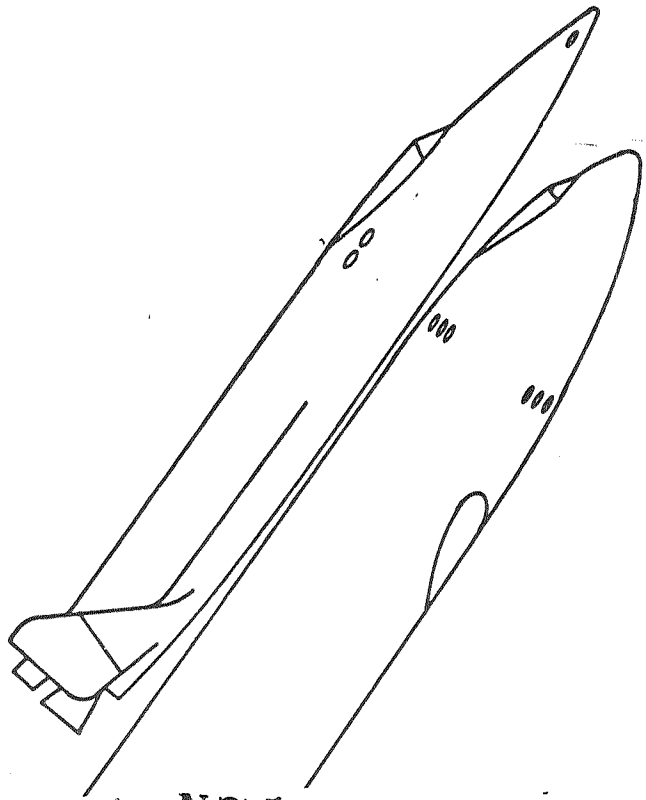

VOLUME IV

CRYOGENS

N71-29609 (ACCESSION NUMBER)
220 (PAGES)
TMX 67248 (NASA CR OR TMX OR AD NUMBER)
N71-29618 (THRU)
G3 (CODE)
28 (CATEGORY)
FACILITY FORM 602

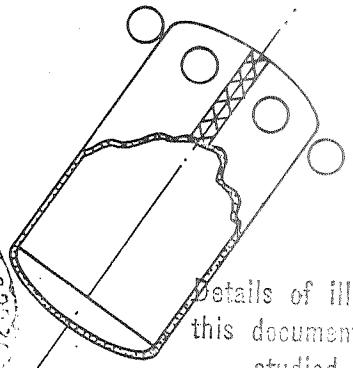

JUN 1971
RECEIVED
NASA STI FACILITY
INPUT BRANCH

Details of illustrations in this document may be better studied on microfiche

NATIONAL AERONAUTICS AND SPACE ADMINISTRATION

Reproduced by
NATIONAL TECHNICAL
INFORMATION SERVICE
Springfield, Va. 22151

PROCEEDINGS
SPACE TRANSPORTATION SYSTEM
PROPULSION TECHNOLOGY CONFERENCE

APRIL 6-7, 1971

MARSHALL SPACE FLIGHT CENTER

VOLUME IV

SESSION V CRYOGENS C. WOOD, CHAIRMAN

April 28, 1971

THIS PAGE INTENTIONALLY LEFT BLANK

PRECEDING PAGE BLANK NOT FILMED

PROPULSION TECHNOLOGY CONFERENCE PAPERS

VOLUME I MAIN PROPULSION

1.	"Final Results of the XLR-129 Program"	P&W
2.	"Two-Phase Flow LH_2 Pump Inducers"	Rocketdyne
3.	"Saturated LH_2 Turbopump Operation"	MSFC
4.	"Characteristics of Feed System Instabilities"	Martin Marietta
5.	"Combustion Oscillations Damping Devices"	P&W
6.	"Minimum Pressure Loss in High Velocity Flow Duct Systems"	S. R. I.
7.	"Engine Onboard Checkout System Study"	Martin Marietta
8.	"Low Frequency Analysis of Rocket Engines Using Compressible Propellants"	Aerojet
9.	"Titanium Pump Impeller Fabrication and Testing"	Rocketdyne
10.	"Advanced Thrust Chamber (Non-tubular)"	Rocketdyne
11.	"High Pressure Hydrogen Effects on Materials"	MSFC

VOLUME II AUXILIARY PROPULSION

1.	"Hydrogen/Oxygen ACPS Engines"	Rocketdyne
2.	"Hydrogen/Oxygen ACPS Engines"	Aerojet
3.	"High Pressure Reverse Flow ACPS Engine"	Bell
4.	"Space Shuttle ACPS Shutoff Valve"	Marquardt
5.	"Space Shuttle ACPS Shutoff Valve"	Rocketdyne
6.	"Ignition Devices for ACPS"	Aerojet
7.	"Spark and Auto Ignition Devices for ACPS"	Rocketdyne
8.	"Catalytic Ignition/Thruster Investigation"	TRW
9.	"Auxiliary Propulsion Subsystem Investigations"	MSFC
10.	"Injector Performance, Heat Flux and Film Cooling in O_2/H_2 Engines"	MSC
11.	"Auxiliary Propulsion Subsystem Definition Study"	TRW
12.	"Auxiliary Propulsion Subsystem Definition Study"	MDAC
13.	"Acoustic Cavity Use for Control of Combustion Instability"	Rocketdyne
14.	"Noncircular Injector Orifices and Advanced Fabrication Techniques"	Rocketdyne

PROPULSION TECHNOLOGY CONFERENCE PAPERS

VOLUME III AUXILIARY POWER UNIT AND AIRBREATHING PROPULSION

1.	"Auxiliary Power Unit Design Studies"	Airesearch
2.	"Auxiliary Power Unit Design Studies"	Rocketdyne
3.	"H_2 Fuel System Investigation"	G. E.
4.	"Booster and Orbiter Engine Studies"	P&W

VOLUME IV CRYOGENS

1.	"Orbital Cryogenic Acquisition and Transfer"	General Dynamics
2.	"Zero Gravity Incipient Boiling Heat Transfer"	Univ. of Michigan
3.	"Zero Gravity Propellant Transfer"	LeRC
4.	"Recent Developments in High Performance Insulation Purge Systems for Shuttle Application"	MDAC
5.	"Effect of Environment on Insulation Materials"	Lockheed
6.	"PPO Foam Internal Insulation"	General Dynamics
7.	"Internal Insulation Systems for LH_2 Tanks" and	MDAC
	"Gas Layer and Reinforced Foam"	Martin Marietta
8.	"Shuttle Cryogen Technology Program"	MSFC

TABLE OF CONTENTS

VOLUME IV

CRYOGENS

			PAGE NO.
1.	Introduction C. C. Wood	MSFC	1265-1273
2.	"Orbital Cryogenic Acquisition and Transfer" M. H. Blatt	General Dynamics	1275-1310
3.	"Zero Gravity Incipient Boiling Heat Transfer" H. Merte, Jr.	Univ. of Michigan	1311-1348
4.	"Zero Gravity Propellant Transfer" E. P. Symons	LeRC	1349-1377
5.	"Recent Developments in High Performance Insulation Purge Systems for Shuttle Application" G. Fredrickson	MDAC	1379-1410
6.	"Effect of Environment on Insulation Materials" R. T. Parmley	Lockheed	1411-1437
7.	"PPO Foam Internal Insulation" G. B. Yates and R. E. Tatro	General Dynamics	1439-1452
8.	"Internal Insulation Systems for LH_2 Tanks" and "Gas Layer and Reinforced Foam" J. M. Stuckey	MDAC Martin Marietta	1453-1480
9.	"Shuttle Cryogen Technology Program" C. C. Wood	MSFC	1481-1500

THIS PAGE INTENTIONALLY LEFT BLANK

MARSHALL SPACE FLIGHT CENTER

SCIENCE & ENGINEERING

LAB: S&E-ASTN-P

NAME: C. C. Wood

DATE: 4-7-71

N71-29610

SHUTTLE CRYOGEN TECHNOLOGY

MSFC - Form 3369 (Rev June 1970)

CHART No. 1

PRECEDING PAGE BLANK NOT FILMED

THIS PAGE INTENTIONALLY LEFT BLANK

SHUTTLE CRYOGEN TECHNOLOGY

Charles C. Wood

NASA/Marshall Space Flight Center
Huntsville, Alabama

THE TECHNICAL PAPERS PRESENTED IN THIS SESSION SUMMARIZE THE EFFORTS OF UNIVERSITIES, INDUSTRY, AND THE GOVERNMENT IN DEVELOPMENT OF CRYOGENIC TECHNOLOGY TO SUPPORT THE SHUTTLE PROGRAM. ALTHOUGH THE TOTAL SPECTRUM OF CRYOGENIC TECHNOLOGY ACTIVITY WILL NOT BE ADDRESSED IN DETAIL, THE LAST PAPER WILL SUMMARIZE MUCH OF THE EFFORT NOT COVERED IN THE PAPERS PRECEDING IT.

PRECEDING PAGE BLANK NOT FILMED

CRYOGEN TECHNOLOGY BASE FOR SPACE SHUTTLE

THE CRYOGEN TECHNOLOGY IS MULTIPLE DISCIPLINE TECHNOLOGY WITH APPLICATION TO MAIN PROPULSION, AUXILIARY PROPULSION, LIFE SUPPORT, AND AUXILIARY POWER SYSTEMS OF THE SPACE SHUTTLE VEHICLE. THE EXTENSIVE TECHNOLOGY BASE AVAILABLE TO SUPPORT CRYOGEN UTILIZATION HAS BEEN DEVELOPED FROM GROUND BASE TECHNOLOGY PROGRAMS AND THE HIGHLY SUCCESSFUL MANNED SPACE FLIGHT PROGRAMS. IN THE INITIAL SHUTTLE TECHNOLOGY CONFERENCE AT THE LEWIS RESEARCH CENTER IN JULY 1970, AN ATTEMPT WAS MADE TO ASSESS THE TECHNOLOGY STATUS AND ESTABLISH SUCH A BASE. THE AREAS OF CHART 2 WERE ADDRESSED IN DETAIL BY THE SPEAKERS WITH EACH SPEAKER ATTEMPTING TO DISCUSS THE SUBJECT MATERIAL FROM THE STANDPOINT OF THE NATION'S CAPABILITY IN A PARTICULAR AREA CONTRASTED TO THAT WHICH MIGHT EXIST WITHIN HIS OWN ORGANIZATION. THESE ASSESSMENTS ARE REPORTED IN THE PROCEEDINGS OF THE LEWIS CONFERENCE - NASA TMX-52876 - VOL. V.

MARSHALL SPACE FLIGHT CENTER

SCIENCE & ENGINEERING

CRYOGEN TECHNOLOGY BASE FOR SPACE SHUTTLE

LAB: S&E-ASTN-P

NAME: C. C. Wood

DATE: 4-7-71

DISCIPLINE	APPLICATION			
	ASCENT		ORBIT	
	O_2	H_2	O_2	H_2
Stratification	x	x	x	x
Mixing	-	-	x	x
Thermal Conditioning				
- Geyser Suppression	x	-	-	-
- Quality Control	x	x	x	x
In-Space Venting	-	-	x	x
Pressurization	x	x	x	x
Mass Gauging				
Tank Insulation Acquisition and Transfer Systems Integration Hardware	DISCUSSED INDIVIDUALLY			

MSFC - Form 3369 (Rev June 1970)

CHART No. 2

CRYOGEN TECHNOLOGY DISCIPLINES

THIS CHART ATTEMPTS TO SHOW QUALITATIVELY THE TECHNOLOGY STATUS AS RELATED TO THE SPACE SHUTTLE PROGRAM. THE ANALYTICAL ASPECTS (SYSTEM PERFORMANCE) OF THE REQUIRED TECHNOLOGY HAVE BEEN SEPARATED FROM THE HARDWARE DESIGN AND MANUFACTURING ASPECTS. WHILE SUCH AN ASSESSMENT MAY BE ARGUMENTATIVE, IT IS READILY APPARENT THAT A SIGNIFICANT TECHNOLOGY BASE DOES EXIST, THAT ADDITIONAL EFFORTS ARE REQUIRED AND THE AREAS REQUIRING THE MAJOR EMPHASIS ARE IDENTIFIED.

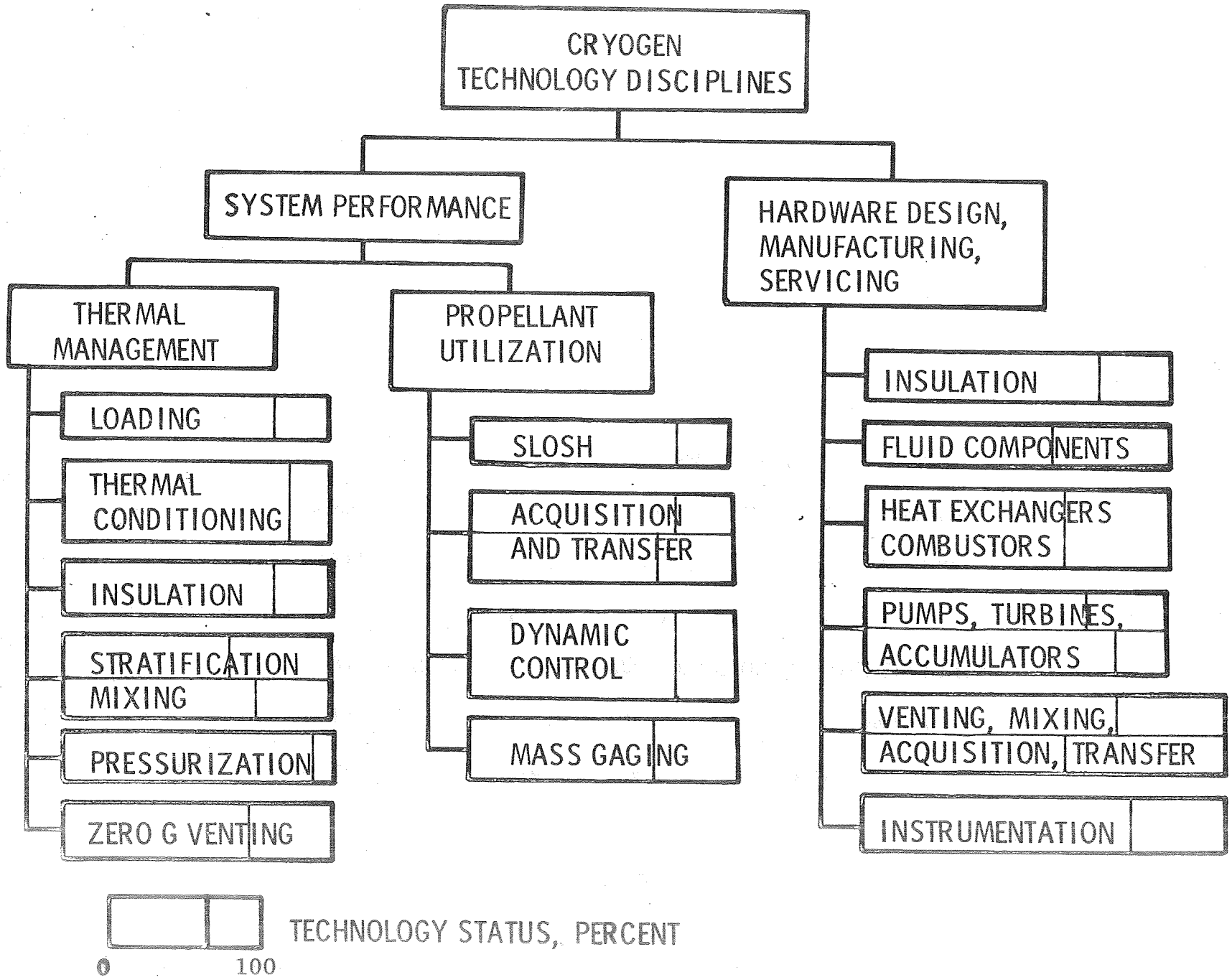
CRYOGEN TECHNOLOGY DISCIPLINES
SYSTEM PERFORMANCE
HARDWARE DESIGN, MANUFACTURING, SERVICING
THERMAL MANAGEMENT
PROPELLANT UTILIZATION
LOADING
THERMAL CONDITIONING
INSULATION
STRATIFICATION MIXING
PRESSURIZATION
ZERO G VENTING
SLOSH
ACQUISITION AND TRANSFER
DYNAMIC CONTROL
MASS GAGING
INSULATION
FLUID COMPONENTS
HEAT EXCHANGERS COMBUSTORS
PUMPS, TURBINES, ACCUMULATORS
VENTING, MIXING, ACQUISITION, TRANSFER
INSTRUMENTATION
0
100
TECHNOLOGY STATUS, PERCENT

SHUTTLE CRYOGEN PROGRAM

THE TECHNOLOGY PLAN IS SHOWN ON CHART 4. THE MANY AREAS FROM THE PRECEDING CHART ARE CONSOLIDATED FOR CONVENIENCE INTO THE FIVE CATEGORIES SHOWN. THE SHUTTLE TECHNOLOGY REQUIREMENTS SHOULD BE MET BY EARLY 1973 WHICH IS COMPATIBLE WITH THE SHUTTLE DEVELOPMENT SCHEDULE. THE TECHNOLOGY POSTURE IS MORE FAVORABLE IN SOME AREAS DUE TO FUNDAMENTAL TECHNOLOGY PROGRAMS IN PROGRESS AT SHUTTLE INCEPTION AND/OR EARLIER FUNDING FROM THE SHUTTLE TECHNOLOGY PROGRAM.

MARSHALL SPACE FLIGHT CENTER

SCIENCE & ENGINEERING

SHUTTLE CRYOGEN PROGRAM

LAB: S&E-ASTN-P

NAME: C. C. Wood

DATE: 4-7-71

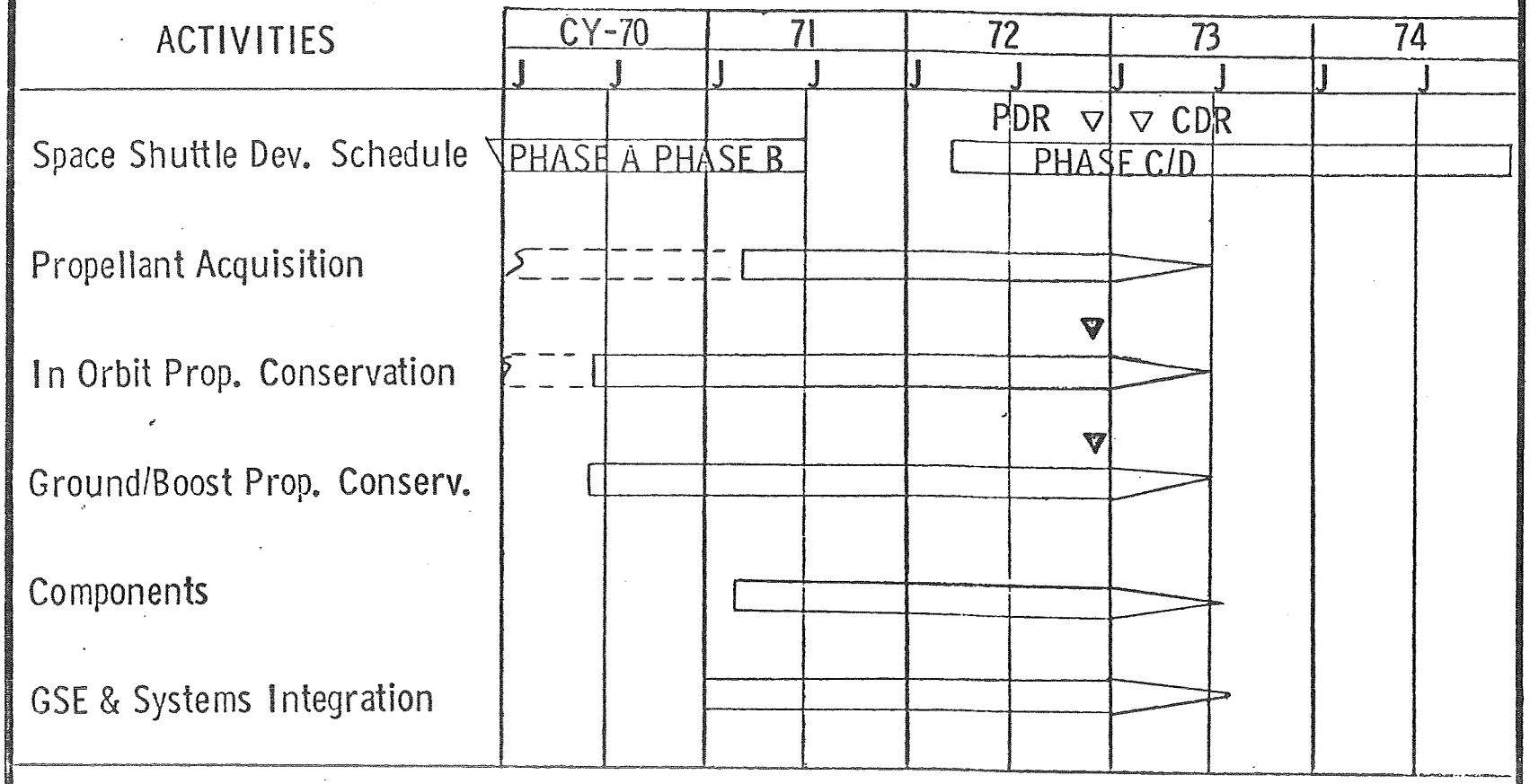

PRE-SHUTTLE EFFORT

SYSTEM DEMONSTRATION

MSFC - Form 3369 (Rev June 1970)

CHART No. _____

THIS PAGE INTENTIONALLY LEFT BLANK

PRECEDING PAGE BLANK NOT FILMED

N71-29611

"ORBITAL CRYOGENIC ACQUISITION AND TRANSFER"

M. H. BLATT

GENERAL DYNAMICS

TECHNICAL MANAGER

L. J. HASTINGS

MARSHALL SPACE FLIGHT CENTER

THIS PAGE INTENTIONALLY LEFT BLANK

PRECEDING PAGE BLANK NOT FILMED

ORBITAL CRYOGENIC ACQUISITION & TRANSFER

GENERAL DYNAMICS
Convair Aerospace Division

MORTON H. BLATT

NAS 8-21465

THIS PAGE INTENTIONALLY LEFT BLANK

PRECEDING PAGE BLANK NOT FILMED

ORBITAL CRYOGENIC ACQUISITION AND TRANSFER

This paper presents the results of Contract NAS8-21465, "Low Gravity Propellant Control Using Capillary Devices in Large Scale Cryogenic Vehicles," as related to cryogenic acquisition and transfer devices for space shuttle. Initially fluid dynamic considerations are discussed including settling, residuals, refilling, retention,wicking, spilling and venting. Thermal conditioning problems centered on thermodynamic vent system cooling of capillary devices and feedlines with consideration of destratification, wicking, liquid collection and tank pressure control. Shuttle mission requirements are then given with a discussion of technology studies required to supplement fluid, thermal and structural design information currently available in a design handbook prepared under the contract.

LOW GRAVITY PROPELLANT CONTROL USING CAPILLARY DEVICES IN LARGE SCALE CRYOGENIC VEHICLES

FLUID ANALYSIS

THERMAL ANALYSIS

STRUCTURAL ANALYSIS

BENCH TESTING

DESIGN HANDBOOK

INTRODUCTION

In orbiting spacecraft containing subcritical storage vessels, periods of orbital drag and disturbing accelerations may position liquid away from the tank outlet. Prior to engine restart or propellant transfer it is necessary to have liquid positioned over the outlet in order to effectively accomplish fluid transfer.

Acquisition devices for controlling propellants prior to transfer come under two categories; partial orientation devices that control only a small percentage of the tank contents and total orientation devices that attempt to control all the propellant in the tank. For the Contract NAS8-21465 study, partial acquisition devices were required for the S-IVC restart mission and total acquisition was required for the LO_2 tanker mission.

Spacecraft low gravity restarts have primarily been accomplished in the past through the use of linear acceleration to provide settling thrust with which to collect fluid over the outlet. This well proven technique introduces weight penalties and operational constraints compared to more advanced methods of acquisition. These methods include positive displacement devices such as bladders, bellows and diaphragms, dielectrophoretic devices and capillary devices.

Capillary devices are particularly attractive because they are lightweight, passive and introduce minimal operational constraints. These devices, while successfully applied to non-cryogenic propellant acquisition, have not been adequately studied for cryogenic fluid applications. Using cryogenic fluids introduces thermodynamic and heat transfer problems which greatly affect capillary control system design.

The purpose of Contract NAS8-21465 was to ascertain the feasibility of using capillary devices such as screens and/or perforated plates, for propellant control in large scale cryogenic vehicles.

The first phase of the two-phase program defined the thermodynamic and heat transfer problems associated with the use of capillary devices, derived methods for solving these problems and selected promising propellant control schemes. This was predominantly an analytical study with some low cost bench testing required to verify basic concepts. Based on the general results of the initial analytical and experimental effort, designs were developed for an S-IVC LH_2 and LO_2 tank restart mission and an S-IIB LOX tanker propellant transfer mission. Promising capillary control designs were compared with other means of propellant control in order to ascertain the feasibility of using capillary devices for propellant control in large-scale cryogenic vehicles.

During the second phase of the study, Phase I results were used as a base for an experimental/analytical program which examined the various problems in detail and developed design solutions. Techniques developed in Phase I were refined and expanded. A series of bench tests were run with noncryogenic fluids to provide information with which to correlate analytical models and develop empirical relationships where analytical models were not applicable. Second phase results were compiled in the form of a design handbook containing useful fluid, thermal and structural information, and a report covering analytical, experimental and design studies performed for the two missions.

S-IVC RESTART MISSION

The S-IVC mission is a single restart of a 60% full S-IVC in order to propel a spacecraft and two S-IVCs into a transplanetary trajectory. The vehicle is basically an S-IVB with J-2S engines and high performance insulation. Total orbital heating is 2140 Btu/Hr (630 watts) with 1300 Btu/Hr (382 watts) in the common bulkhead area.

Due to orbital drag, liquid will be positioned in the forward end of the tank. The objective of a restart capillary device is to position liquid at the outlet in order to provide continuous liquid flow until the thrust produced by this flow causes the main body of liquid to collect over the outlet.

S-IVC RESTART MISSION

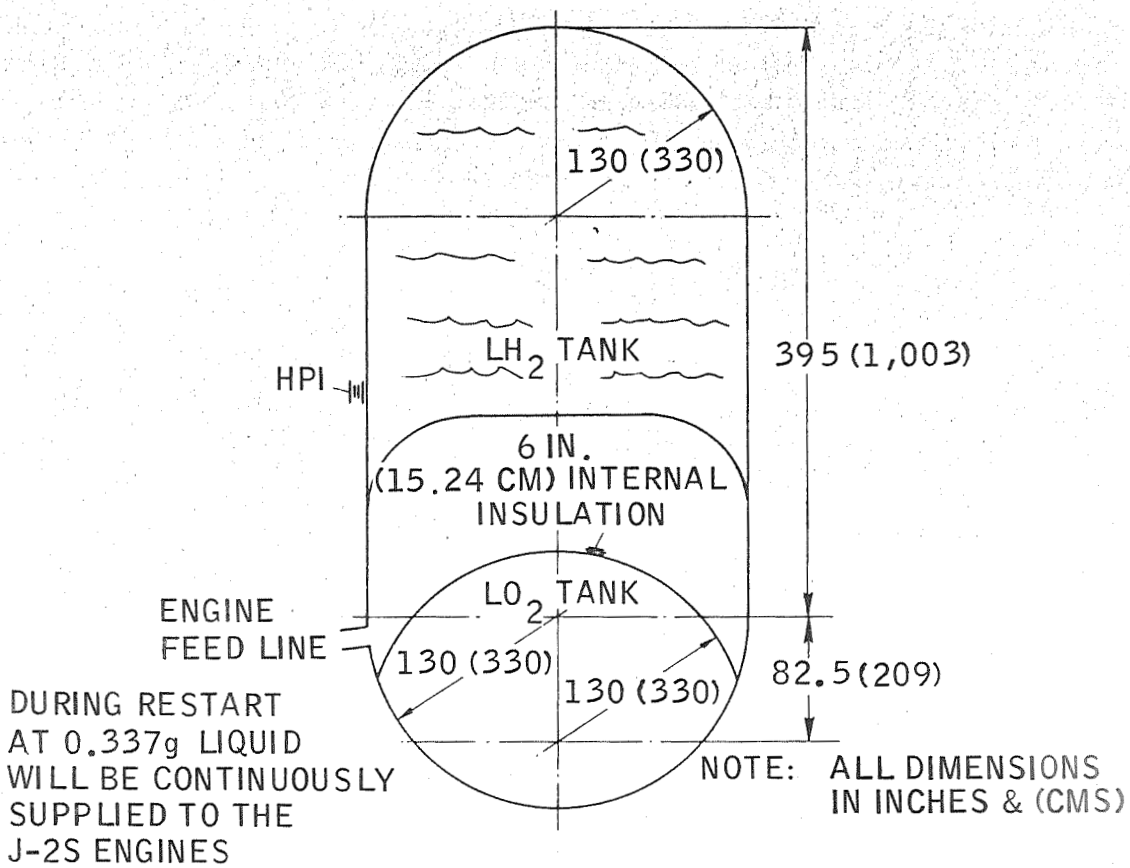

LO_2 TANKER MISSION

The tanker mission has the objective of filling an S-II B LO_2 tank in orbit from 3 LO_2 tankers. For orbital propellant transfer where the liquid flowing does not provide thrust to settle the propellants, a much larger surface area is required for the capillary device. The propellant transfer device must maintain continuous contact with the liquid in order to prevent vapor from entering the capillary device and interrupting the liquid path to the feedline.

The LO_2 tanker is a 218"(554 cm) diameter sphere with high performance insulation limiting boiloff to 8,050 lbs (3630 kg) during the 163-day mission. The major portion of the transfer occurs at 3×10^{-5} g's with a scavenging accerleration during the final seconds of transfer of 6.5×10^{-4} g's to minimize residuals.

LO_2 TANKER MISSION

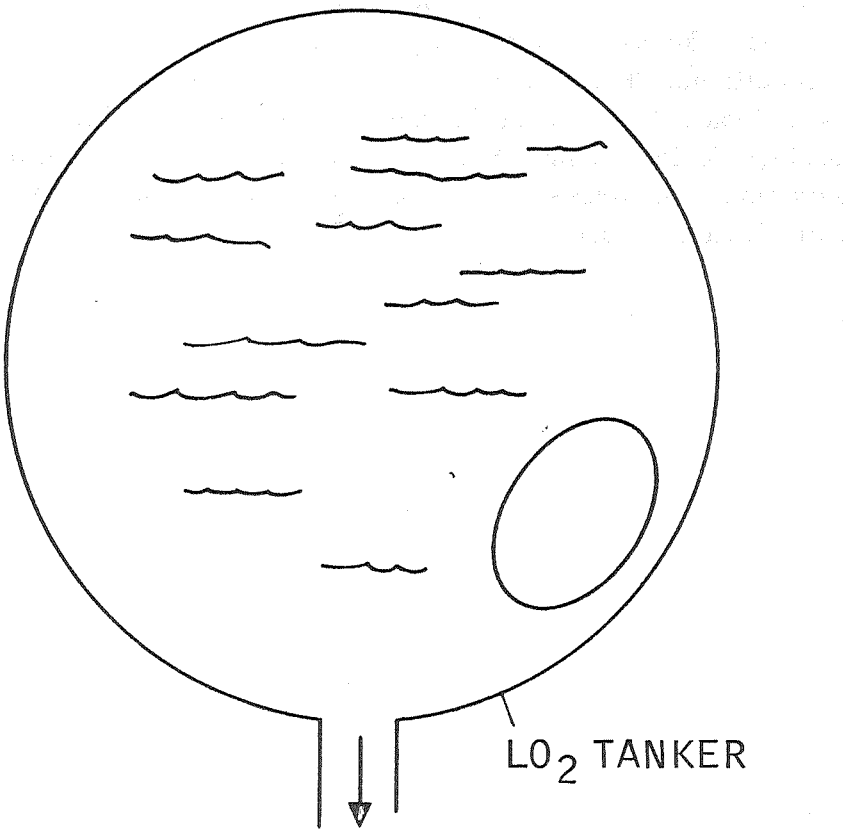

CONTINUOUS LOW-GRAVITY TRANSFER
REQUIRED TO S-IIB LO_2 TANK

CAPILLARY RETENTION HEAD

An important fluid parameter is the surface tension retention head capable of being held by a capillary barrier in low gravity. The curves indicate that considerable hear can be contained under static conditions for the missions considered. Static conditions, however, are not the critical design conditions. For example, for the S-IVC the restart period, where the acceleration is .337 g's and vapor is entering the capillary device to replace liquid flowing to the engine determines capillary device sizing. For the tanker mission the critical period is when the tank is relatively empty and pressure drop of fluid flowing through the capillary device approach the surface tension retention pressure.

LIQUID HYDROGEN HEAD OR TRAPPED VAPOR HEAD CONTAINED BY CAPILLARY VS. ACCELERATION

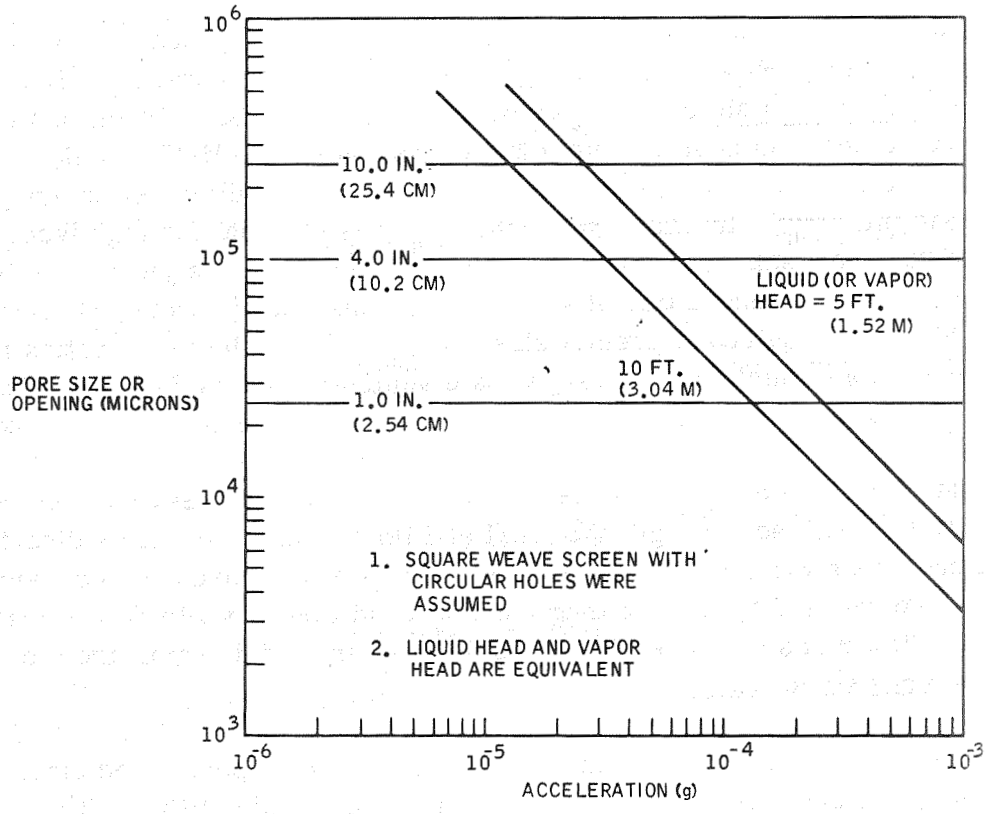

FLUID DYNAMIC CONSIDERATIONS

Transfer time for a restart case is determined by the time required for propellants to be r oriented and to cover the engine outlet completely. Start basket volume is directly proportional to this collection time. Settling and collection predictions were attempted using both empirical correlations and the MAC model for the S-IVC restart case.

Initial fluid conditions were representative of a 10^{-6} g drag acceleration on an LH_2 tank 60% full at 25 psia (172 KN/M^2). A 0.337 g acceleration representative of liquid flow to the engi was applied to the vehicle to induce settling. The empirical correlations indicated that settling would occur in approximately 3 seconds, while the MAC model, for this case, indicated that considerable recirculation and geysering would exist delaying collection to well beyond this time. Implications of this analysis are that for high Weber numbers in excess of 200, conventional means of predicting settling times yield optimistic values. For a more accurate representation of settling, a sophisticated numerical technique such as MAC or SURF is required to predict slosh decay and turbulent dissipation for high Weber number conditions which exist in large scale vehicles such as the space shuttle. These predictions are required to determine capillary device volume and refilling provisions.

For restart capillary devices, screen selection depends upon several competing criteria. The ability to resist adverse gravitational and impingement forces is directly increased by decreasing pore size; refilling is hindered by such a decrease. Screen wicking promotes wetting of the capillary device; aiding thermal conditioning while detracting from filling and refilling. Flow rates and liquid levels during restart and draining are a complex function of screen sizes selected.

Impingement velocities for penetrating a welted screen or perforated plate are shown. These velocities are found from MAC model runs of liquid settling. If vapor cannot be prevented from entering the capillary device outer surfaces, deflector screens may be provide to repel vapor bubbles from entering the tank outlet.

Screen wicking may be computed from the semiempirical relationship. Wicking fluid is

$$\Delta P = \frac{\phi \sigma}{D_{BP}} = \frac{A_W \mu V L}{D_a^2 g_c} \qquad (1)$$

used to replace liquid evaporated from the screen surface and thus prevent screen drying.

VELOCITY REQUIREMENTS FOR PENETRATION OF VAPOR OR LIQUID THROUGH A LH_2-WETTED SCREEN OR PLATE

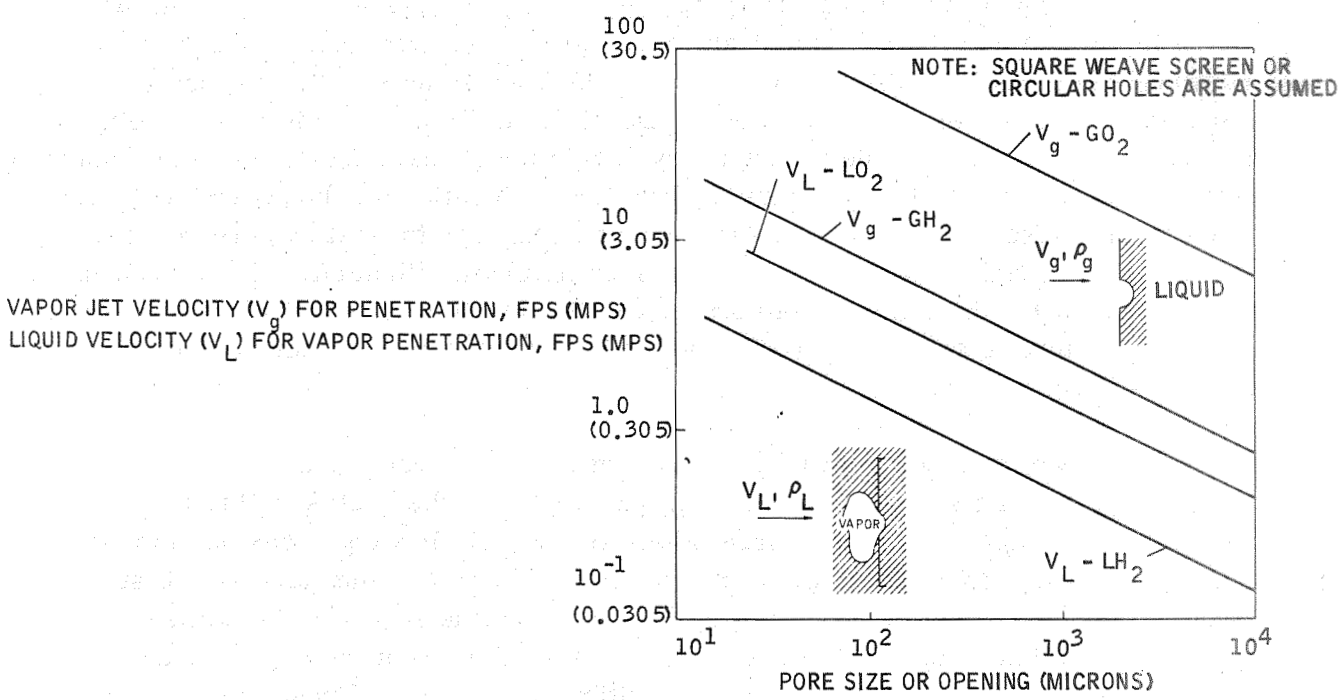

FLUID DYNAMIC CONSIDERATIONS

During restart, high accelerations are imposed upon the capillary device which tend to cause liquid spillage out of the capillary device. Screen drying due to vapor inflow will also promote liquid spillage from the capillary device during restart when the capillary device is surrounded by vapor. A method was devised for preventing spilling, as shown, by making the pressure drop across the top screen greater than the head of liquid in the capillary device. This makes the pressure inside the capillary device lower than outside tending to make vapor ingest through the side of the capillary device. This ingestion can be prevented because surface tension forces will resist vapor penetration through the wetted screen. The opposite is not true; e.g., liquid cannot be prevented from spilling with surface forces because the wetting nature of the propellants used for space vehicles such as space shuttle causes the radius of curvature to approach infinity and the liquid retention pressure due to surface tension to approach zero.

A general program to predict spilling, vapor ingestion, and vapor pullthrough in capillary devices during restart was formulated using the results of the analysis illustrated in the following analysis and pullthrough correlations and screen flow equations obtained from Convair Aerospace IRAD programs. The program, INGASP, computes in time steps, for a given outflow rate, the flow rates through the top and side screen which satisfy conservation of volume and balancing of the pressure drops. Refilling of the capillary device due to collected fluid is also considered in the calculations as well as all possible liquid level combinations in the tank and capillary device. The cases considered include liquid level in the capillary device both above and below the screened area and no liquid initially in the device with liquid subsequently collected outside the capillary device and consequent refilling calculations.

Residuals were determined for the S-IVC case by analyzing the flow in the capillary device region during draining using the DREGS2 computer program. This program using techniques similar to INGASP computes relative liquid levels and pullthrough in the capillary device as a function of liquid flow rates, acceleration, liquid and capillary device properties and tank and capillary device geometry.

FLUID CONFIGURATION FOR SPILLING & VAPOR INGESTION ANALYSES

$\Delta P_L = HG - HT$

IF $\Delta P_L < 0$, LIQUID WILL SPILL FROM CAPILLARY DEVICE

IF $\Delta P_L > 0$, & > HS (SURFACE TENSION PRESSURE HEAD), VAPOR WILL BE INGESTED INTO CAPILLARY DEVICE

IF $\Delta P_L > 0$, & > HS, NO FLOW WILL OCCUR AT THIS POINT

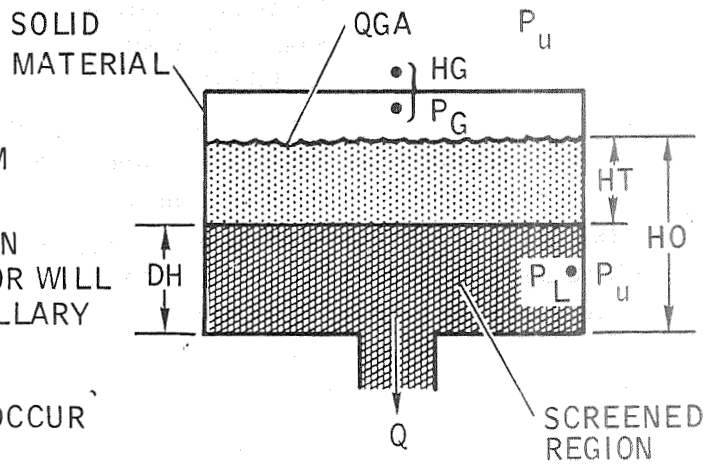

BULK BOILING DURING TANK BLOWDOWN

Information necessary to size a surface-tension device properly for cryogenic propellant control includes propellant transfer time, outflow rates, gravity levels, and tank pressure. For applications where a surface-tension device is to be used, it is advantageous to hold tank pressure constant, thus eliminating vapor generation within the capillary device caused by tank pressure blowdown below the vapor pressure of the liquid. Results of an analysis to determine whether liquid boiling would be appreciable are shown for LH_2 tanks that are initially at 25 psia (172 KN/M^2). Even a 2-psia (13.8 KN/M^2) drop in liquid vapor pressure will generate substantial vapor. A large amount of bulk boiling is likely to cause vapor formation within the start basket. To minimize bulk boiling, a thermodynamic vent system will be operated during orbit to permit essentially constant pressure venting. These results apply directly to space shuttle tankage and thus establish the need for a thermodynamic vent system on the shuttle.

GH_2 VAPOR GENERATED WITHIN CAPILLARY DEVICE
DURING TANK VENTING BLOWDOWN SEQUENCE

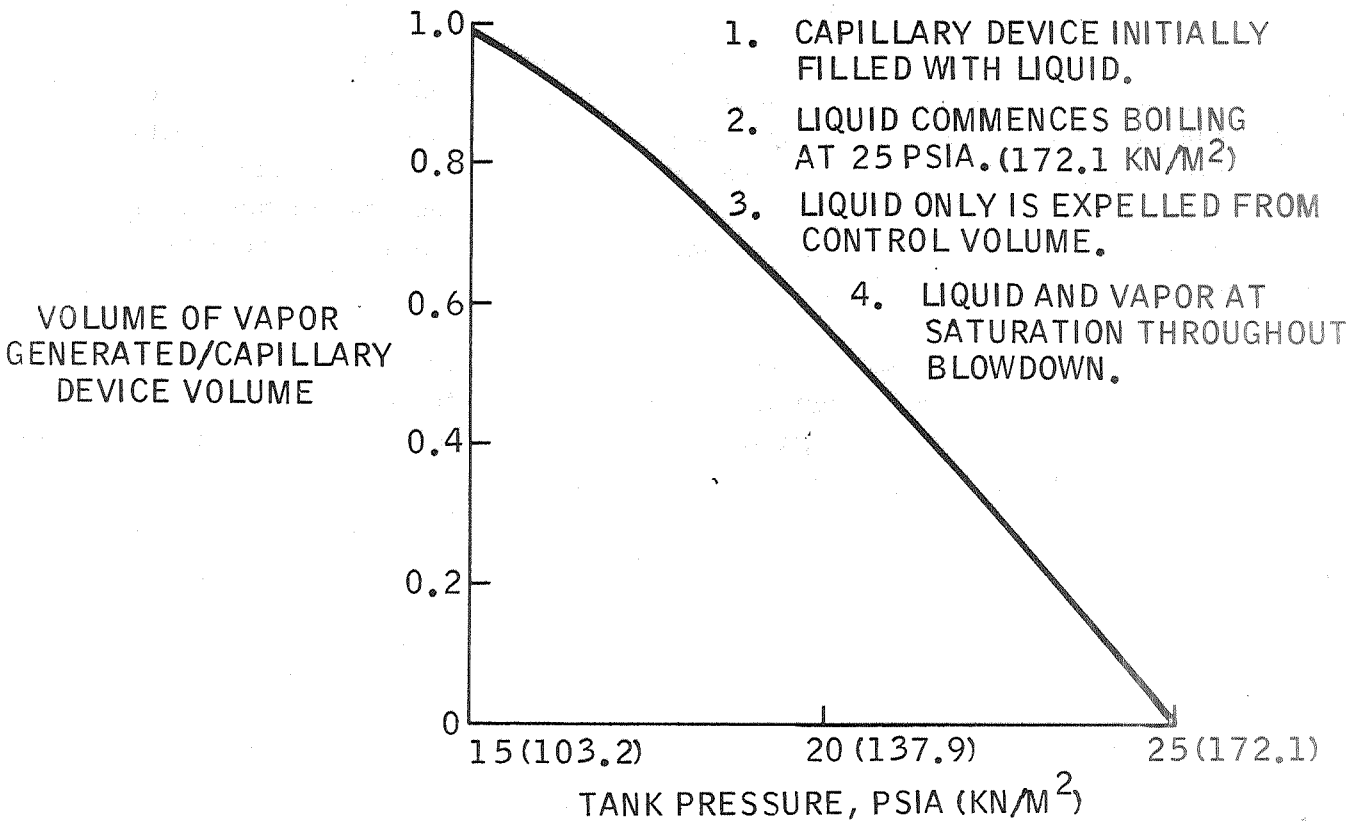

S-IVC LH_2 START BASKET

Because of the inverted bulkhead design of the S-IVC LH_2 tank, liquid spilling was a major consideration in determining the geometry and screen selections for the LH_2 capillary device. The INGASP and DREGS2 programs were used to minimize spelling and vapor ingestion, and liquid residuals resulting in the configuration shown. The top screen is 200 x 600 mesh while the side screen is 200 x 1400 mesh. Both internal deflectors and pullthrough suppression screens are used to resist entrance of vapor into the outlet. The volume of the start basket is based on a ten second collection time for the main liquid pool. The surface area of the device has been minimized for this volume in order to minimize weight and cooling requirements.

The design uses aluminum screen and an aluminum skin-stringer support system. The philosophy in the structural design was to minimize deflections due to impingement loads and pressure gradients. The weight of the LH_2 capillary device, including the thermal conditioning system, was approximately 400 lbs (180 kg).

FUEL START BASKET GENERAL ASSEMBLY & DESIGN GROUND RULES

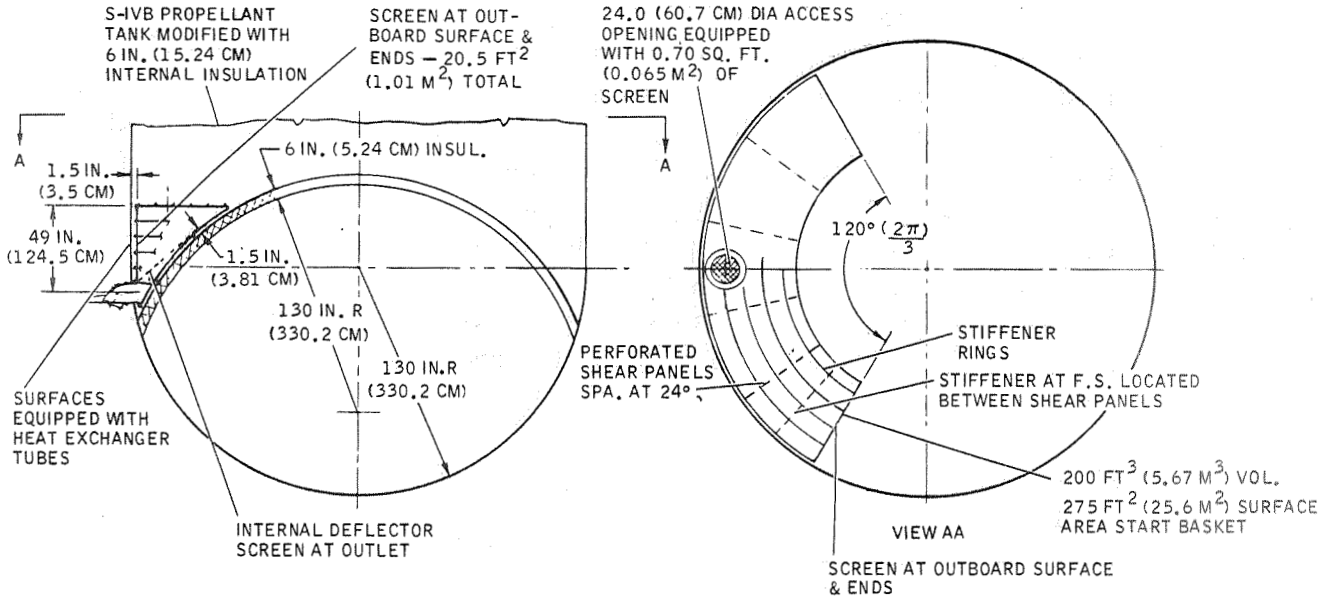

S-IVC HEAT EXCHANGER SYSTEM SCHEMATIC

Of major importance in the design of capillary control devices for cryogenic fluids is the prevention of liquid evaporation in the capillary device. The design approach was to eliminate all vapor formation in both the feed line and capillary device for both missions considered. In the case of a perfectly mixed tank fluid (no superheated gas) at constant pressure with capillary device fluid not in direct contact with the tank walls, no vaporization would occur in the capillary device. Under actual conditions, however, basket supports are required, tank mixing is not complete and tank pressure is not constant. The cooling capacity of a thermodynamic vent system may be used to prevent vaporization under actual conditions. The objective of the second phase thermal analysis was to perform detailed analysis and sizing of capillary device cooling systems for the S-IVC restart and LO_2 tanker propellant transfer missions. For the S-IVC LH_2 and LO_2 tanks a thermal conditioning system as shown will be utilized to cool the start baskets, engine feed lines and to maintain uniform tank pressures.

Vented fluid is throttled to below tank pressure to create a ΔT for cooling the capillary devices and feedline. Cooling coils passing over the conditioned components cause the throttled liquid to be vaporized and thus be vented in vapor form. Liquid inlet to the throttling device is provided by capillary collector tubes placed along the tank wall penetrating the main liquid mass in order to obtain sufficient cooling capacity to prevent vapor formation within the LH_2 capillary device and feed line. After cooling the capillary device, vent fluid will then cool the feedline. Alternate design configurations use independent or integrated pressure control vent systems downstream of the LH_2 feed line. The vent fluid is then used to cool the LO_2 tank capillary device and control tank pressure in the LO_2 tank with an external cooling configuration as shown.

HEAT EXCHANGER SYSTEM SCHEMATIC

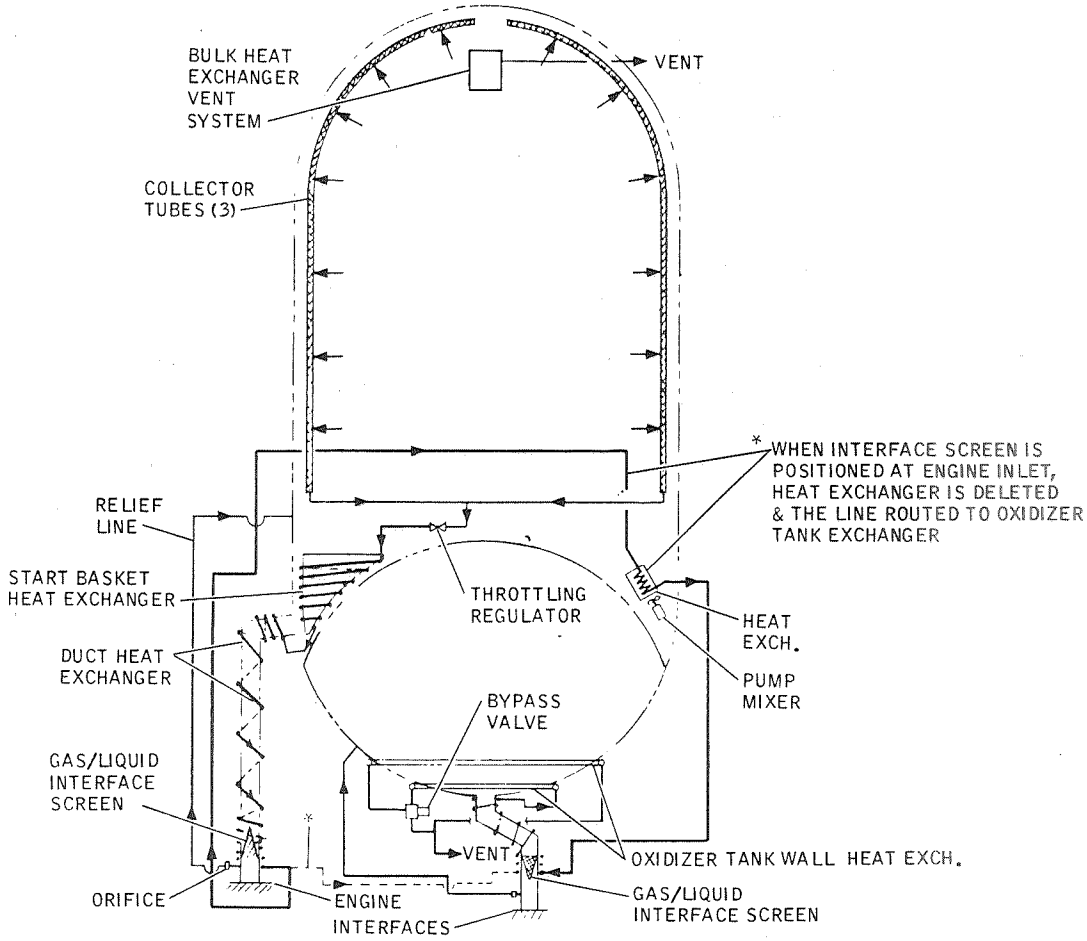

LO_2 TANKER

The LO_2 tanker propellant transfer capillary device consists of eight channels radiating from the outlet with a single channel connecting these eight channels at the equator. These channels are designed to maintain continuous contact with the main liquid pool which will be wall bound at the low gravity levels experienced during the orbital period. The reservoir over the outlet is to provide continuous liquid flow in the event a disturbing acceleration temporarily positions the liquid away from the wall.

This design was chosen in preference to a full liner configuration because the liner configuration cannot be cooled with the normal boiloff from the tank. For the channel-reservoir configuration normal boiloff rates can be utilized to prevent vapor formation in the capillary device because it does not project over the full surface area of the tank.

OXIDIZER TANKER GENERAL ARRANGEMENT & DESIGN GROUND RULES

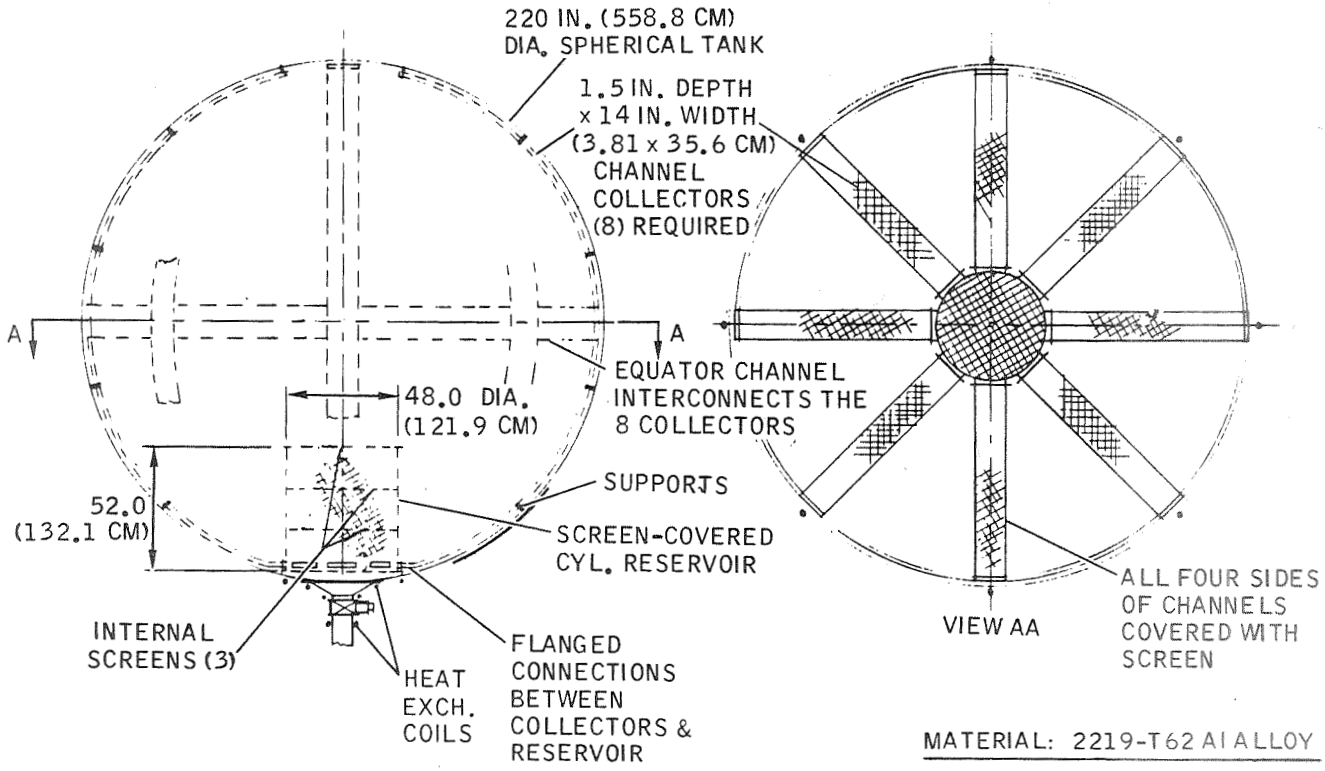

LO_2 TANKER COLLECTOR

For the LO_2 tanker, the higher ratio of capillary device area to total tank area makes the thermal-conditioning system more difficult to design. Overcooling must be minimized if sufficient cooling capacity is to be available from the normal boiloff vent rate. Placing the cooling tubes inside the collection channels proved to transfer too much heat to the cooling channels. In order to minimize overcooling, the configuration selected was to place the cooling tubes outside the tank attached at discrete points along the collector channels and reservoir. These discrete attachments correspond to the channel support locations as shown. A configuration of this type relies on mixing and wicking to prevent vapor formation in the channel from heat incident on the bulk fluid side of the capillary device. Cooling was analyzed in a manner similar to that of the S-IVC LO_2 tank.

The channel support structure consists of one drag strut and two links pinned to the collector and welded to the tank wall. Perforated shear panels carry the load from the stringers to the support links.

OXIDIZER TANKER COLLECTOR SUPPORT FITTING ARRANGEMENT

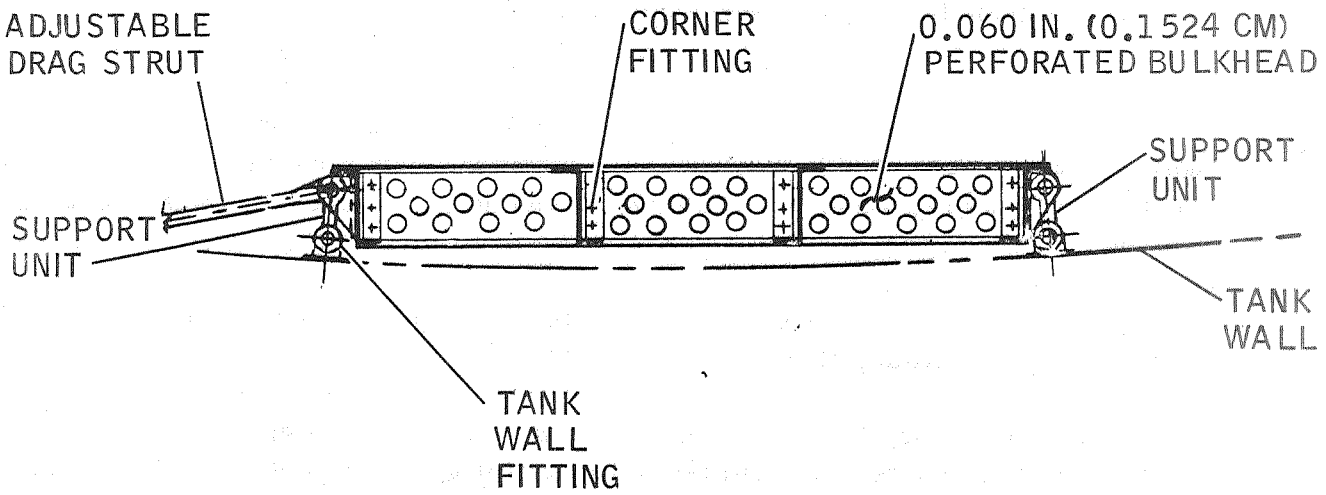

EXPERIMENTAL PROGRAM - SCALE MODEL OUTFLOW TESTS

Experiments were run to determine screen capillary retention when subjected to heat transfer, spilling, vapor ingestion and draining of capillary devices, pullthrough suppression using screen baffles, wicking rates in screens, and screen flow pressure drop. Experimentation consisting of non-cryogenic scale model bench testing was successful in providing correlations and verification of computer models and design techniques.

A test article was designed to provide visual data for correlation with DREGS2 and INGASP computer programs. A plexiglas tank and capillary device scaled from the S-IVC LH_2 tank and capillary device were used to monitor liquid levels and vapor and liquid flow during simulated restart and draining conditions. The test set-up for the pentane and water tests is shown schematically. Water and pentane were used as the test fluids and runs were visually recorded over a range of outflow rates using a high-speed motion picture camera. Tests were run initially with no capillary device to obtain pullthrough correlations for the flow rate range to be tested with the capillary device.

Vapor ingestion and spilling tests runs were compared with INGASP simulation runs and residual tests were compared with DREGS2 computer program predictions. On the basis of successful correlation of the computer models with the test data, DREGS2 and INGASP were used to develop optimum configurations for the S-IVC LH_2 and LO_2 tank capillary devices. The programs are written in general form in order to make them useful for a wide range of capillary restart device configurations and flow conditions.

Outflow tests were also performed in a cylindrical plexiglas tank to evaluate the effect of screens on retarding pullthrough during outflow. Screens were stretched across the bottom of the tank and sealed with gaskets. Several flow rates were run using water and Freon TF and 400 x 400, 165 x 1400 and 200 x 1400 screen and no screen, and recorded with high-speed motion pictures. Pullthrough was experienced at a liquid level as high as .60 inches (1.53 cms) with no screen over the outlet, using both water and Freon TF. With screens placed at heights varying from .23 to .30 inches (.584 to .762 cm) above the outlet, no pullthrough was visually observable above the screen with either screen in place, using either fluid. This was consistent with calculations made using interface shapes during draining, screen pressure drop, and screen surface tension retention pressure.

OUTFLOW TEST SCHEMATIC

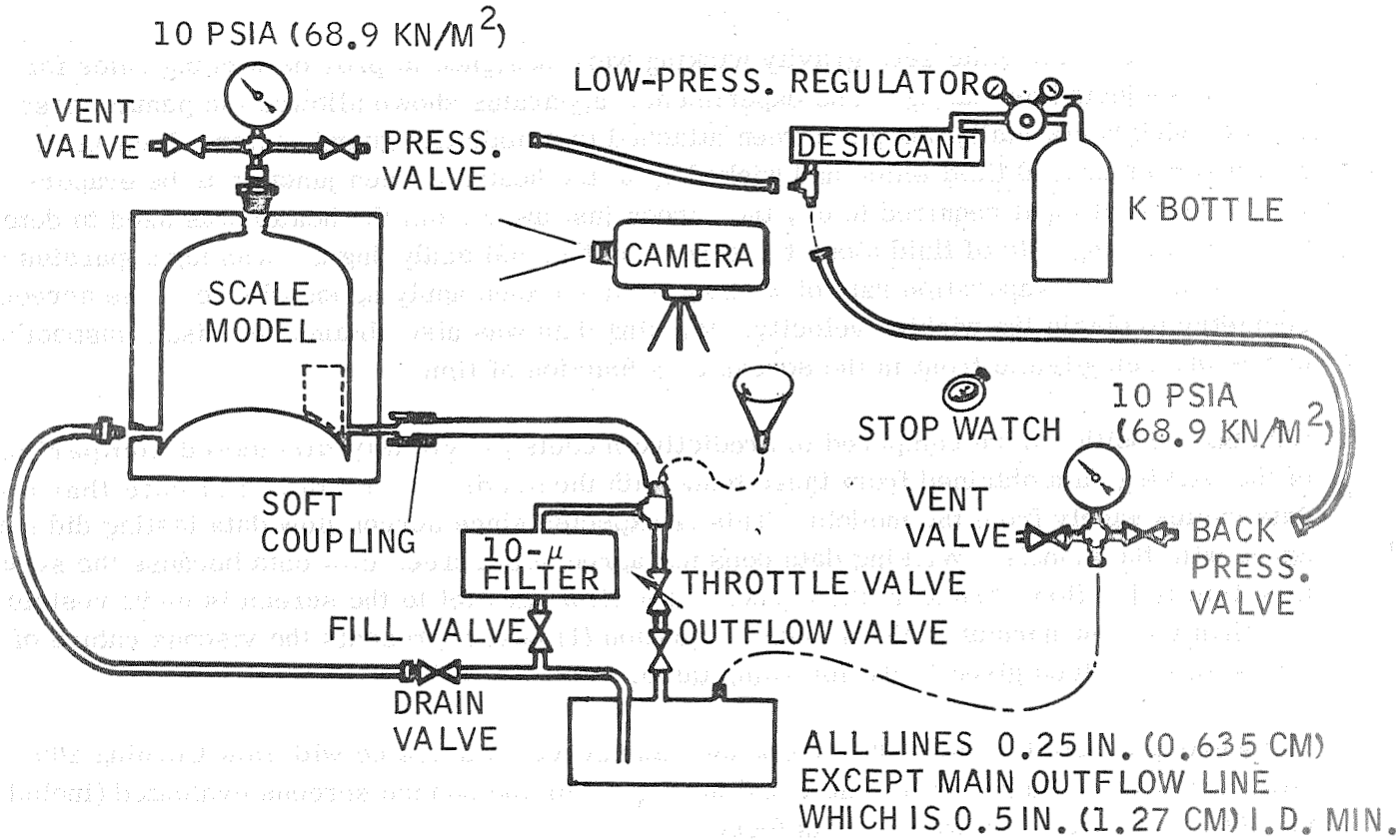

WICKING TESTS

Wicking tests to simulate zero gravity wicking were designed to provide wicking rates for screens subjected to heating. The experimental apparatus shown allowed the pentane test fluid to wick horizontally along a screen attached to a main and guard heater. Heat input to the screen caused fluid which had wicked up to the heater screen junction to be evaporated. The heat input required to dry the screen just away from the heater was used to determine the wicking rate of fluid along the screen by thermal analyzing the wicking apparatus to determine the evaporation rate of wicking fluid and then applying knowledge of the screen geometry to obtain the wicking velocity. Wicking data was also obtained by visual inspection of the advancing liquid front in the screen as a function of time.

Wicking velocities were compared to predictive models previously discussed comparison of the wicking data obtained from these tests with the predictive models indicate that the data varies widely from the models. This is expected since screen flow data testing did not agree with the models. Wicking data does not agree with screen flow data because the screen flow data is for flow normal to the screen. The flow parallel to the screen is more restrictive than the flow normal to the screen. Equation (1) best represents the viscous nature of the flow with A_W values given in the following table.

For wicking parallel to the warp wire a 30 x 250 screen was tested with Dow Corning 200 Silicone Oil and a value of 755 was found for A_W. For the square screens evaluated (including 400 x 400 mesh), no wicking was found.

This information can be used directly to predict wicking rates which will prevent screen drying when subjected to both distributed and local heat sources.

WICKING TEST SET-UP

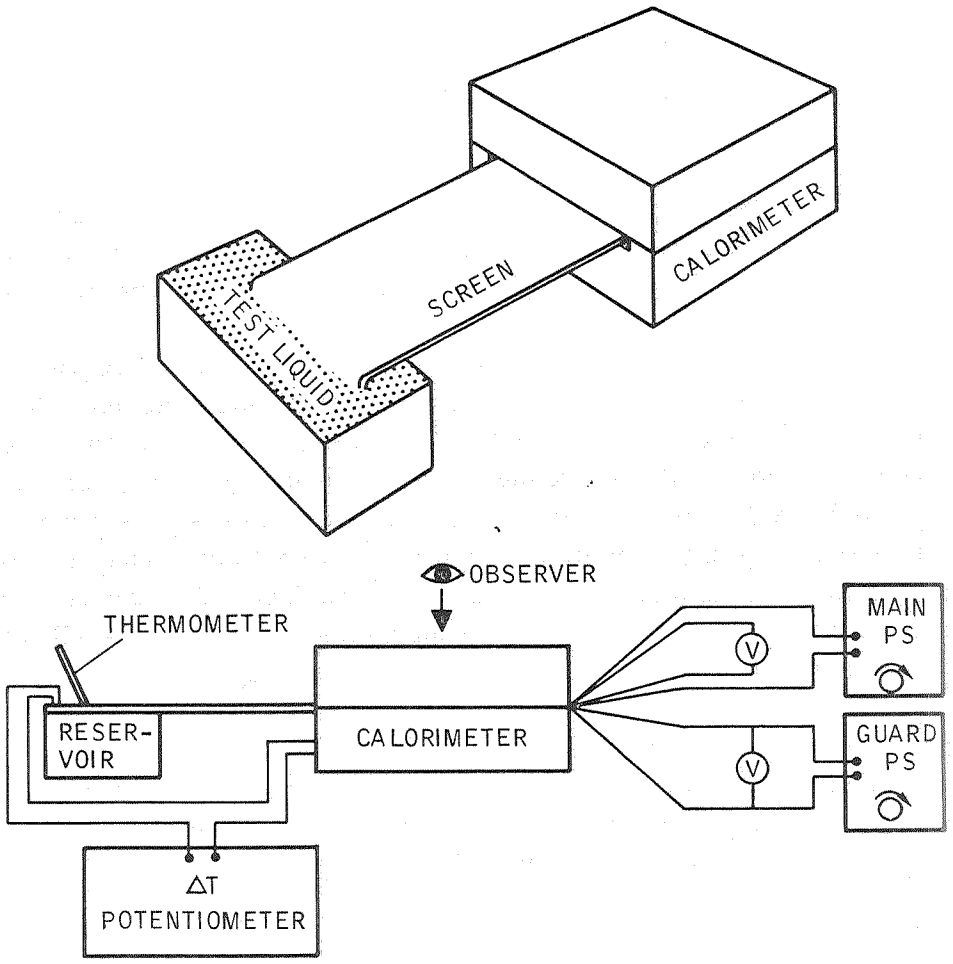

DESIGN HANDBOOK FOR CRYOGENIC CAPILLARY CONTROL DEVICES

Based on the information briefly summarized herein, a design handbook was formulated which consisted of parametric information, equations, principles and computer programs in order to hydrodynamically, thermally and structurally design large scale cryogenic capillary devices.

Hydrodynamic considerations such as screen pressure drop, wicking, refilling, filling, settling, venting, impingement and bubble dynamics are discussed. The information presented in the design handbook is directly applicable to shuttle capillary device design.

Basic principles of actively cooling capillary devices in large scale cryogenic vehicles as shown in the design handbook are directly applicable to the shuttle vehicle. This includes how to determine capillary device heat transfer coefficients, mixing requirements for destratification, consideration of ullage pressure collapse subsequent to engine shutdown, vent coil configuration and spacing to conserve cooling capacity while still subcooling the capillary device, feedline cooling principles, external and internal heat exchanger operation, liquid collection channel sizing and vent system pressure drop calculations. Using this information in conjunction with shuttle mission groundrules and conditions will allow efficient design of shuttle subcritical acquisition thermal conditioning systems.

Structural considerations which are discussed are methods of limiting capillary device deflections, minimizing capillary device weight and computing and handling forces due to impingement loading and pressure drops. Subassembly procedures for large scale capillary devices and methods of checkout and repair of devices are summarized.

DESIGN HANDBOOK FOR CRYOGENIC CAPILLARY CONTROL DEVICES

FLUID DESIGN

- OUTFLOW COMPUTER PROGRAMS
- SCREEN PROPERTIES — GEOMETRY PRESSURE DROP, WICKING
- OPERATIONAL CONSIDERATIONS — REFILLING, FILLING, SETTLING, VENTING, IMPINGEMENT, BUBBLE DYNAMICS

THERMAL DESIGN

- ACTIVE COOLING DESIGN PRINCIPLES
- HEAT TRANSFER — CAPILLARY DEVICES, FEEDLINES
- PRESSURE CONTROL — MIXING

STRUCTURAL DESIGN

- LOADS — PRESSURE GRADIENTS, VIBRATION, ACCELERATION, DEFLECTIONS
- FABRICATION — ATTACHMENTS, ASSEMBLY, CHECKOUT, REPAIR

SHUTTLE TECHNOLOGY REQUIREMENTS

As indicated in previous slides, it is possible to design the shuttle vehicle using existing technology. This, however, requires a conservative design approach resulting in less than optimum vehicle weight and performance. Additional technology studies are thus recommended to increase capillary device versatility, reduce weight and improve performance by providing information with which to reduce design conservatism.

In addition to the specific pressurization, restart and propellant transfer considerations discussed above for shuttle applications, the following technology investigations should be undertaken.

In order to predict low gravity destratification and resulting mixing velocity effects on the capillary device studies should be considered using drop tower testing and future orbital experiments. As a foundation for this low gravity testing, normal gravity destratification and capillary device-mixer interaction effects should be studied.

A primary uncertainty in designing capillary devices is the settling and collection time during restart, before capillary device refilling occurs. For large vehicles, such as the shuttle, this settling process involves high Bond and Weber Number reorientation flows. Analytical tools, such as the MAC method, should be used in conjunction with experimentation to extend collection time correlations into this range. Techniques for reducing settling time such as dual mode thrusting or using anti-slosh baffles to collect fluid while damping out turbulence and high amplitude recirculation should be investigated. In conjunction with these settling studies, capillary device refilling with collected fluid should be studied using several different configurations such as wicking or non-wicking screens or refill valves.

In the area of thermal conditioning, in addition to the mixing studies recommended above, subscale prototype testing should be accomplished at normal gravity with subsequent low gravity orbital experimentation with full scale hardware. As an important part of this thermal conditioning study, feedline conditioning concepts such as the use of an optically impervious baffle should be empirically verified. For capillary device thermal conditioning, screen thermal conductivity determinations are required. Wicking to prevent screen drying should be investigated for screens of interest in addition to those tested in NAS 8-21465 bench tests.

Fabrication studies should be initiated to establish practical methods of assembly, checkout, cleaning and refurbishment of large scale capillary devices for cryogenic applications. A typical device should be built and cycled in a simulated shuttle environment to demonstrate reusability and ease of checkout.

TECHNOLOGY REQUIREMENTS

LOW-GRAVITY DESTRATIFICATION

SETTLING & CAPILLARY DEVICE REFILLING

THERMAL CONDITIONING

FABRICATION

SUMMARY

CAPILLARY DEVICES ARE AN ATTRACTIVE MEANS OF PROPELLANT CONTROL FOR LARGE SCALE CRYOGENIC VEHICLES.

DESIGN HANDBOOK RESULTS PROVIDE STATE OF THE ART CRYOGENIC CAPILLARY DEVICE DESIGN PRINCIPLES.

WORK IN THIS AREA SHOULD BE CONTINUED IN THE AREAS INDICATED TO INCREASE SHUTTLE EFFICIENCY AND RE-USABILITY.

N71-29612

"ZERO GRAVITY INCIPIENT BOILING HEAT TRANSFER"

H. MERTÈ, JR.

THE UNIVERSITY OF MICHIGAN

TECHNICAL MANAGER

J. W. LITTLE

MARSHALL SPACE FLIGHT CENTER

ZERO GRAVITY INCIPIENT BOILING HEAT TRANSFER

H. Merte, Jr.
The University of Michigan
Ann Arbor, Michigan

J. W. Littles
Marshall Space Flight Center
Huntsville, Alabama

The need for information on vapor formation characteristics and incipient boiling under very low gravity arises in the storage of cryogenic liquids in space. For optimizing the long-term storage of cryogenic liquids it is necessary to be able to predict the velocity and temperature fields in both the liquid and vapor.

A procedure had been developed to compute the pressure rise in a closed cylindrical container whose side walls are subjected to an imposed heat flux (1).* The model is shown in Fig. 1. The system pressure is related to the temperature at the liquid-vapor interface, which is in turn governed by how the liquid (and vapor) heated at the wall proceeds to the vicinity of the liquid-vapor interface. The model takes into account the heat capacity of the wall. With self pressurization the heated wall will always be higher in temperature than the liquid-vapor interface, hence the liquid in contact with the heated wall must become superheated. The degree of superheat depends on the local heat flux, fluid properties, system configuration, and local fluid velocity.

* References are appended.

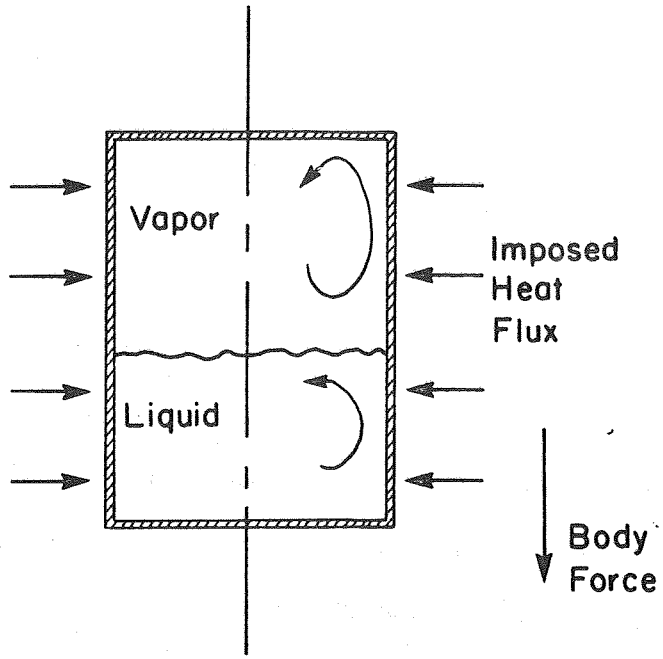

FIG. 1. MODEL FOR NUMERICAL COMPUTATION OF SELF-PRESSURIZATION

If boiling takes place, the vapor bubbles will influence the flow of liquid toward the liquid-vapor interface, and hence affect the pressure rise rate. Complicating the process further would be the interaction between the vapor bubbles and bulk subcooled liquid which will be present. Typical results are given in Fig. 2 computed with the technique of Ref. 1, and shows the temperature distribution at selected points in the liquid. Temperature is plotted in the upper portion as the degree of subcooling or superheat above the saturation temperature which exists at the liquid-vapor interface. The liquid is subcooled near the center, and simultaneously superheated toward the wall. An interesting point to be noted here is that even though the entire process is transient, once the initial starting transients have died out, which takes about 1000 seconds in this case, the remainder of the heating process can be considered to be pseudo-steady state. Approximate calculations assuming thermodynamic equilibrium within the entire tank give pressure rise rates which agree within 25% with the non-equilibrium case at 1800 seconds in Fig. 2.

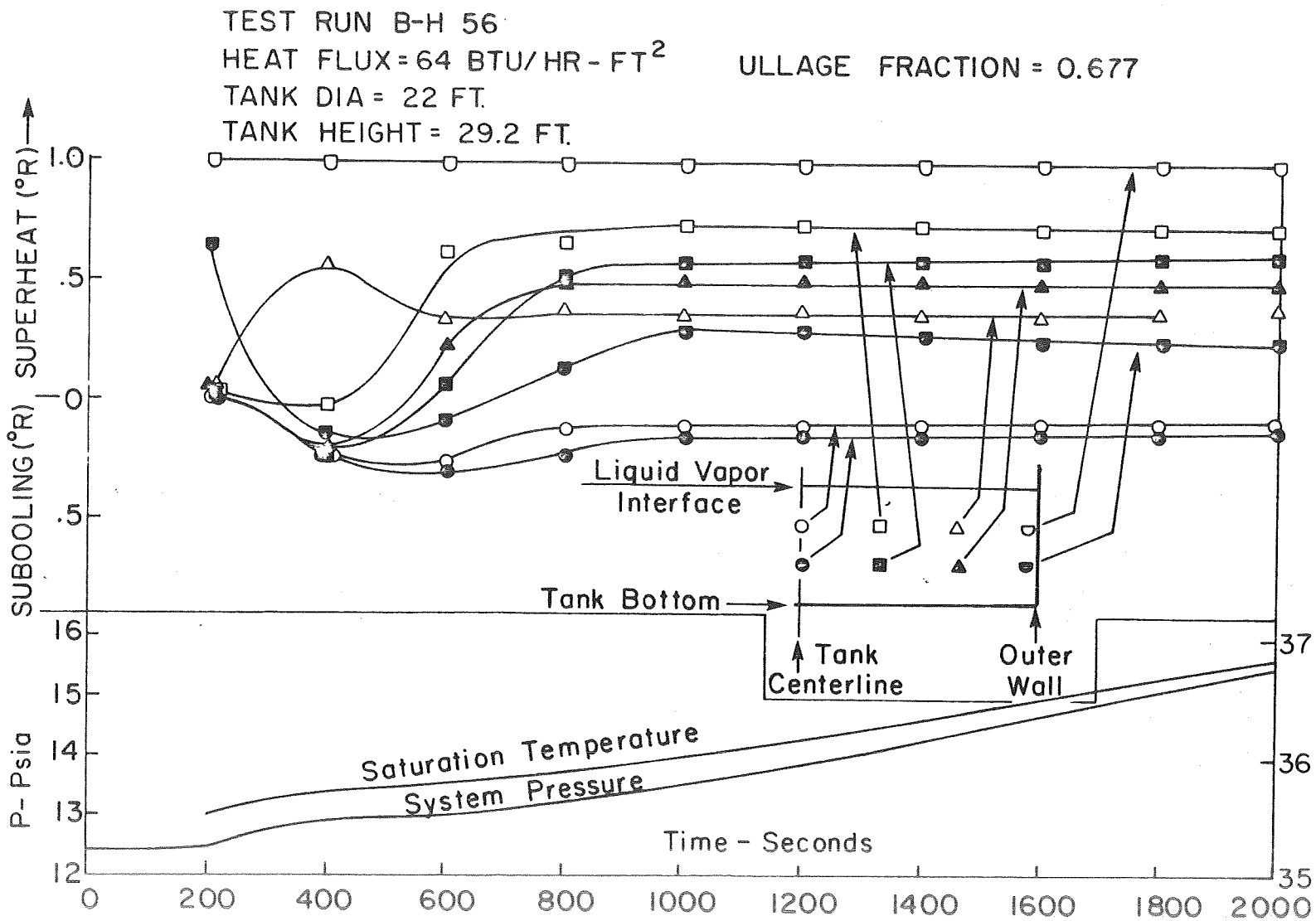

FIG. 2. FINITE DIFFERENCE COMPUTATION OF PRESSURE RISE

Information about incipient boiling is necessary not only for long-term storage, but in applications involving short term storage as well. It should be understood that the expressions long and short terms are purely relative. It is important to be able to predict the conditions necessary for nucleation of the first bubble. If the liquid is extensively superheated, the first bubble could initiate a process of catastrophic vapor generation, resulting in a phenomena similar to geysering if it takes place in a tube, or a rapid pressure increase similar to that which arises with "bumping" in the distillation of water. The severity depends on the relative amounts of liquid and vapor present, the degree and distribution of the superheat in the liquid, and the system configuration.

Bulk nucleation will take place only if the surfaces of the container are very smooth, and generally does not occur with engineering surfaces. Consideration of thermodynamic equilibrium gives the conditions necessary for the growth of a vapor bubble, the results of which are shown in Fig. 3. The liquid superheat ($Tv^* - Ts$) must be equal to greater than the expression on the right side, for a vapor bubble of radius r^* to grow (2). If the liquid superheat is less than this the vapor bubble will collapse.

Although this expression applies to bulk liquid nucleation, it forms the basis for a number of models for incipient boiling at a surface (3,4,5).

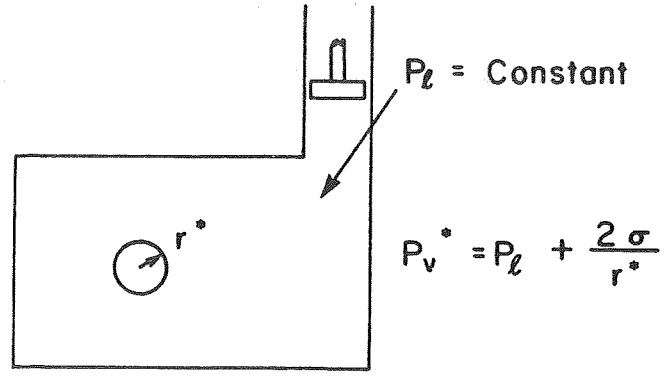

MINIMUM SUPERHEAT REQUIRED FOR VAPOR BUBBLE OF RADIUS r^* TO GROW

$$= T_v^* - T_s = \frac{2\sigma}{\rho_v h_{fg}} \frac{T}{r^*}$$

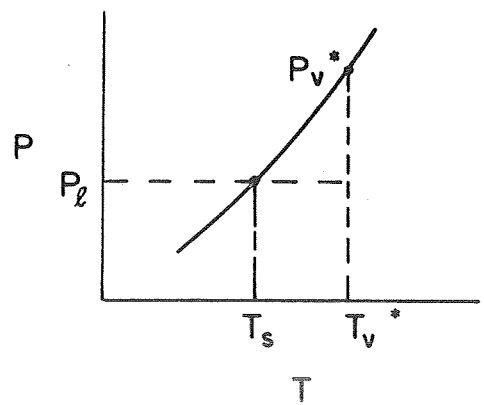

FIG. 3. THERMODYNAMIC EQUILIBRIUM FOR VAPOR BUBBLES

The lower equation in Fig. 3 is plotted at the top of Fig. 4, with r^* being the distance from the heated wall. The several incipient boiling theories consider that hemispherical vapor bubbles of radius r protrude from idealized cavitites of radius r on the surface. The bubble grows, and hence the site is activated, when the liquid superheat at the top of the bubble is equal to or exceeds the minimum superheat for equilibrium. Temperature distribution A in Fig. 4 will not produce any active sites, while temperature distribution C will activate all cavities of sizes between r_{cmin} and r_{cmax}, and temperature distribution B will activate a cavity of size r_B. The various models differ essentially in how the temperature distribution in the liquid is determined. These consider only the influence of the geometry of the cavities (cavity size) and not the surface material. For a given material they predict the effect of pressure on incipient boiling reasonably well in that as pressure increases the heater surface superheat for incipient boiling decreases in fact as well as theory (6).

For a given specific surface, the ratio of the heater surface superheat for incipient boiling for different fluids should be given approximately by the ratio of the fluid properties given in Fig. 3. Since the same surface is used, the cavity size radius is cancelled. The expression for this ratio is given at the bottom of Fig. 4, with calculations and measurements in LH_2 and LN_2 for several different surfaces (7). The comparison is reasonably good, considering that differences in liquid-solid surface energy is not taken into consideration here.

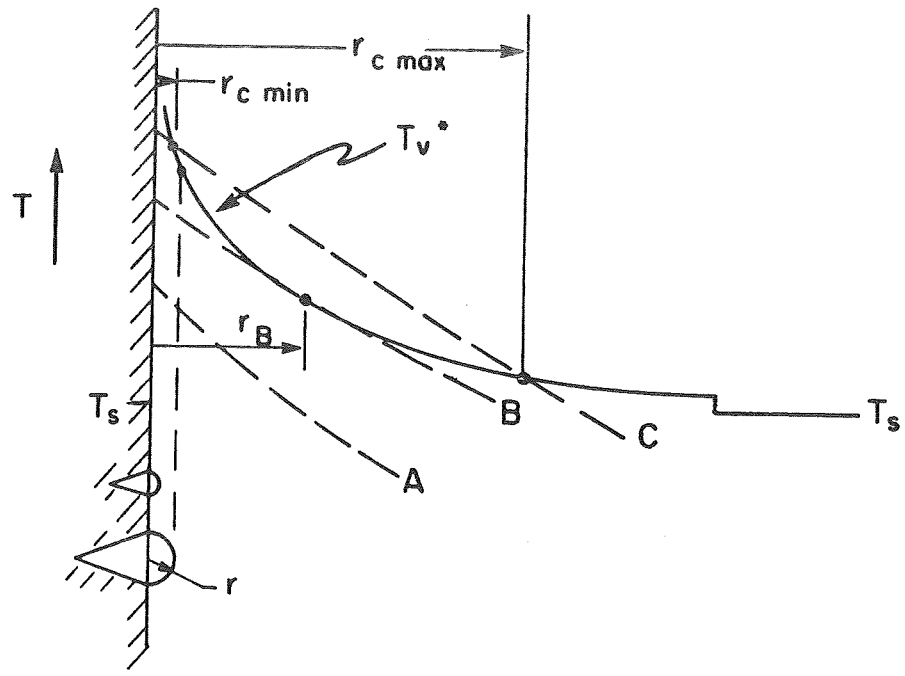

FOR INCIPIENT BOILING

$$\frac{(\Delta T_{SAT})_{LN_2}}{(\Delta T_{SAT})_{LH_2}} = \frac{\left(\frac{\sigma T_{SAT}}{\rho_v h_{fg}}\right)_{LN_2}}{\left(\frac{\sigma T_{SAT}}{\rho_v h_{fg}}\right)_{LH_2}}$$

CALCULATED	9.4
MEASURED	
POLISHED S. S.	4.6
600 GRIT S. S.	2.3
POLISHED COPPER	9.1

FIG. 4 INCIPIENT BOILING AT A SOLID SURFACE

Owing to the lack of a comprehensive theory on incipient nucleate boiling at a surface, which is able to take into account the significant parameters, one must conduct experiments with specific situations. Examples are shown in Figs. 5-8 obtained at a/g = 1 with liquid hydrogen. In each of these the heat flux is plotted as a function of the heater surface superheat.

Figure 5 shows results with a horizontal polished stainless heating surface (8). The transition between natural convection and nucleate boiling is quite well defined, and the results on decreasing the heat flux reproduce those obtained with increasing heat flux.

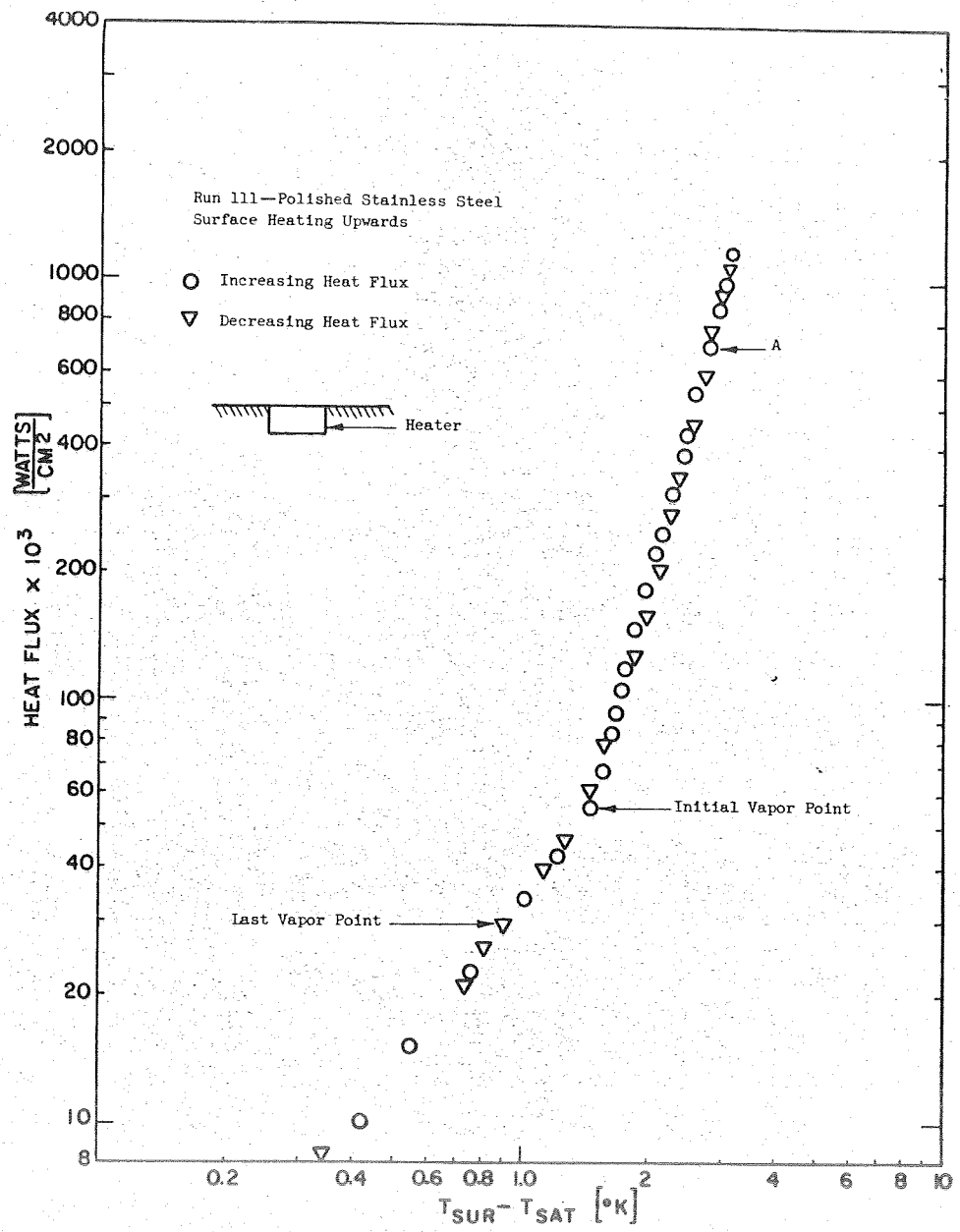

Figure 5. Incipient Boiling on Polished S.S. Surface in LH_2.

If the horizontal stainless heating surface is roughened, as in Fig. 6, the initial nucleation point is shifted to a lower ΔT, and a hysteresis effect is now present, where the heater surface superheat is smaller with a decreasing heat flux. Hysteresis appears to be an indication that a cavity, once activated, requires less superheat to remain activated. If vapor is trapped, then the superheat to sustain the active site should be smaller. The lack of hysteresis observed with the highly polished surface could mean that the cavities activated are not able to trap or retain vapor, and hence are easily deactivated. This was confirmed by the observation of spreading of "patchwise" boiling on a highly polished surface as the heat flux is increased (7).

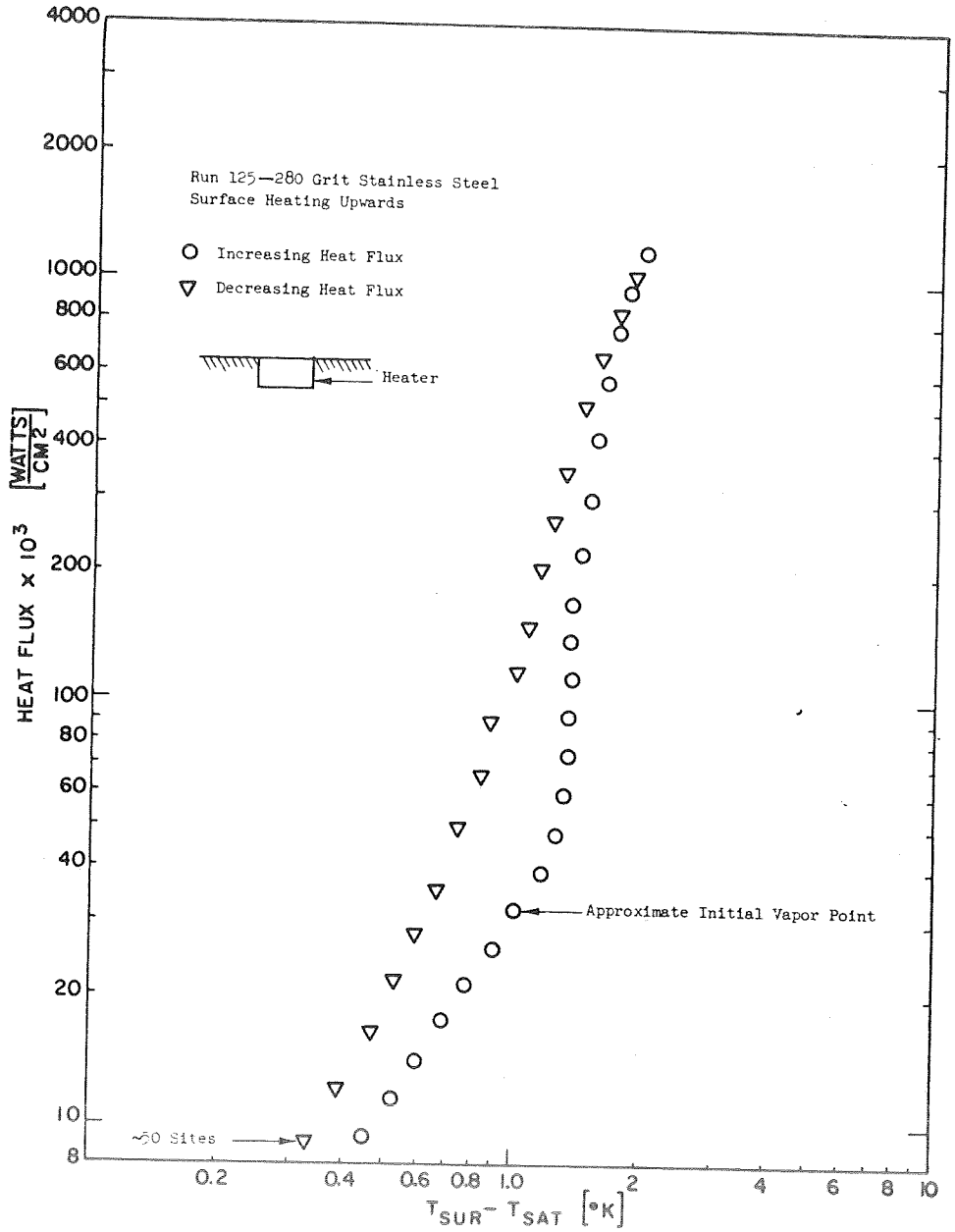

Figure 6. Hysteresis of 280 Grit S.S. Surface in LH_2.

Figure 7 shows the effect of differences in heater surface material on incipient and low heat flux nucleate boiling in liquid hydrogen. It is obvious that the wettability of a surface by a liquid is insufficient to explain these differences. The limited data available claims that liquid hydrogen wets all material.

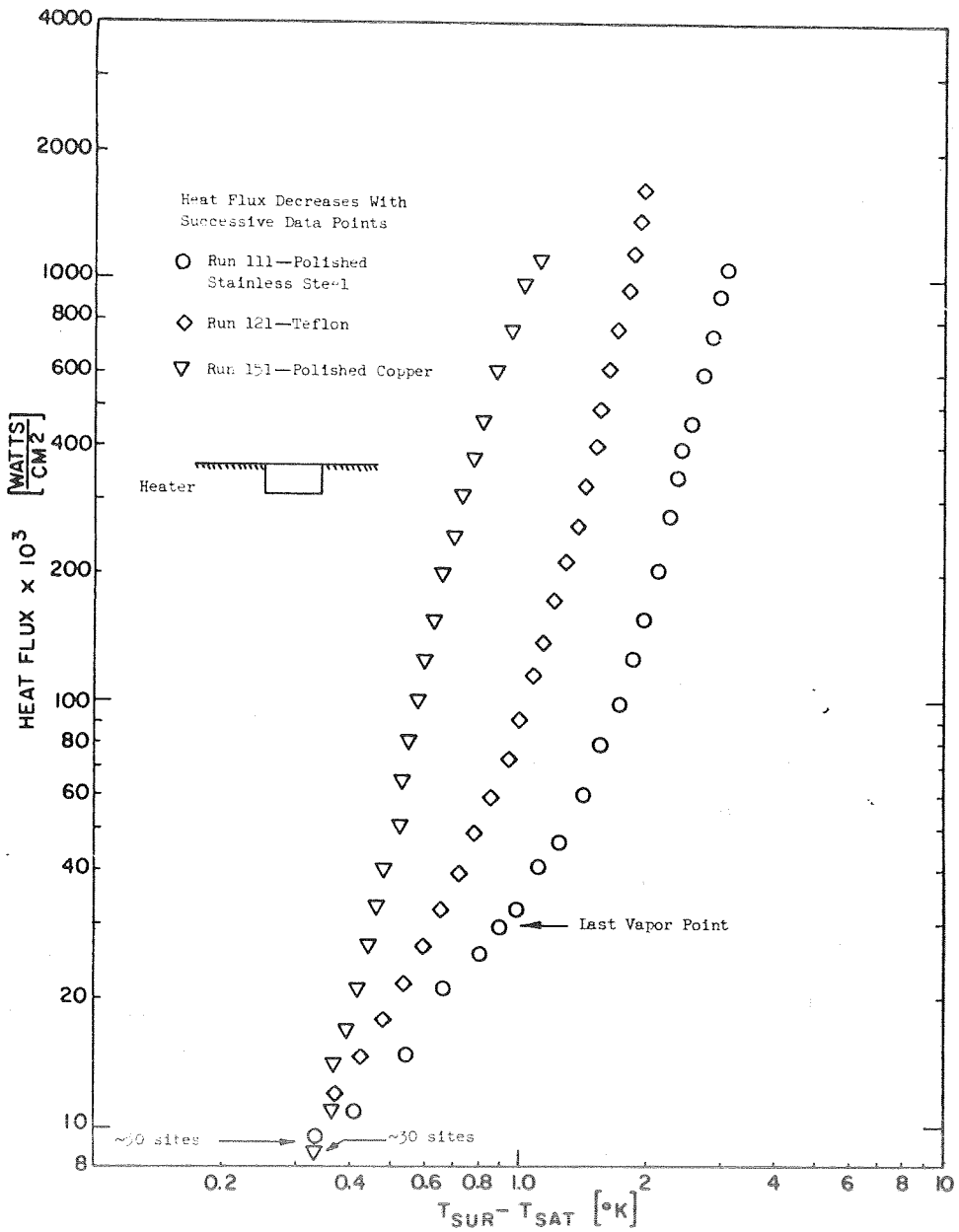

Figure 7. Effect of Surface Material with Nucleate Boiling of LH_2 on Polished Surfaces.

A sample of the internal insulation for the S-IVB LH_2 tank was furnished, and the fiberglas-resin coating on the interior was carefully removed from its backing and glued to a copper surface. Incipient boiling data were obtained for this surface and are shown in Fig. 8 (9). As heat flux was increased the behavior followed the natural convection path to higher liquid superheats. The number of active sites did not increase significantly with heat flux, as contrasted to the behavior of the metal surfaces, and is believed due to the extreme smoothness of the resin, like glass over the greatest part of the surface. The few sites activated are believed due to surface imperfections.

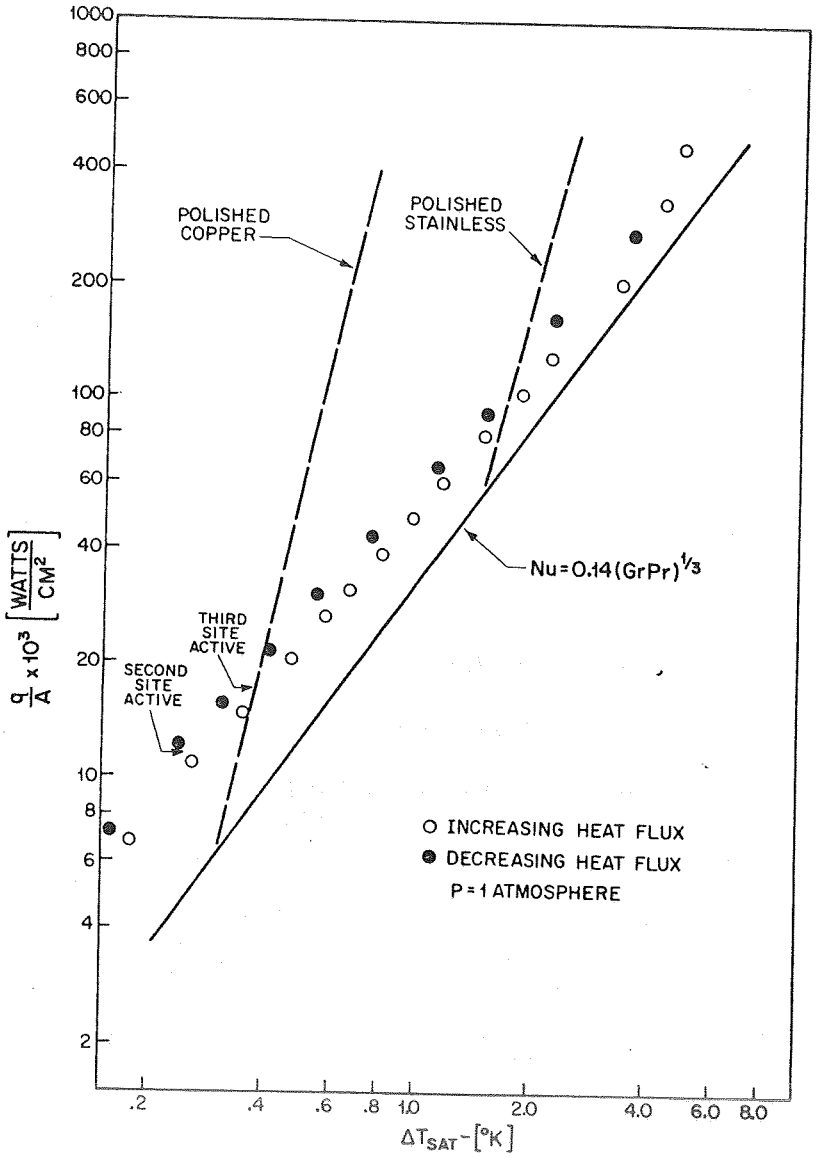

Figure 8. Incipient Boiling of LH_2 from SIV-B Fiber-Glass Lining. Horizontal Up.

Regarding the space storage of cryogens, the question now arises as to the role of body forces in the incipient boiling process, particularly very low body forces. One might consider zero gravity as the ultimate, but is doesn't exist. $a/g = 10^{-9}$ may be sufficiently large to be effective under proper circumstances. One might postulate from the nucleation model represented in Figs. 3 and 4 that under the action of very low gravity, where conduction is predominant, that the incipient boiling point should be a function primarily of heater surface superheat, and not heat flux.

To examine the role of body forces on incipient boiling two approaches were made. In the first we attempt to simulate zero "g" by inverting the heated surface with a suitable convection shielded as shown in Fig. 9 (8). If convection were completely eliminated the measured liquid temperatures should be linear. This is seen to be approximately the case only very near the heating surface.

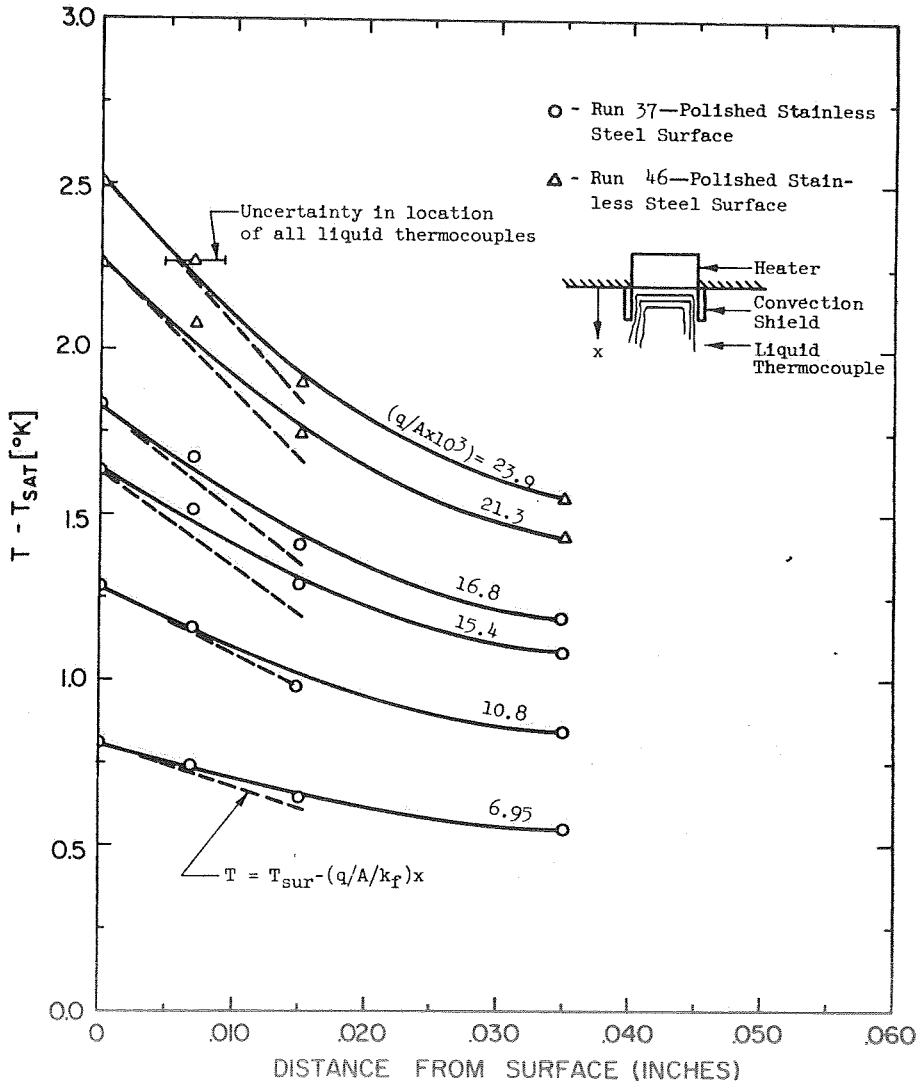

Figure 9. Temperature Distribution in LN_2 Heating Downwards.

Another way of viewing the role of body forces is to express the non-boiling results in terms of the standard dimensionless parameters - Nusselt versus Rayleigh number as in Fig. 10. The upper data and correlations apply to upward facing surfaces at $a/g = 1$, and the lower data apply to the simulated zero gravity. If convection were totally lacking, the Nusselt number should have a value of one. Such is not the case. However, the influence of convection is reduced by an order of magnitude. A line with a slope of 1/4, which is generally representative of laminar type flows, is drawn through the simulated zero gravity points. In the inverted position the superheated liquid stays adjacent to the surface, and once the initial nucleation occurs the vapor completely fills the convection shield space, terminating the test.

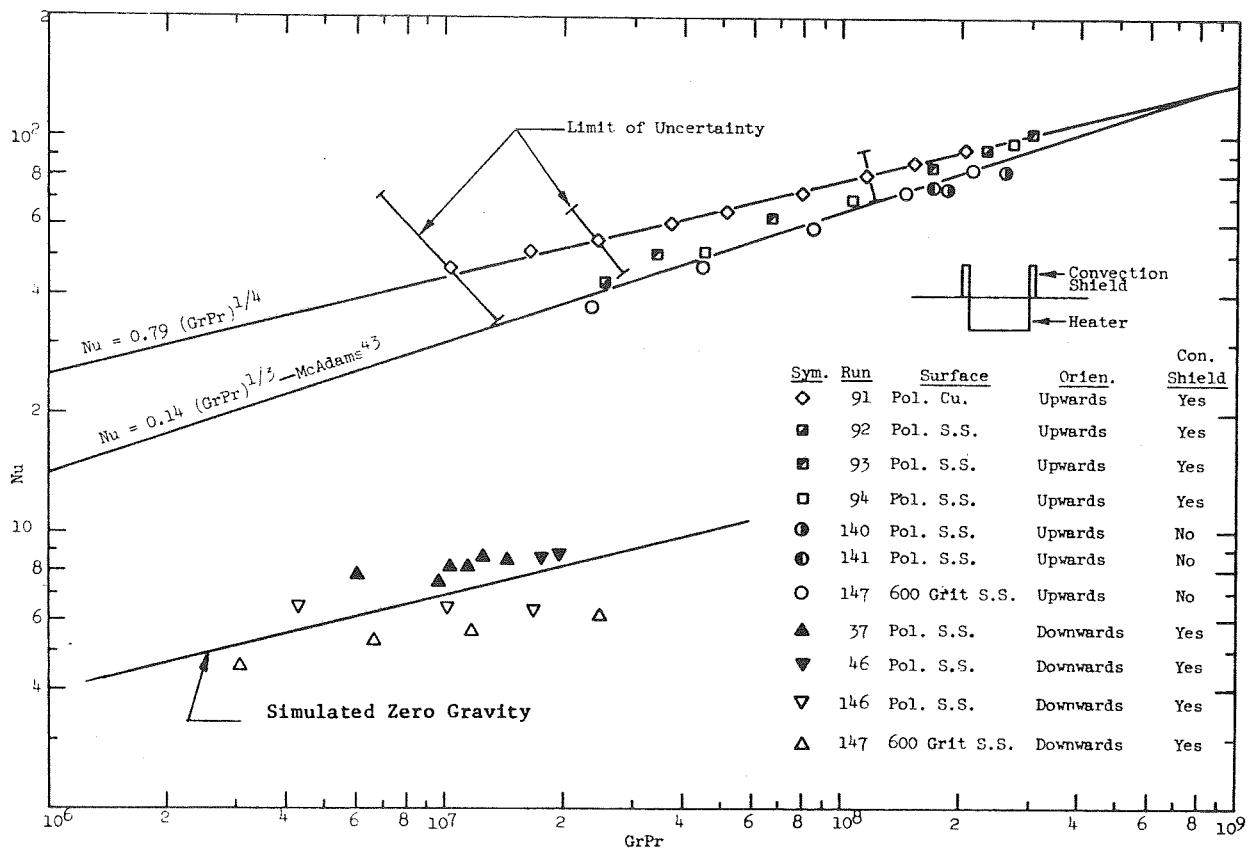

Figure 10. Natural Convection Heat Transfer to LN_2.

The initial nucleation points for all of the tests conducted are plotted in Fig. 11, as heat flux versus the heater surface superheat, and as might be expected fall on the natural convection correlation. Data with LH_2 are on the left side and with LN_2 are on the right. The results for the simulated zero gravity with LN_2 are also included, and indicate that incipient nucleation depends primarily on the heater surface superheat, and not on heat flux. Corresponding simulated zero gravity tests were attempted with LH_2, but were discontinued when it became apparent that an undue investment in time would be required. It was felt that the relative behavior would be the same as for LN_2.

The technique just described we call simulated zero gravity testing. It is desirable to determine if this provides results representative of true low gravity. The only means for obtaining reduced gravity at reasonable costs was the drop tower, which gives 1-5 seconds depending on height. The steady state procedures described above required about 1 hour for each test, and so a transient technique was adopted in conjunction with a drop tower.

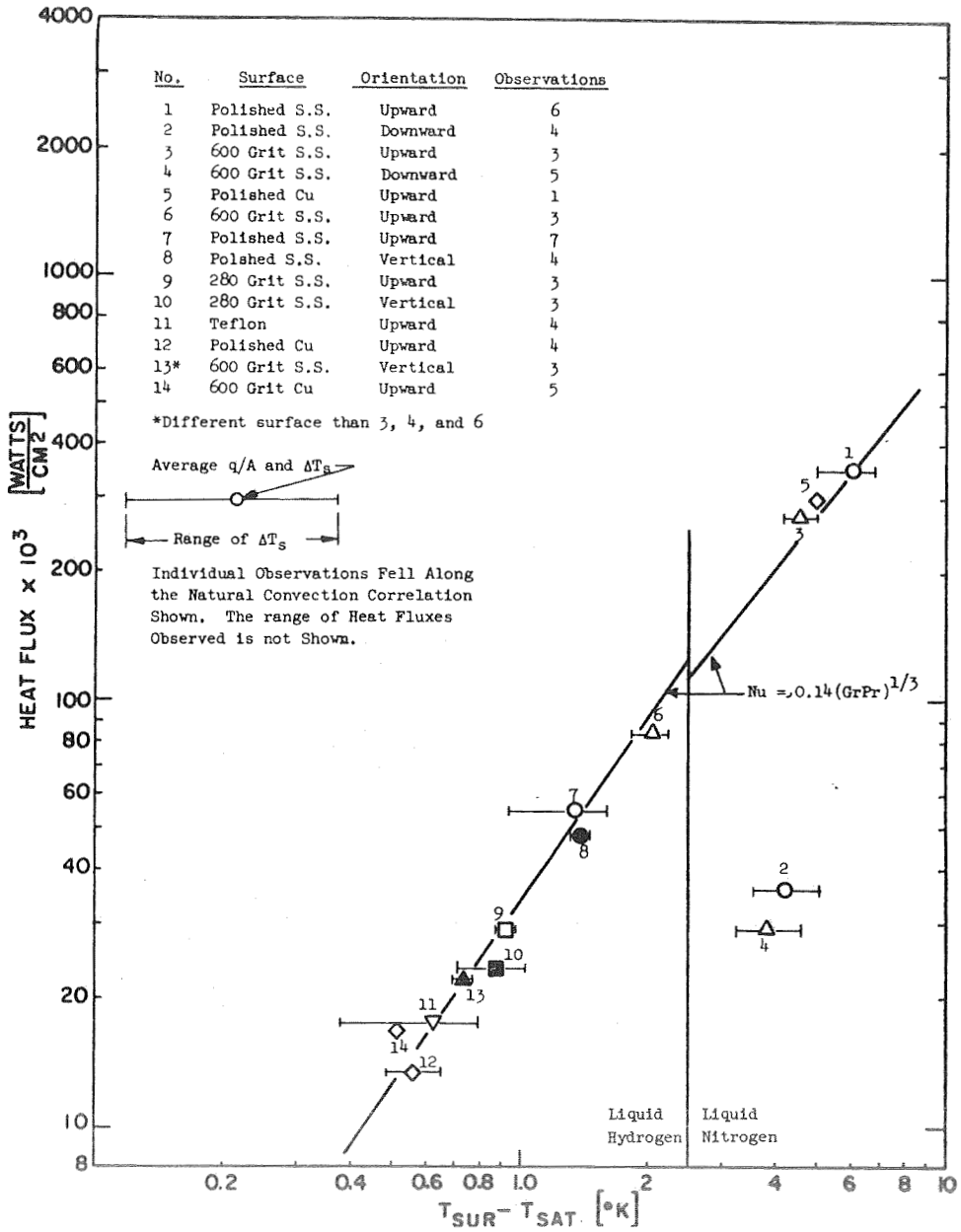

Figure 11. Initial Vapor Formation Conditions.

Figure 12 shows a cross section of the drop tower located at The University of Michigan, which is designed so as to permit its safe use with LH_2. This gives a free fall time of 1.4 seconds, with a present maximum body force of $a/g = 0.008$. This could be reduced further by the use of an air shield.

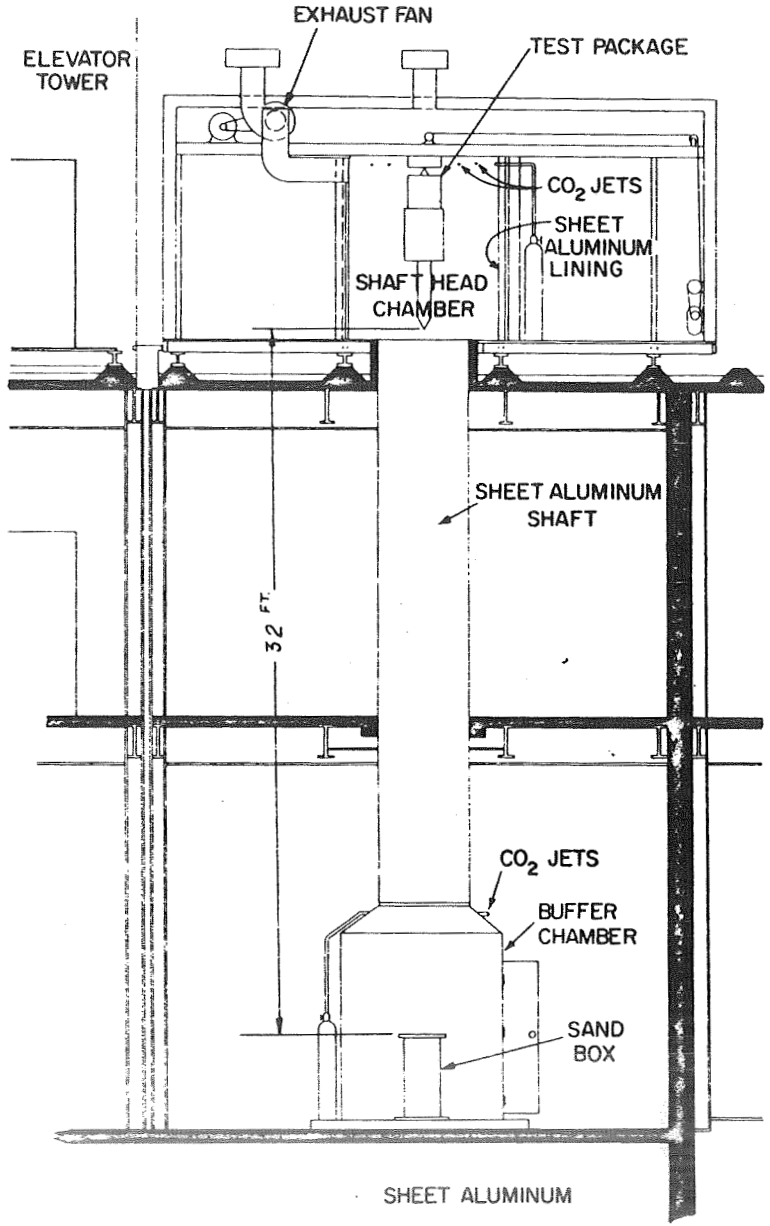

Figure 12. Drop Tower Elevation.

Since the time available during a test is small, it was desired to keep the heat capacity of the heater surface as small as possible. A small platinum wire was used, shown in Fig. 13, and permits the direct measurement of instantaneous resistance, which is a function of the mean wire temperature. D.C. power to the wire is suddenly turned on, and the transient temperature of the wire is recorded.

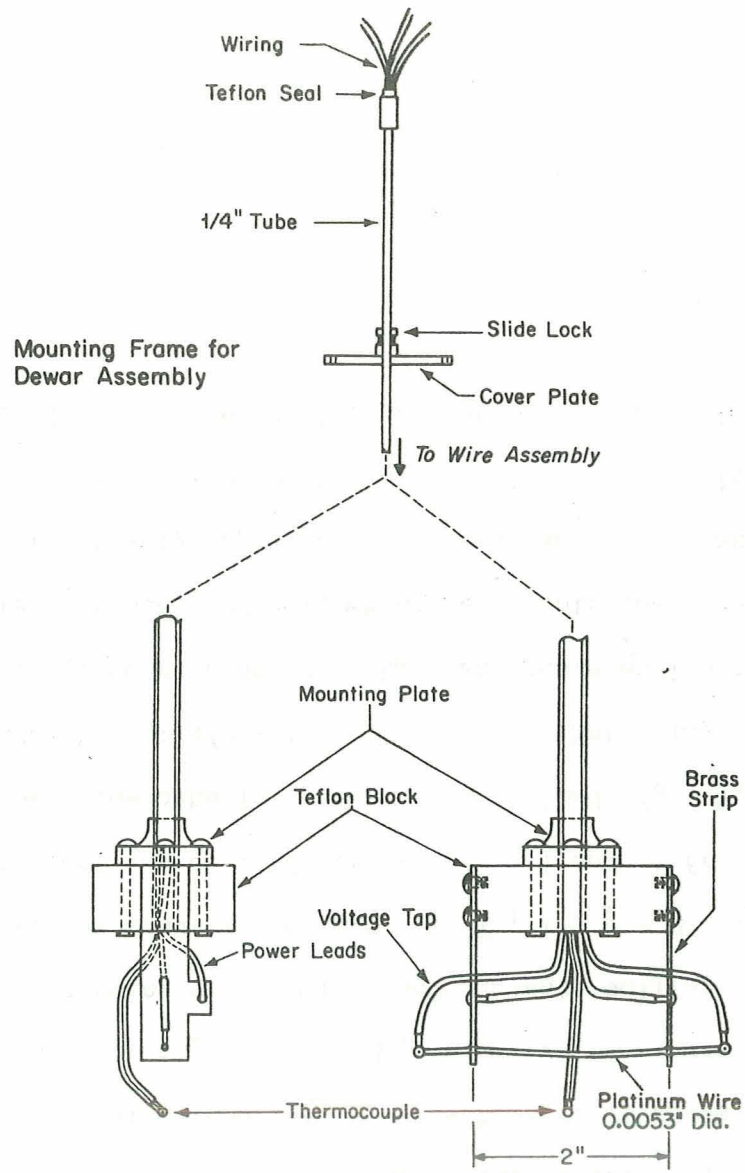

Figure 13. Platinum Wire Assembly.

An example of the data obtained with the platinum wire is shown in Fig. 14. Since the resistance of the platinum wire is small compared to the system resistance, the voltage drop across the wire is a direct measure of the wire temperature. A schematic is shown on the right side of Fig. 14. The temperature rises to a maximum E_{max} in time τ_1, at which point a plateau of duration τ_2 exists. Nucleation then commences at a point on the wire, and nucleate boiling spreads across the wire in time $_3$, at which time a steady condition exists. If $\tau_1 + \tau_2 + \tau_3$ is less than the 1.4 second free fall period, then this test can be conducted at a/g = 1 and at free fall, and the behavior compared. In order to compare the behavior between a/g = 1 and a/g = 0, one must have parameters which are themselves reproducible at a/g = 1. It was found that delay times τ_2 and τ_3 were not reproducible. However, ΔT_{max}, corresponding to E_{max} and representing the maximum temperature at which initial nucleation takes place, and τ_1, which represents the time for the wire to reach a steady maximum value, were relatively reproducible. These were then taken as the parameters to determine if incipient boiling is influenced by the body force. This is an indirect test only, in that if the behavior is different, the difference cannot be meaningfully quantized with this technique.

NOT REPRODUCIBLE

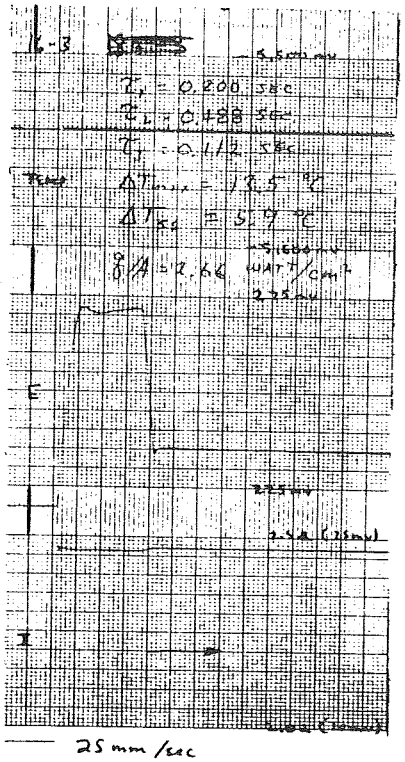

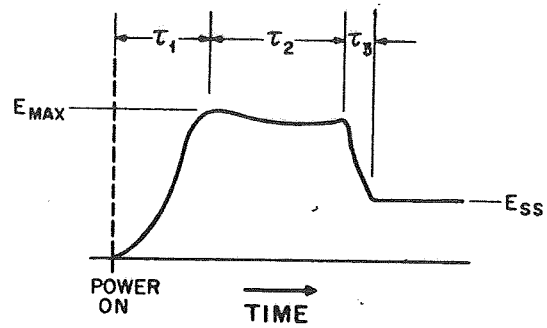

b. Schematic.

Figure 14. Definitions of Delay Times.

Figure 15 shows comparison of the steady state data with the non-boiling correlation for a horizontal cylinder, and the nucleate boiling data at a/g = 1. This served as a check on the adequacy of the instrumentation. Data for incipient boiling with larger surfaces are included. With the small wire used, it was necessary to restrict the level of heat flux used to a relatively narrow range. If the heat flux was too low, boiling would not begin within 1.4 seconds; if the heat flux was too high, the system would revert directly to film boiling once nucleation was begun.

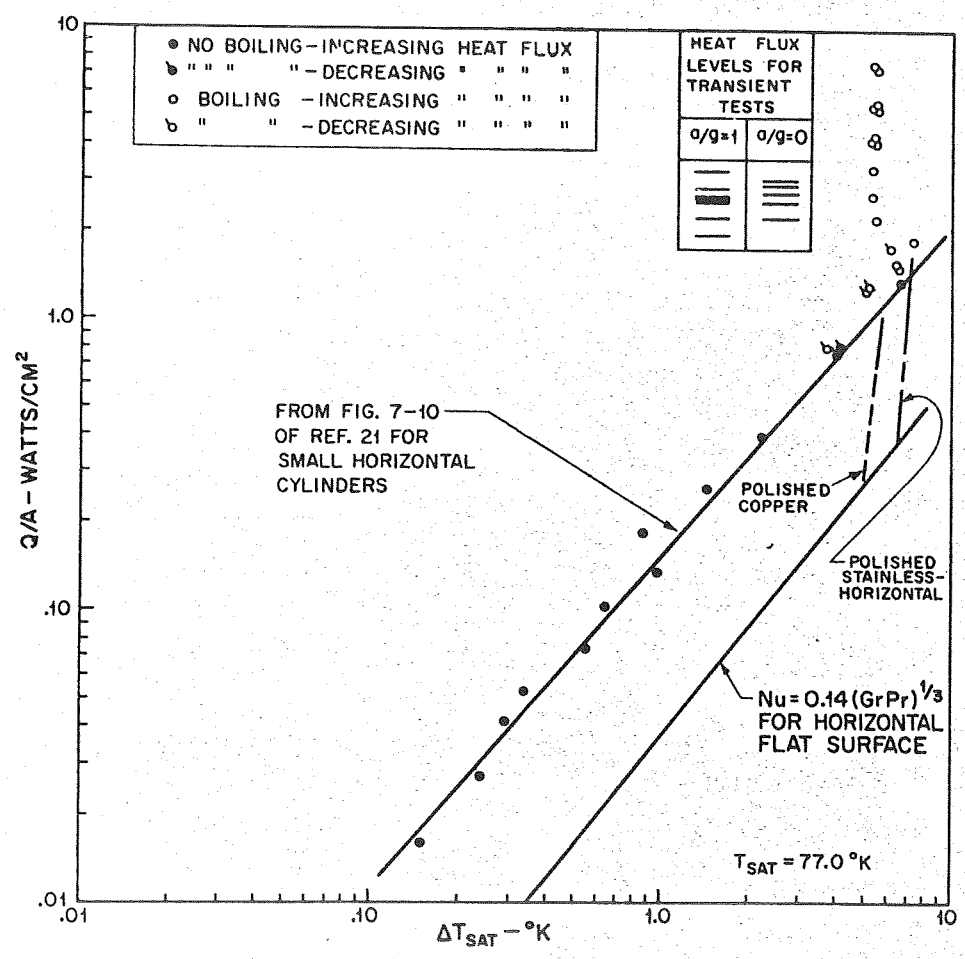

Figure 15. Nucleate Boiling with Platinum Wire in LN_2.

Figure 16 shows the comparison of τ_1 at a/g = 1 and a/g = 0. As heat flux increases, τ_1 decreases, as one might expect, but no particular effect of body force is obvious.

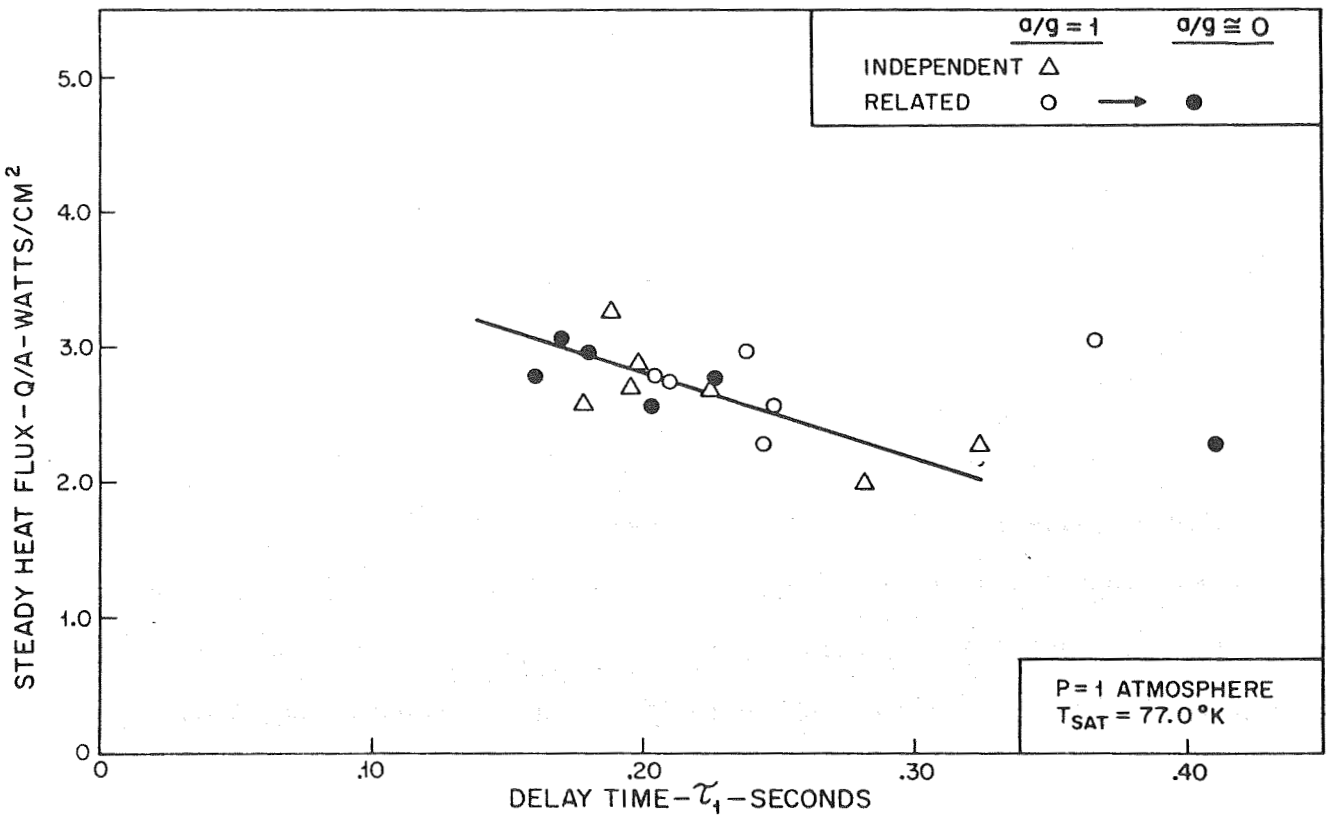

Figure 16. Delay Time τ_1. Platinum Wire in LN_2.

Figure 17 shows the comparisons of ΔT_{max} at $a/g = 1$ and $a/g = 0$. ΔT_{max} increases as heat flux increases, but again, no particular effect of body force is present. Included here are results for the platinum wire with the steady tests. The temperature overshoot due to the transient process is obvious here. These tests were repeated with LH_2, with similar results, and are presented in detail in Ref. (9). To eliminate the geometry effects due to the small wire, we are preparing to conduct corresponding tests with flat surfaces.

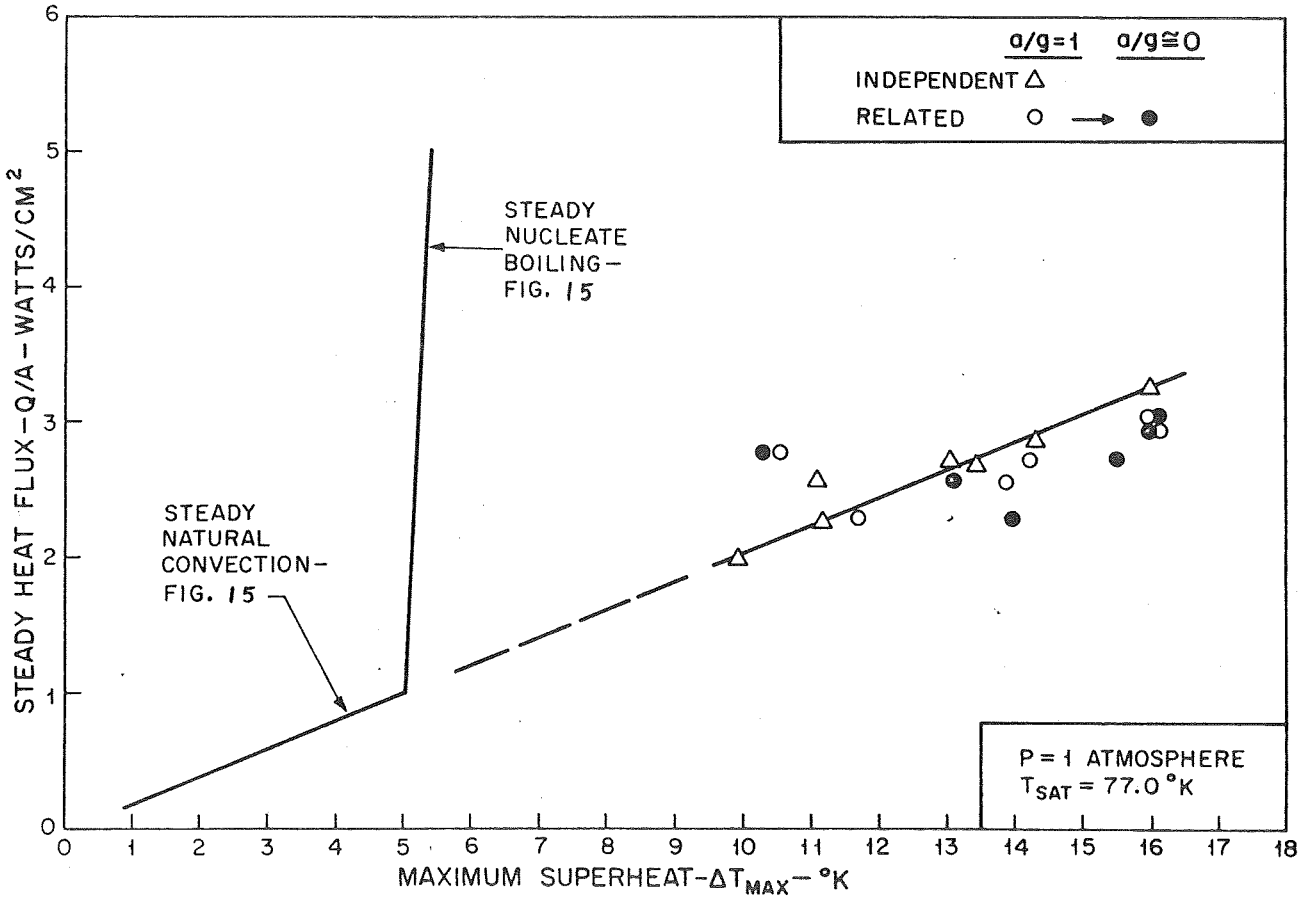

Figure 17. Maximum Transient Superheat. Platinum Wire in LN_2.

The tentative conclusion of these experiments is that we believe that one can test for incipient boiling at very low gravity by conducting tests at standard gravity, provided that adequate precautions are made to keep the convection quite small. A nagging question mark will always remain, however, when extrapolating these results to long term zero or reduced gravity behavior, with steady heating. The final answer can come only with long-time orbital testing.

Several other questions still remain:

(1) What is the role of subcooling on nucleation or incipient boiling at low gravity? For nucleation to occur, local liquid superheat must be present. If local superheating is unavoidable, can nucleation be prevented by subcooling the bulk liquid sufficiently? If so, how much? If not, will subcooling prevent or minimize the undesirable effects associated with the vapor formation. Will bubbles collapse on departure? Will they depart? To a large extent, these depend on the distribution of the subcooling, and hence become in part a systems problem.

(2) Given the fluid, heating surface material properties, and some description of the microtopography of the surface which can be related to the initiation of nucleation, is it possible to predict the initial nucleation point? The latter - relating topography or surface finish to nucleation has not yet been done. Were this possible, one could predict the nucleate boiling curve a priori.

References

(1) Merte, H., et al, "Transient Pressure Rise of a Liquid-Vapor System in a Closed Container Under Variable Gravity", Proceedings of 4th International Heat Transfer Conference, Vol. VI, Paper B.8.8, Paris, Aug. 31 - Sept. 5, 1970.

(2) Tong, L.S., "Boiling Heat Transfer and Two-Phase Flow", John Wiley and Sons, Inc., New York, 1965.

(3) Hsu, Y.Y., "On the Size Range of Active Nucleation Cavitites on a Heating Surface", Trans. ASME, 84C (J. Heat Transfer), #3, 207-216, Aug. 1962.

(4) Han, C-Y. and Griffith, P., "The Mechanism of Heat Transfer in Nucleate Pool Boiling: Part 1, Bubble Initiation, Growth and Departure", Int. J. Heat Mass Transfer 8, #6, 887-904, June 1965.

(5) Bergles, A.E. and Rohsenow, W.M., "The Determination of Forced Convection Surface-Boiling Heat Transfer", Trans. ASME, 86C (J. Heat Transfer), 365, 1964.

(6) Elrod, W.C., et al, "Boiling Heat Transfer Data at Low Heat Flux", Trans. ASME, 89C (J. Heat Transfer), #3, 235-243, Aug. 1967.

(7) Coeling, K.J. and Merte, H., Jr., "Incipient and Nucleate Boiling of Liquid Hydrogen", Trans. ASME, 91B (J. Engineering for Industry), #2, 513, May 1969.

(8) Coeling, K.J., et al, "Incipient Boiling of Cryogenic Liquids", Technical Report No. 3, ORA Report 07461-28-T. Heat Transfer Laboratory, Department of Mechanical Engineering, The University of Michigan, Ann Arbor, Michigan, Contract NAS8-20228, Dec. 1967.

(9) Merte, Herman Jr., "Incipient and Steady Boiling of Liquid Nitorgen and Liquid Hydrogen under Reduced Gravity", Technical Report No. 7, ORA Report 07461-51-T. Heat Transfer Laboratory, Department of Mechanical Engineering, The University of Michigan, Ann Arbor, Michigan, Contract NAS8-20228, Nov. 1970.

N71-29613

"ZERO GRAVITY PROPELLANT TRANSFER"

E. P. SYMONS

LEWIS RESEARCH CENTER

THIS PAGE INTENTIONALLY LEFT BLANK

PRECEDING PAGE BLANK NOT FILMED

ZERO GRAVITY PROPELLANT TRANSFER

by

Eugene P. Symons
National Aeronautics and Space Administration
Lewis Research Center
Cleveland, Ohio

THIS PAGE INTENTIONALLY LEFT BLANK

PRECEDING PAGE BLANK NOT FILMED

INTRODUCTION

In-orbit propellant transfer and the transfer of liquids between containers as in regenerative life support systems will be required for future space missions. The knowledge of both the outflow characteristics from a storage tank and the subsequent fluid behavior during the filling of the receiver tank in weightlessness will be required for the design of efficient transfer systems.

The Lewis Research Center has been conducting an extensive program concerned with liquid transfer in zero gravity. The majority of the work to date has been conducted in ground based facilities (2 and 5/10 second drop towers) and has dealt with the liquid outflow phase of fluid transfer and more recently with fluid behavior during inflow. This paper will review the results of these studies, concentrating on zero gravity liquid transfer between unbaffled cylindrical tanks having either flat or hemispherical ends.

LIQUID OUTFLOW

The first study of liquid outflow was conducted several years ago and was effective in illustrating some of the basic problems which exist. The results of that study can be seen in this figure. Typical interface configurations during outflow are shown for a flat bottomed cylindrical tank in weightlessness. The sketch at the far left shows the liquid-vapor interface configuration in an unbaffled tank at a relatively low outflow velocity at the instant of vapor ingestion into the tank outlet. Note that at this velocity, a large quantity of liquid remains in the tank as residual. Increasing the outflow velocity, as in sketch two, caused an increase in liquid residual. The remaining three sketches show interface configurations in baffled tanks at essentially the same outflow velocity. In each case, proceeding from left to right, progressively smaller liquid residuals occurred. For example, inclusion of a disc shaped baffle above the tank drain increased draining time and reduced residuals over those obtained in the unbaffled tank at comparable flow rates. Addition of a baffle over the pressurant gas inlet increased the drain time and reduced the liquid residuals still further. The addition of both baffles in the tank incorporated the best features of each and was responsible for even greater improvement in reducing residuals and increasing draining time.

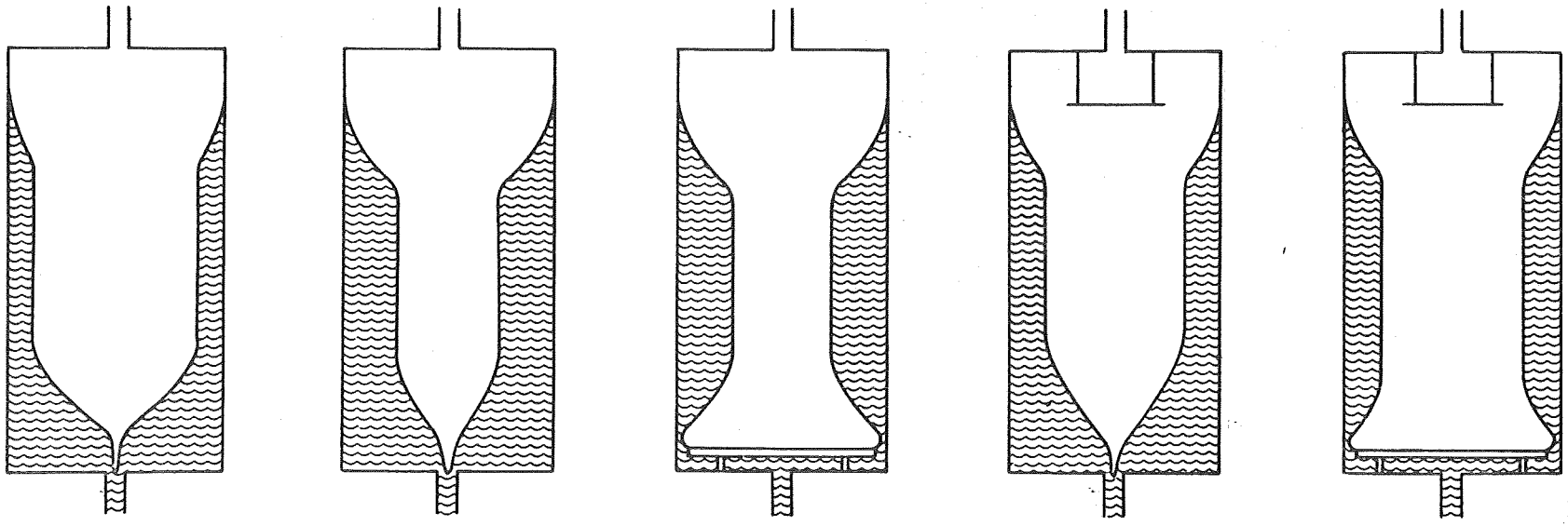

Outlet velocity, 291 centimeters per second; expelled liquid, 47 cubic centimeters.

Outlet velocity, 1408 centimeters per second; expelled liquid, 18.7 cubic centimeters.

Outlet velocity, 1330 centimeters per second; expelled liquid, 26 cubic centimeters.

Outlet velocity, 1427 centimeters per second; expelled liquid, 32 cubic centimeters.

Outlet velocity, 1348 centimeters per second; expelled liquid, 45 cubic centimeters.

Typical interface configuration during outflow from cylindrical tank in weightlessness.

The next study investigated the distortion of the liquid-vapor interface during draining. The results are shown in this figure where distortion parameter is plotted against outflow Weber number. V_m is the mean liquid-vapor interface velocity, which from continuity, is simply the area ratio, A_o/A_T, times the liquid velocity in the outlet. V is the liquid-vapor interface velocity at the tank centerline. Of course, if the liquid retained its equilibrium hemispherical shape during draining, V would equal V_m and the distortion would be zero. Unfortunately, the interface distorts during draining in weightlessness and the distortion parameter indicates the magnitude of that distortion. The distortion parameter was found to increase to a maximum of about 0.27 at an outflow Weber number of 2, remaining at this maximum value for all higher values of the Weber number. The data shown is for initial fillings of 3 tank radii. Additional data showed that the distortion parameter increased as the initial liquid filling decreased.

NASA
CS-39826

OUTFLOW DISTORTION IN CYLINDRICAL TANKS

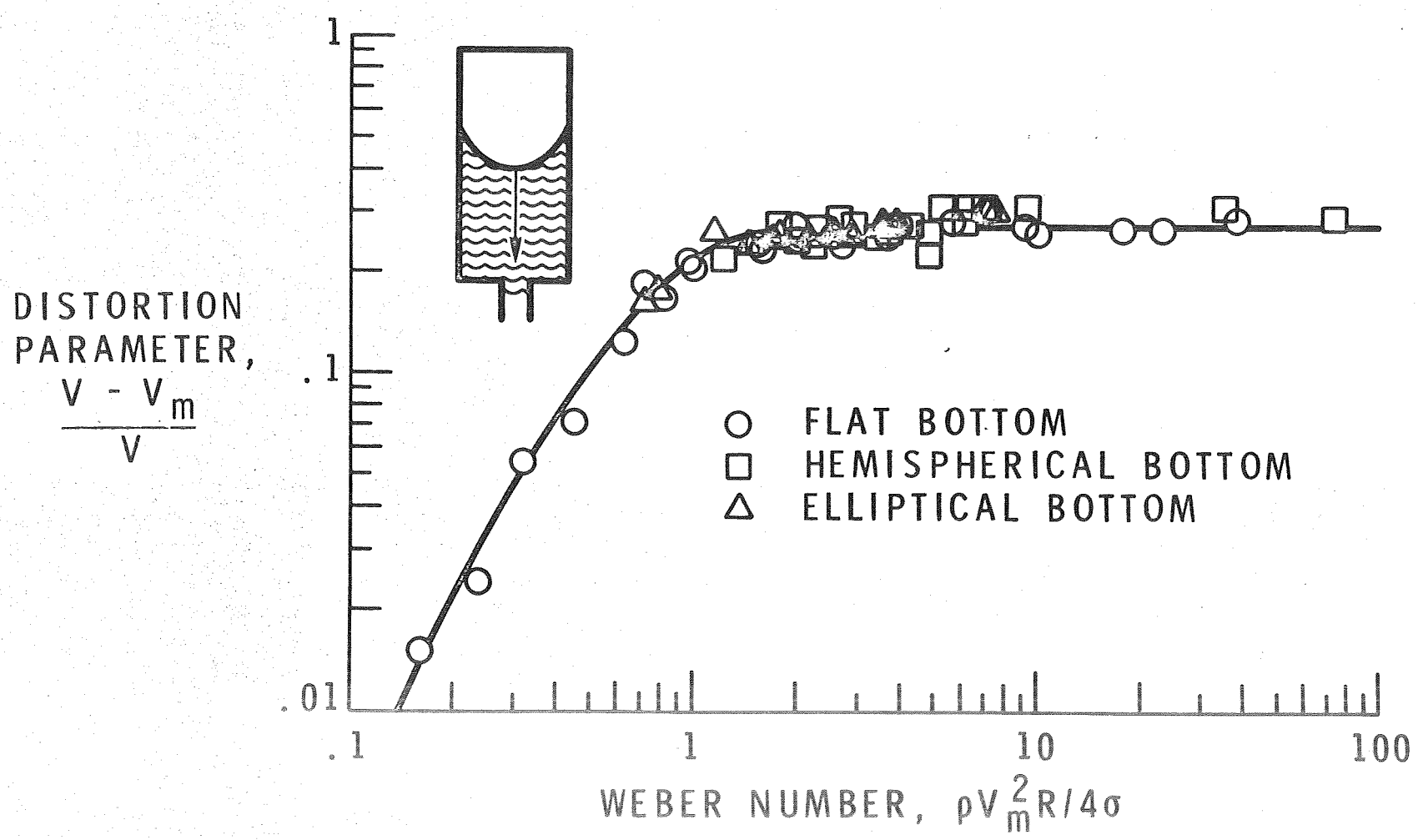

The vapor ingestion phenomena in weightlessness can be described by the use of this figure. During tank draining, there exists a time when the center of the liquid-vapor interface (directly above the tank outlet) is suddenly and rapidly accelerated toward the tank outlet. As previously noted, the liquid-vapor interface in a cylindrical tank is hemispherical prior to tank draining. During draining the interface distorts from this configuration, but the liquid surface at the tank centerline moves at a constant velocity (implying constant distortion) until the incipience of vapor ingestion and then moves rapidly toward the drain. The critical height is defined as the height of liquid above the drain at this time.

VAPOR INGESTION PHENOMENON

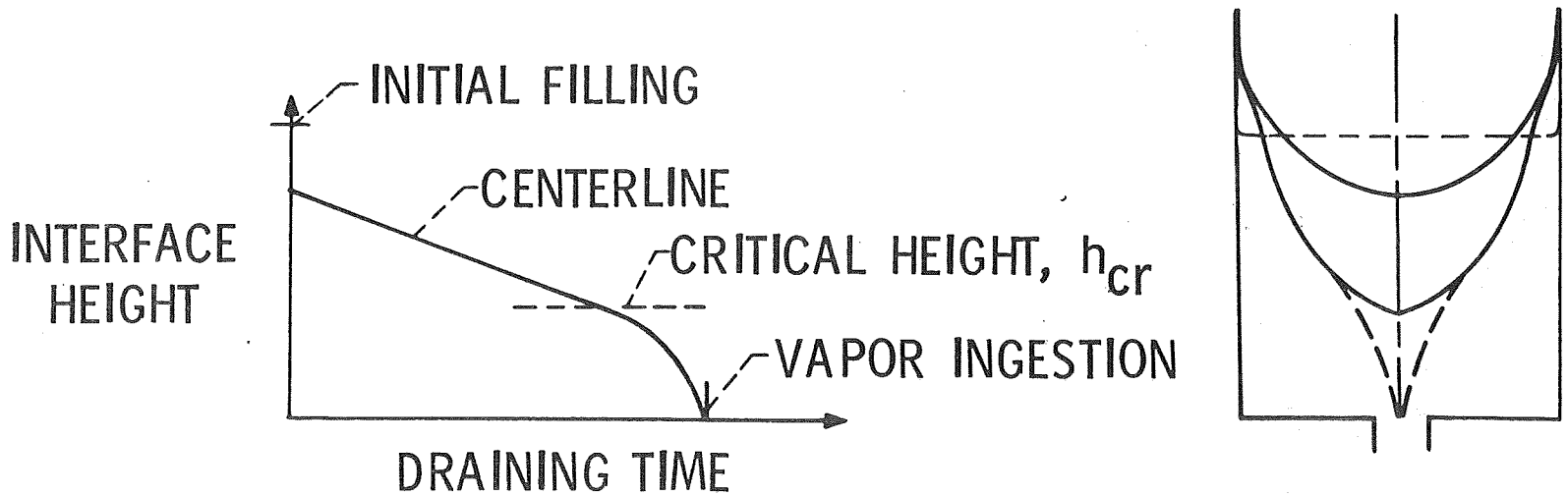

CS-57985

The results of an investigation of the vapor ingestion phenomena in weightlessness are shown in this figure. The ratio of critical height to tank radius is plotted against an outflow Weber number. The correlation shows that the critical height increases with the outflow Weber number according to the empirical equation shown. No variation with initial filling was found.

PREDICTION OF INCIPIENCE OF VAPOR INGESTION IN WEIGHTLESSNESS BY OUTFLOW WEBER NUMBER

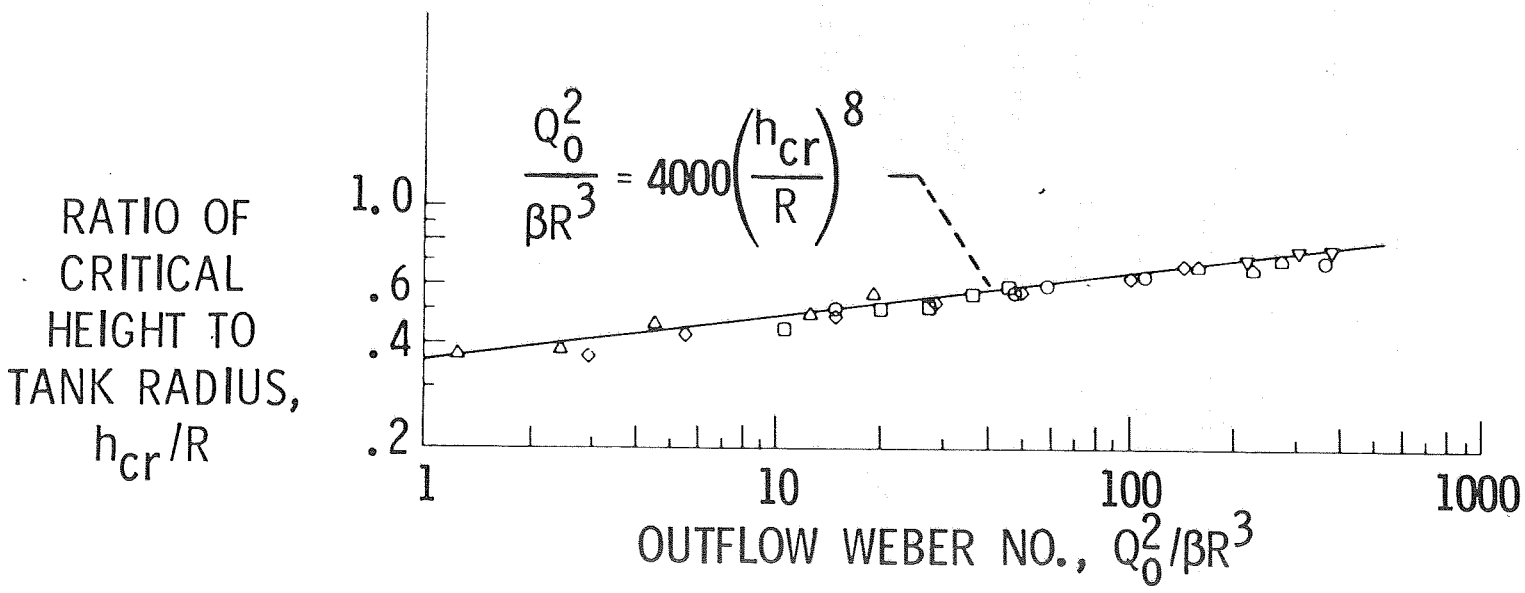

CS-57989

From the data obtained in the vapor ingestion study, it is possible to predict liquid residuals. Values of liquid residuals were determined by using the draining time to vapor ingestion and the outflow rate. This volume was subtracted from the initial liquid volume to give liquid residuals. The results of these calculations are shown in this figure as residual fractions versus outflow Weber number. The residual fraction is defined as the residual liquid volume divided by the initial liquid volume. Results show that the residual fraction increases with increasing Weber number over a narrow range. Above a Weber number of about 25, the residual fraction levels off at a maximum value of about .70. This leveling off is primarily due to the interface distortion during draining; just as the distortion parameter leveled off so did the residual fraction.

RESIDUAL FRACTION WEIGHTLESSNESS

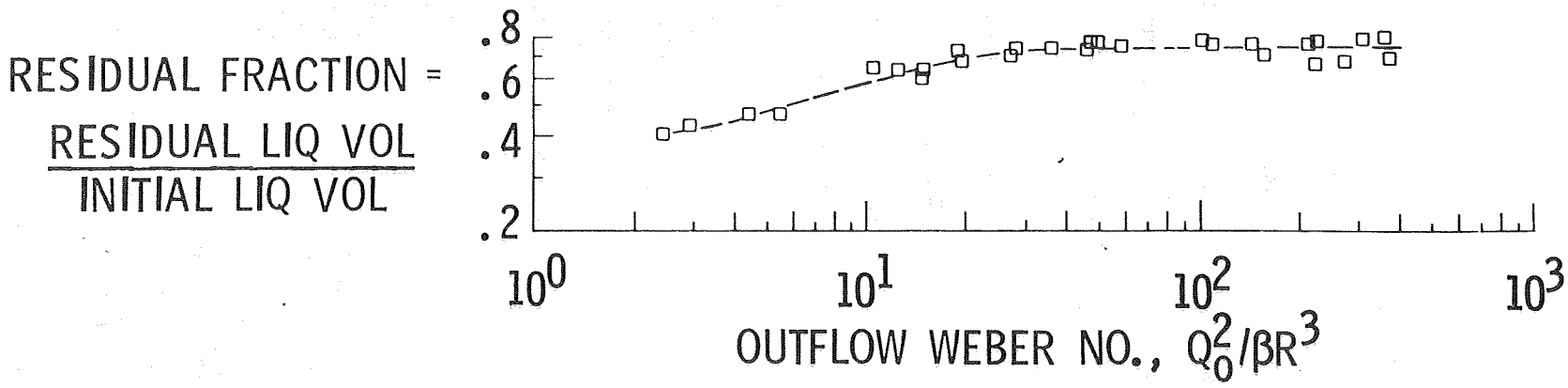

CS-57988

CONCLUSIONS

The results of these zero gravity studies of draining from cylindrical tanks having flat ends can be summarized as follows:

1. Direct impingement of the pressurant gas on the liquid vapor interface increases the distortion of the interface. This problem was alleviated in part by placing a disc shaped baffle over the pressurant gas inlet. This baffle was employed in obtaining all the outflow data presented in this paper.

2. The liquid vapor interface distorts as a result of the draining process. The magnitude of the distortion was found to be Weber number dependent, increasing with Weber number over a narrow range and then achieving a constant value.

3. Critical height at the incipience of vapor ingestion was found to be a function of outflow Weber number. As the Weber number increased, so did the critical height. The resulting empirical equation is:

$$\frac{Q_o^2}{gR^3} = 4000 \left(\frac{h_{cr}}{R}\right)^8$$

4. Liquid residual were found to increase with outflow Weber number over a narrow range, reaching a constant of 70% as the Weber number exceeds 25.

THIS PAGE INTENTIONALLY LEFT BLANK

PRECEDING PAGE BLANK NOT FILMED

LIQUID INFLOW

A sketch showing the inflow phenomena is presented in this figure. In a tank initially void of liquid at the initiation of inflow, both stable and unstable filling can occur, depending on inflow velocity. If the inflow velocity is low enough, the incoming liquid jet is stabilized by the action of surface tension and the liquid tends to puddle or collect over the inlet as shown, resulting in stable inflow. Above a certain inflow velocity, termed the critical inflow velocity, the incoming liquid jet forms a geyser which moves across the tank and impinges on the tank vent, resulting in unstable inflow.

For tanks containing a quantity of liquid at the initiation of inflow, a similar situation occurs. The main difference between the two cases, that of an initially empty tank and one which contains some liquid at the initiation of inflow, is that the incoming liquid jet tends to diffuse or spread in passing through the liquid in the partially full tank. As a result, the formed geyser is wider than in an empty tank and higher values of critical inflow velocity are obtained.

LIQUID INFLOW

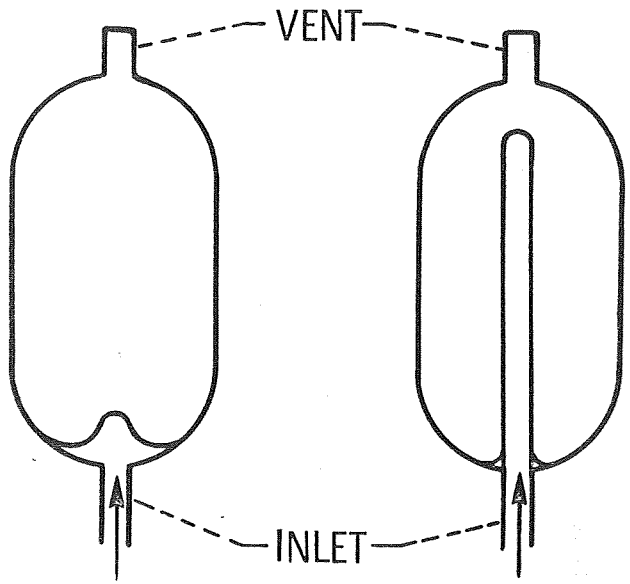

STABLE UNSTABLE

INITIAL CONDITION - EMPTY TANK

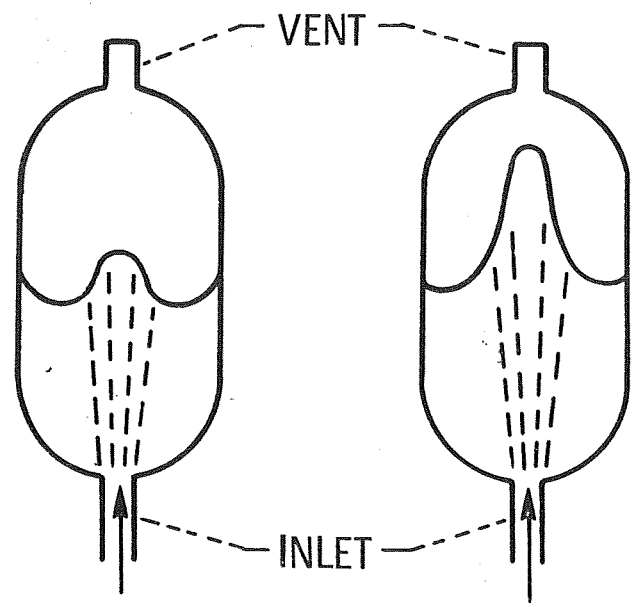

STABLE UNSTABLE

INITIAL CONDITION - PARTIALLY FULL TANK

CS-57987

A form of the Weber number should delineate between stable and unstable interface behavior. A simple energy balance results in the various forms of the Weber number shown in this figure. $V_{i,av}$ is the average inflow velocity at the inlet line exit, β is the specific surface tension, R_i is the inlet radius and R_j the radius of the incoming liquid jet at the liquid vapor interface. R_j is identical to R_i for the case in which the tank is initially void of liquid and, thus, all forms are equivalent except for the constant. This constant is a function of the velocity profile of the incoming liquid in the inlet as shown and may have a value of 1/2 to 2/3 dependent on profile shape. Unfortunately, these forms necessitate a knowledge of the incoming jet radius at the liquid vapor interface for the tanks partially full at the initiation of inflow. The jet radius (R_j) is a function of the angle of spread and is dependent on initial profile shape as well as jet Reynolds number. For jet Reynolds numbers greater than about 1500 and uniform velocity profiles, the jet has been experimentally determined to spread at about 7° for approximately 6 inlet diameters and then at about 11°. For Reynolds numbers between about 500 and 2000 and initially parabolic velocity profiles, a constant spread angle of 3° was found. Since larger angles of spread yield larger values of R_j and, hence, larger values of the critical inflow velocity, it should be expected that optimum inflow to unbaffled cylindrical tanks would occur when the inlet line shape was configured so as to impart a uniform velocity profile to the incoming jet.

PREDICTED WEBER NUMBER

INITIALLY EMPTY TANK

UNIFORM VELOCITY PROFILE $WE_{cr} = \dfrac{V_{i_{av}}^2 R_i}{2\beta}$

PARABOLIC VELOCITY PROFILE $WE_{cr} = \dfrac{2V_{i_{av}}^2 R_i}{3\beta}$

PARTIALLY FULL TANK

UNIFORM VELOCITY PROFILE $WE_{cr} = \dfrac{V_{i_{av}}^2 R_i^2}{2\beta R_j}$

PARABOLIC VELOCITY PROFILE $WE_{cr} = \dfrac{2V_{i_{av}}^2 R_i^2}{3\beta R_j}$

CS-57983

The first study conducted to study liquid inflow to hemispherical ended cylinders initially void of liquid yielded the results shown in this figure. Average inflow velocity, $V_{i,av}$, is plotted against the ratio of specific surface tension β, to inlet line radius, R_i. The straight line shown delineates between a region of stable and a region of unstable interface behavior and indicates a Weber number correlation exists. Since the velocity profile shape of the incoming jet was not precisely known, a coefficient midway between the two extremes of 2/3 and 1/2 was chosen. With the value of 7/12 thus chosen, the magnitude of the critical Weber number is 1.5.

STABILITY OF LIQUID VAPOR INTERFACE DELINEATED BY WEBER NUMBER

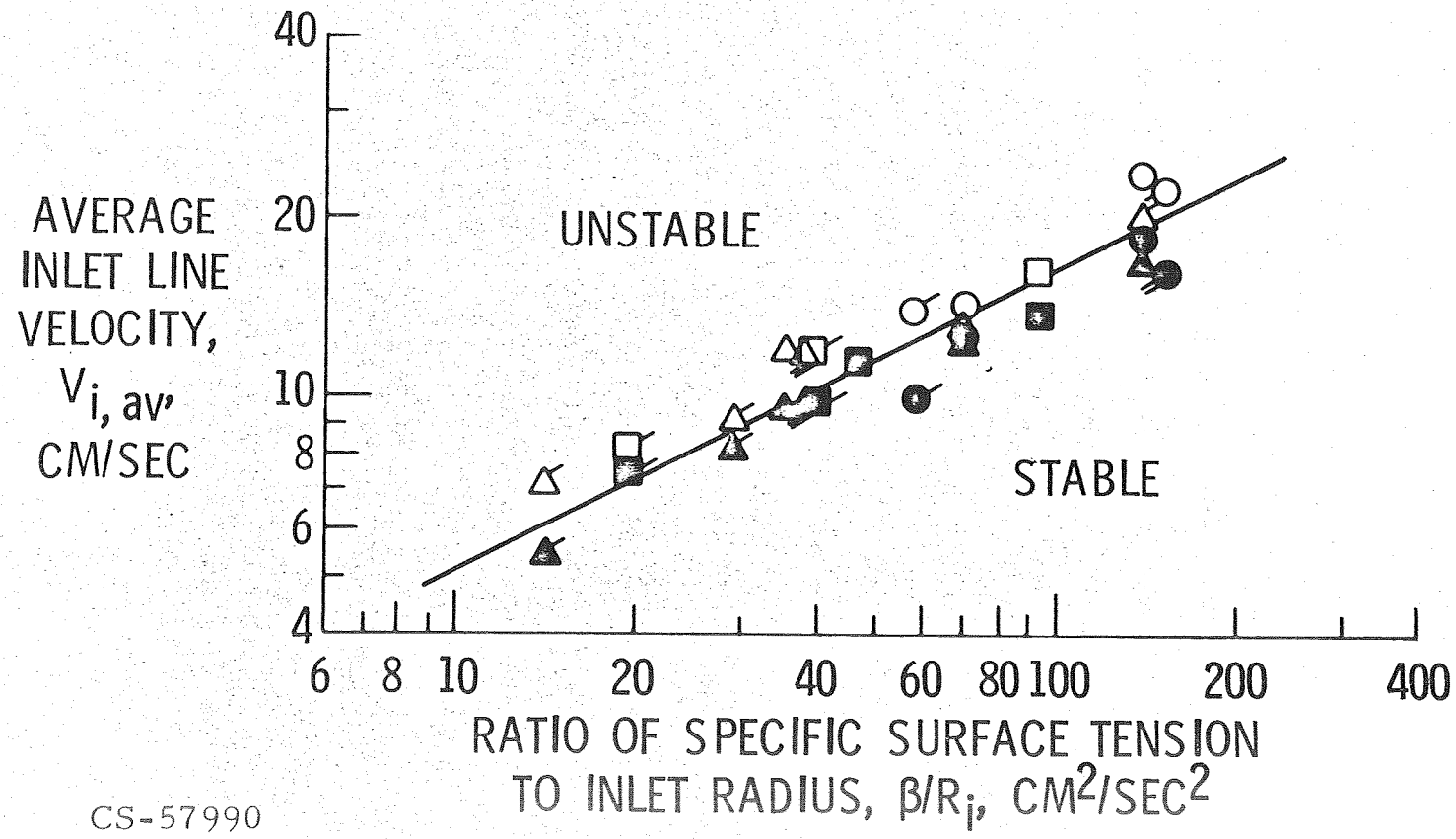

CS-57990

The logical extension of that study was an investigation of inflow to a hemispherical ended cylinder partially full of liquid at the initiation of inflow. The effect of both initial liquid height and velocity profile in the inlet on the critical inflow velocity is shown in this figure. Average inflow velocity ($V_{i,av}$) is plotted versus dimensionless distance from the inlet (H_i/D_i). H_i is the height of liquid above the inlet at the initiation of inflow and D_i is the diameter of the inlet line. The solid line shown delineates between regions of unstable and stable interface behavior for a tank having an inlet configuration which provided the incoming liquid jet with a velocity profile which was neither fully parabolic nor uniform. The actual data points shown were obtained for the same tank and test liquid but with an inlet configured so as to provide the incoming jet with a uniform velocity profile. Note that for any value of H_i/D_i, the critical inflow velocity is higher for the latter tests. This effectively illustrates the advantage of designing an inlet so as to provide the incoming liquid jet with a uniform velocity profile.

EFFECT OF INITIAL VELOCITY PROFILE ON CRITICAL INFLOW VELOCITY

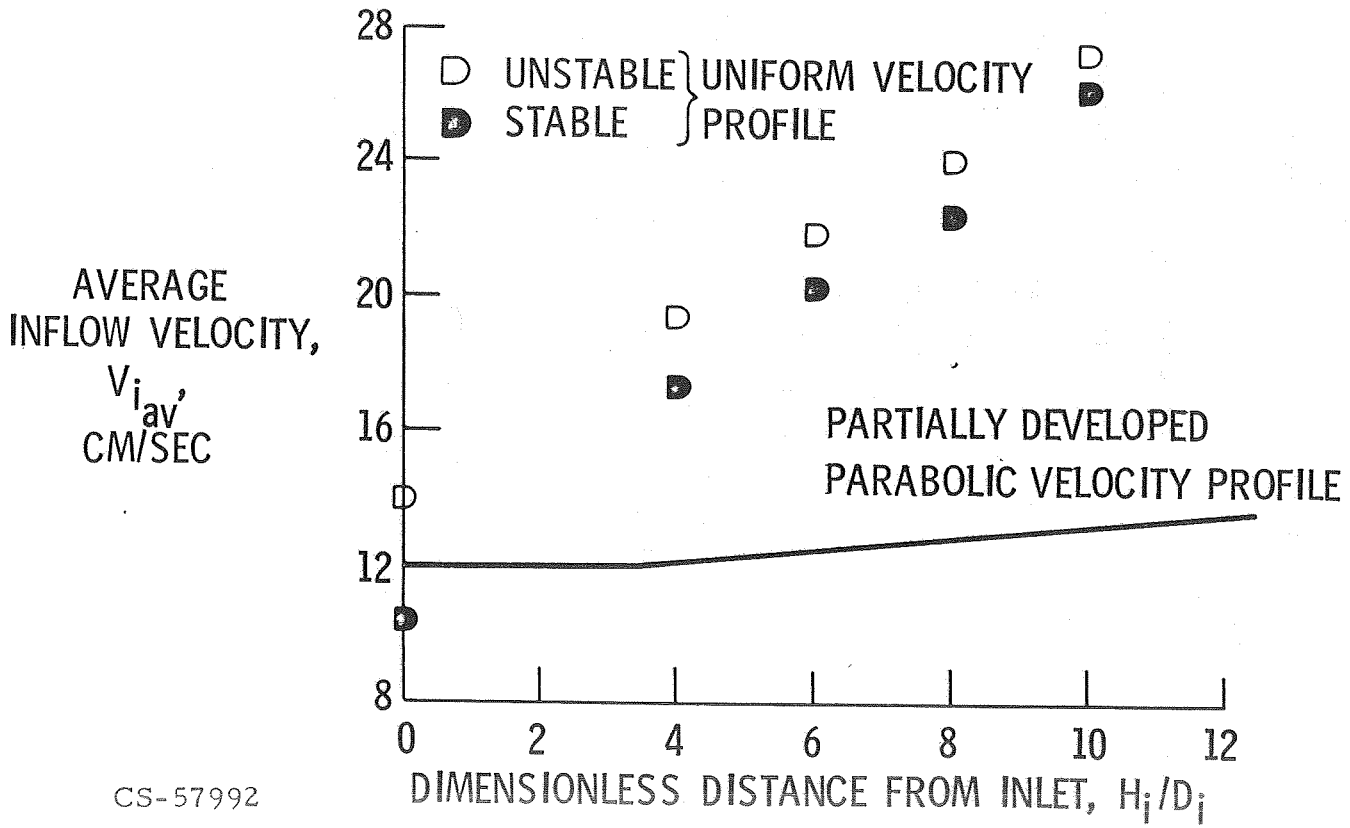

CS-57992

It is possible to compare the results obtained for the uniform profile with known experimental results if the Weber number correlation is assumed. Weber number is plotted against dimensionless distance from the inlet as shown in this figure and the solid line shown delineates between stable and unstable interface behavior. The plotted Weber number differs from the expected critical Weber number only by a radius ratio R_i/R_j. It is thus possible to calculate values of R_i/R_j required to make the magnitude of the critical Weber number 1.5. Knowing R_j versus H_i/D_i, the angle of spread for the group of data can be determined. The angles thus determined are 7° and 11° agreeing with experiment values previously cited. The validity of the critical Weber number developed earlier in this paper is, therefore, supported. However, it should be emphasized that the plotted data does not conclusively prove that the critical Weber number is the correlating parameter for inflow to partially full tanks since tank and inlet size were not varied in this study. More studies are required in which these parameters are varied. However, should the critical Weber number be proven valid by a parametric study, it would be extremely valuable in predicting critical inflow velocities as the tank fills and could be used to compute a throttling technique for inflow to unbaffled hemispherical ended cylinders.

WEBER NUMBER AS FUNCTION OF DIMENSIONLESS DISTANCE FROM INLET

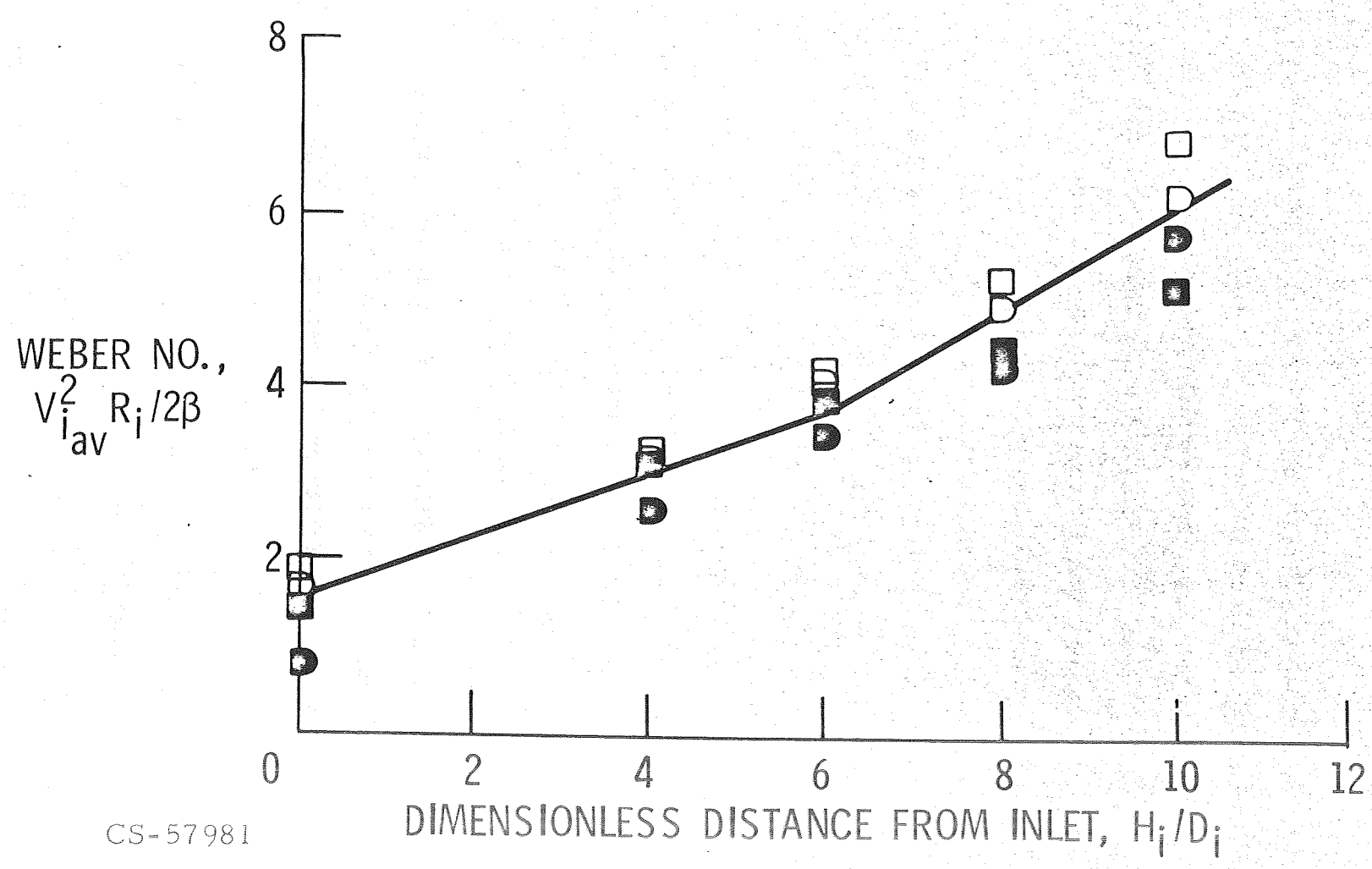

CS-57981

CONCLUSIONS

The results of zero-gravity studies of liquid inflow to unbaffled cylindrical tanks having hemispherical ends may be summarized as follows:

1. Both stable and unstable interface behavior exist. The stable interface is characterized by a small liquid geyser which either remains at the same height or decreases in height with respect to the lowest point on the liquid vapor interface during inflow. The unstable interface is characterized by a geyser which continues to grow in height with respect to the lowest point of the liquid vapor interface.

2. A critical Weber number based on inlet line radius and average inflow velocity delineates between a region of stable and unstable interface behavior for a tank void of liquid at the initiation of inflow. The magnitude of the critical Weber number is approximately 1.5.

3. Velocity profile shape of the incoming liquid jet is important in inflow. An incoming liquid jet with a uniform velocity profile permits the highest critical inflow velocity for either empty or partially full tanks.

4. A critical Weber number based on inlet line radius, average inflow velocity, and liquid jet radius at the liquid vapor interface may be useful in predicting critical inflow velocity to partially full tanks.

BIBLIOGRAPHY

Liquid Outflow

1. Nussle, Ralph C.; Derdul, Joseph D.; and Petrash, Donald A.: Photographic Study of Propellant Outflow from a Cylindrical Tank During Weightlessness. NASA TN D-2572, 1965.

2. Derdul, Joseph D., Grubb, Lynn S.; and Petrash, Donald A.: Experimental Investigation of Liquid Outflow from Cylindrical Tanks During Weightlessness. NASA TN D-3746, 1966.

3. Abdalla, Kaleel L., and Berenyi, Steven, G.: Vapor Ingestion Phenomenon in Weightlessness. NASA TN D-5210, 1969.

4. Berenyi, Steven G., Abdalla, Kaleel L.: Vapor Ingestion Phenomenon in Hemispherically Bottomed Tanks in Normal Gravity and in Weightlessness. NASA TN D-5704, 1970.

5. Berenyi, Steven G.: Effect of Outlet Baffling on Liquid Residuals for Outflow From Cylinders in Weightlessness. NASA TM X-2018, 1970.

6. Berenyi, Steven G.: Effect of Pressurant Inlet Configuration on Liquid Outflow in Weightlessness. NASA TM X-2108, 1970.

Liquid Inflow

1. Symons, Eugene P.; Nussle, Ralph C., and Abdalla, Kaleel L.: Liquid Inflow to Initially Empty Hemispherical Ended Cylinders During Weightlessness. NASA TN D-4628, 1968.

2. Symons, Eugene P.; Nussle, Ralph C.: Observations of Interface Behavior During Inflow to Elliptical Ended Cylinder in Weightlessness. NASA TM X-1719, 1969.

3. Symons, Eugene P.: Liquid Inflow to Partially Full, Hemispherical Ended Cylinders During Weightlessness. NASA TM X-1934, 1969.

4. Symons, Eugene P.: Interface Stability During Liquid Inflow to Initially Empty Hemispherical Ended Cylinders in Weightlessness. NASA TM X-2003, 1970.

THIS PAGE INTENTIONALLY LEFT BLANK

N71-29614

PRECEDING PAGE BLANK NOT FILMED

"RECENT DEVELOPMENTS IN HIGH PERFORMANCE INSULATION PURGE SYSTEMS FOR SHUTTLE APPLICATION"

G. FREDRICKSON

D. KRAUSE

P. KLEVATT

J. NAVICKAS

McDONNELL DOUGLAS

TECHNICAL MANAGER

J. STUCKEY

MARSHALL SPACE FLIGHT CENTER

THIS PAGE INTENTIONALLY LEFT BLANK

PRECEDING PAGE BLANK NOT FILMED

RECENT DEVELOPMENTS IN HIGH PERFORMANCE INSULATION PURGE SYSTEMS FOR SHUTTLE APPLICATION

G. Fredrickson
D. Krause
P. Klevatt
J. Navickas

McDonnell Douglas Astronautics Corporation

April 1971

THIS PAGE INTENTIONALLY LEFT BLANK

PRECEDING PAGE BLANK NOT FILMED

INTRODUCTION

This paper, "Recent Developments in High Performance Insulation Purge Systems for shuttle Applications," represents the contributions of the following McDonnell Douglas Astronautics personnel: G. Fredrickson, D. Krause, P. Klevatt, and J. Navickas. The material presented shows some of the results of two MDAC contracts with the Marshall Space Flight Center, as well as other current MDAC studies. Material reported by others is also discussed.

The scope of the paper covers the multi-layer insulation (MLI) required on the Orbital Maneuvering Propulsion System Tankage of the Earth Orbiting Shuttle Craft. Specifically, the paper discusses the required protection of this insulation during the atmospheric flight phases of the vehicle mission.

THIS PAGE INTENTIONALLY LEFT BLANK

EOS CRYOGENIC TANKS WHICH REQUIRE MLI

The figure shows one of the latest typical high cross-range EOS configurations. The two tanks of interest are the secondary hydrogen tank, located directly beneath the crew compartment, and the secondary oxygen tank mounted directly forward of the main engines. These tanks are typically quite large. For example, their volume might be compared with a 17-foot diameter sphere, hydrogen, and an 8-foot diameter sphere, oxygen. Both tanks require MLI mounted on them in order to achieve adequate propellant storability. The other tanks shown, boost and cruise, are of no concern here since they do not require multi-layer insulation.

Note the unusual configuration of the hydrogen tank. Due to packaging requirements, it has neither the usual cylindrical form nor the common spherical form. It is recognized that the configuration will go through many iterations before final design is selected. But, it should be noted that tank configuration can have an important impact on the MLI installation method and the approach taken to protect it during in-atmosphere flight. For example, attempting to make a tank with this shape into a double wall dewar would be clearly impractical.

20397

TYPICAL EOS ORBITER CONFIGURATION

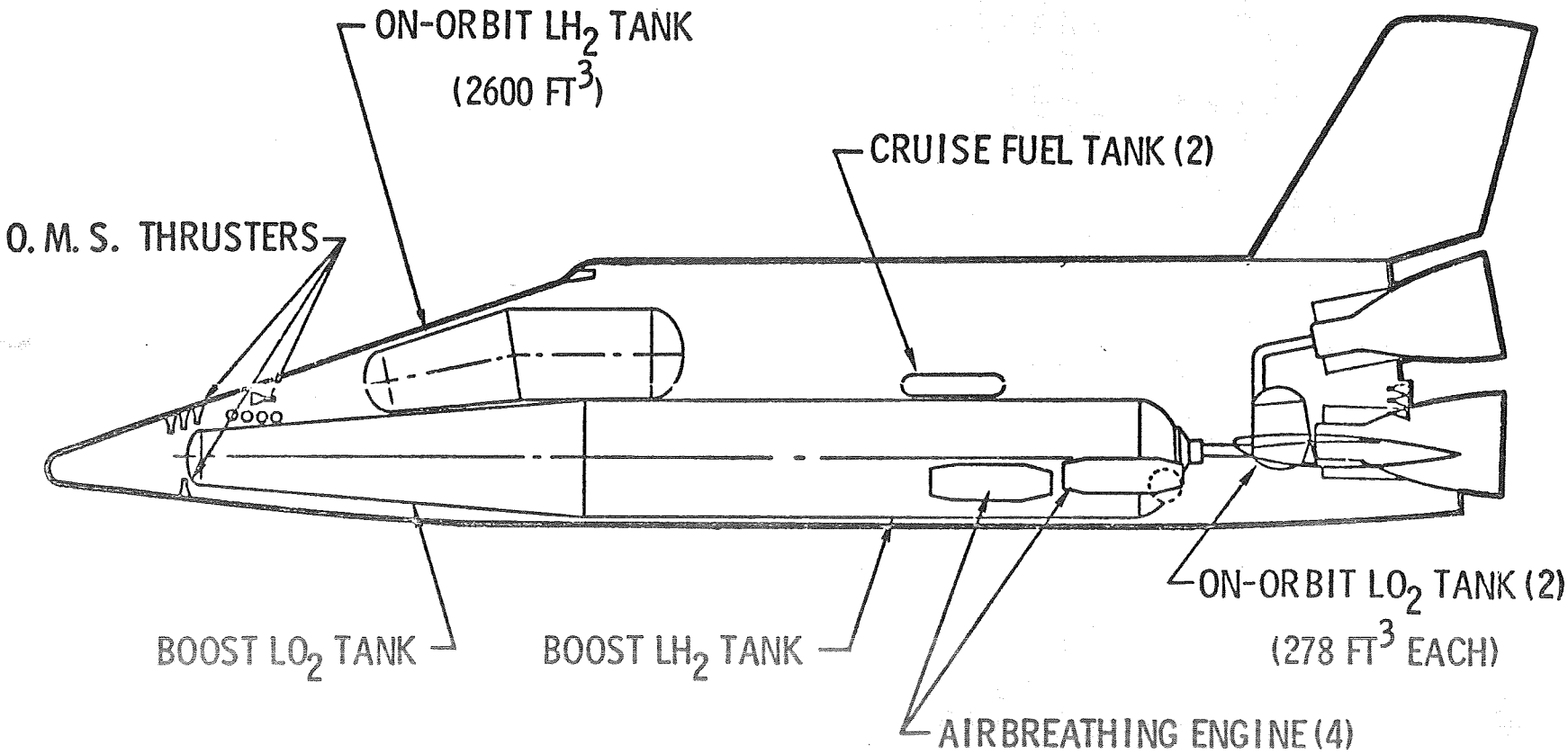

IN-ATMOSPHERE MLI PROTECTION APPROACHES

Protection of the MLI is required during the in-atmosphere phases of the flight. Specifically, atmospheric constituents such as water vapor and oxygen must be prevented from condensing within the insulation layers. As shown in the figure, there are three alternate systems which can be considered for providing this protection: the vacuum jacket; gaseous purge; and self-evacuating. The vacuum jacket is a hard shell mounted over the MLI which is evacuated on the ground and throughout all portions of the flight. The gaseous purge concept provides protection by introducing a non-condensible gas such as helium, or with proper design, nitrogen within the multi-layer sheets. This gas is evacuated in space. The self-evacuating concept typically utilizes a gas (such as carbon dioxide) filled bag containing the MLI. Upon tank cooling, the gas solidifies providing a vacuum in the bag.

Each of these alternatives, at present, requires development. The vacuum jacket requires a light-weight, reliable non-leaking outer shell with low thermal shorts. The gas distribution, evacuating methodology and hardware are the major areas requiring development in the gaseous purge. The flexible non-leak vacuum bag is seen as the major obstacle to developing a self-evacuating system.

30

20398

IN ATMOSPHERE MLI PROTECTION APPROACHES

SYSTEM ALTERNATIVES	MAJOR DEVELOPMENT AREA
VACUUM JACKET	OUTER SHELL: LIGHT, LEAKTIGHT, LOW THERMAL SHORTS
GASEOUS PURGE	GAS DISTRIBUTION AND EVACUATION
SELF EVACUATING	FLEXIBLE VACUUM BAG

TRADEOFF ANALYSES OF COMPETING APPROACHES

To provide a foundation for selecting which system should be emphasized in new development work, weight tradeoff studies have been underway within MDAC, NASA and industry. The figure shows a sketch of the insulation configurations used for one of the MDAC studies. Shown is the vacuum jacket with its hard shell and multi-layer insulation mounted between it and the tank. The other two configurations are gaseous purge approaches. One is simply multi-layer insulation on the tank. This requires an all-helium purge on the hydrogen tank. The other configuration is MLI with a substrate, typically a foam which is mounted either inside or outside the tank wall. The substrate allows the use of a nitrogen purge during pre-launch ground hold on the hydrogen tank because the foam raises the temperature of the inner-most sheet of insulation above the liquifaction point of nitrogen during this period. However, both configurations require the use of a helium repressurization system upon reentry as the outer surface of the foam would be close to the tank propellant temperature. On the hydrogen tank, this is below the liquifaction temperature of nitrogen. A non-substrate configuration is suitable with a nitrogen purge on the oxygen tank since the liquifaction temperature of nitrogen is below that of oxygen.

20399

CANDIDATE INSULATION CONFIGURATIONS
SYSTEMS TRADEOFF ANALYSES

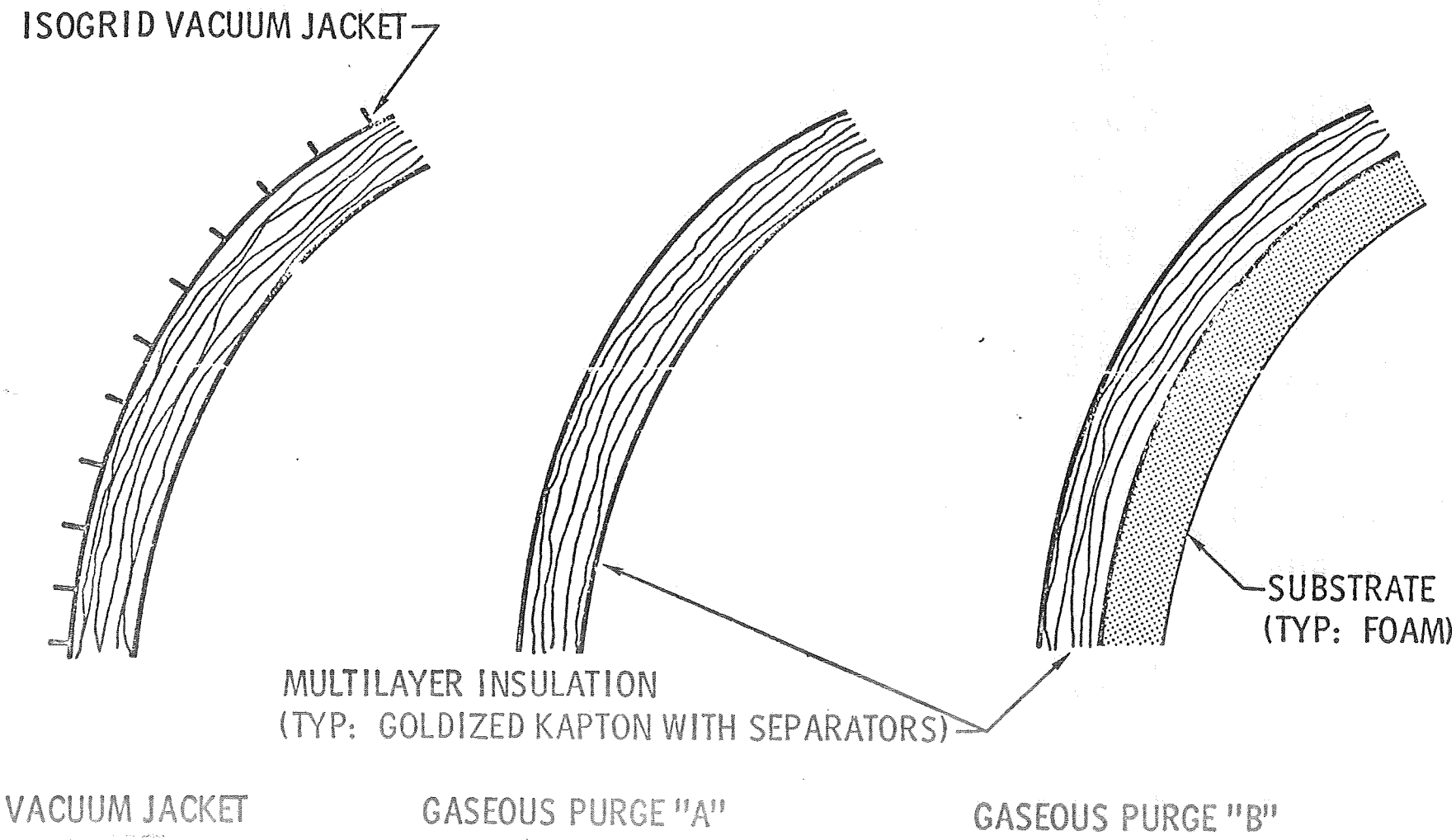

MLI PROTECTION SYSTEM WEIGHT ESTIMATES

The figure shows the resulting weights computed for a low cross-range orbiter configuration. It is recognized that the low cross-range orbiter is no longer a potential approach. However, analyses for a high cross-range vehicle, shown earlier, show the same purge system weight trends except for re-entry. The vacuum jacketed system was not investigated due to the odd configuration of the tank which would clearly make this system impractical.

Note that the purged systems are consistently lighter than their vacuum jacketed counterparts. The structural weight of the vacuum shell was found to be sufficiently large to outweigh its advantages. Therefore, although the analysis must be considered as cursory, it can be concluded that the purged system clearly merits additional investigation at this time.

PURGE AND REPRESSURIZATION SYSTEM DESIGN CONSIDERATIONS

This figure shows the various purge operational phases and associated system design considerations. The first phase is elimination of condensibles from within the insulation prior to tank loading. The important design parameters here are the desired end concentration of condensibles (typically one percent), the purge time, and purge bag leak areas where air can diffuse back into the purge volume. Prefill hold is a period during which other vehicle readiness operations are being conducted. Here the purge volume must be maintained at the low level of condensibles since the back diffusion of air will attempt to increase them. The most critical period is tank fill (chill-down). Here, the gas pressure within the purge volume must be maintained. As the tank is chilled, additional gas must be supplied since the purge gas chills and contracts, reducing pressure. The required makeup flow is influenced by the tank chill rate, bag volume, and tank mass. Post-fill is similar to pre-fill hold where leaks must be made up to maintain the low level of condensibles. There are no purge requirements during launch and orbit. However, during reentry, another critical period is encountered. Here the hydrogen tank purge volume must be repressurized with helium (atmospheric constituents or nitrogen would be condensed). But, it is possible that at some point during reentry the outer surface of the foam substrate would be at a temperature sufficiently high to allow the introduction of nitrogen. The important parameters here, from the design standpoint, are clearly the bag volume, the rate of pressure increase on the bag exterior, and the insulation temperature distribution history.

PURGE AND REPRESSURIZATION SYSTEM DESIGN CONSIDERATIONS

OPERATIONAL PHASE	DESIGN OBJECTIVE	DESIGN PARAMETERS
1 REDUCTION OF CONDENSIBLES	ELIMINATE H_2O & O_2	ρ_F/ρ_i, τ, A_e
2 PREFILL HOLD	LEAKAGE MAKEUP	ρ_F/ρ_i, A_e
3 TANK CHILLDOWN - FILL	MAINTAIN BAG PRESSURE	m_{H_2}, V_p, M_t
4 POST-FILL HOLD	LEAKAGE MAKEUP	ρ_F/ρ_i, A_e
5 LAUNCH & ORBIT	(NO PURGE REQUIREMENT)	--
6 REENTRY	REPRESSURIZE; He/N_2	T_i, V_p

PURGE GAS MANIFOLD CONCEPTS

This figure shows several concepts for manifolding the purge gas into the insulation as reported by General Dynamics*. Four alternatives are shown. The first shows the insulation covered with a purge bag. The gas is ducted into the bag at one point, the bottom, and taken out at the top. The second configuration shows a perforated purge bag acting as a manifold mounted on the tank. The gas comes into the bag and out through the perforations to percolate through the insulation. The third configuration, an external manifold, has a matrix of gas distribution lines installed over and on the outside of the insulation. Gas is injected through purge pins into the insulation panels. The fourth approach is very similar to the above external manifold concept, except here the matrix of gas distribution lines are mounted underneath the multi-layer insulation within a foam substrate. The gas is injected into the MLI in the same manner as with the external manifold system.

---

* Cryogenic Insulation Development, Second Quarterly Progress Report, Contract NAS 8-26129, General Dynamics, Convair Aerospace Division Report, GDC 584-4-568, 21 December 1970.

PURGE GAS MANIFOLD DESIGN CONCEPTS*

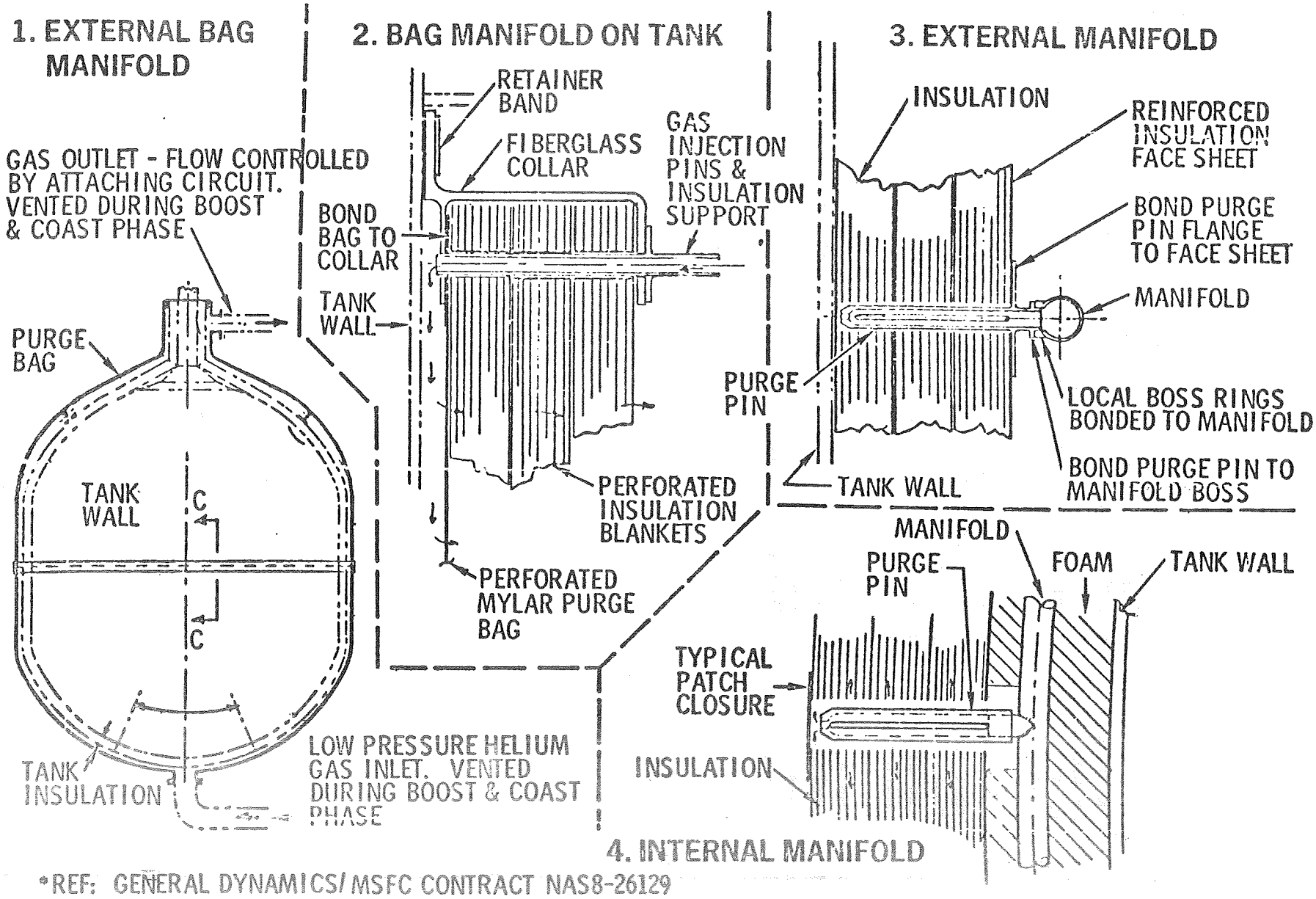

*REF: GENERAL DYNAMICS/MSFC CONTRACT NAS8-26129

INTEGRAL MANIFOLD DESIGN CONCEPT

This figure shows a MDAC concept for manifolding gas into the multi-layer insulation. Shown is an installation adapted to a conical tank support. The purge lines are fiberglas tubes bonded directly into the support sturcture. The concept has the advantage of minimizing conductive heat transfer from the warm exterior into the tank area underneath the insulation. Additionally, existing DC-8 technology can be used in forming the fiberglas tubes. This method allows for design flexibility; inlet and outlet lines can be run side by side as an integral unit if required. The design features low weight and cost.

Some tankage configurations require inlet and outlet lines run side by side such as the conical support shown. Here the dome area insulation is separated from the sidewall by the cone. Purge gas must be introduced into and taken out from the dome area while at the same time gas must be introduced underneath the insulation in the sidewall area.

For a shuttle vehicle, which uses tubular tank supports (some of the recent configurations), the support itself might be used for purge inlets. Should this prove to be undesirable or if additional lines are needed, the bonded fiberglas line method shown here can be used.

20394

MDAC INTEGRAL PURGE MANIFOLD CONCEPT

TYPE

- FIBERGLAS BONDED INTO SUPPORT STRUCTURE

ADVANTAGES

- MINIMUM CONDUCTIVE HEAT TRANSFER
- EXISTING DC-8 TECHNOLOGY
- DESIGN FLEXIBILITY - INLETS & OUTLET LINES SIDE BY SIDE
- LOW WEIGHT
- LOW COST

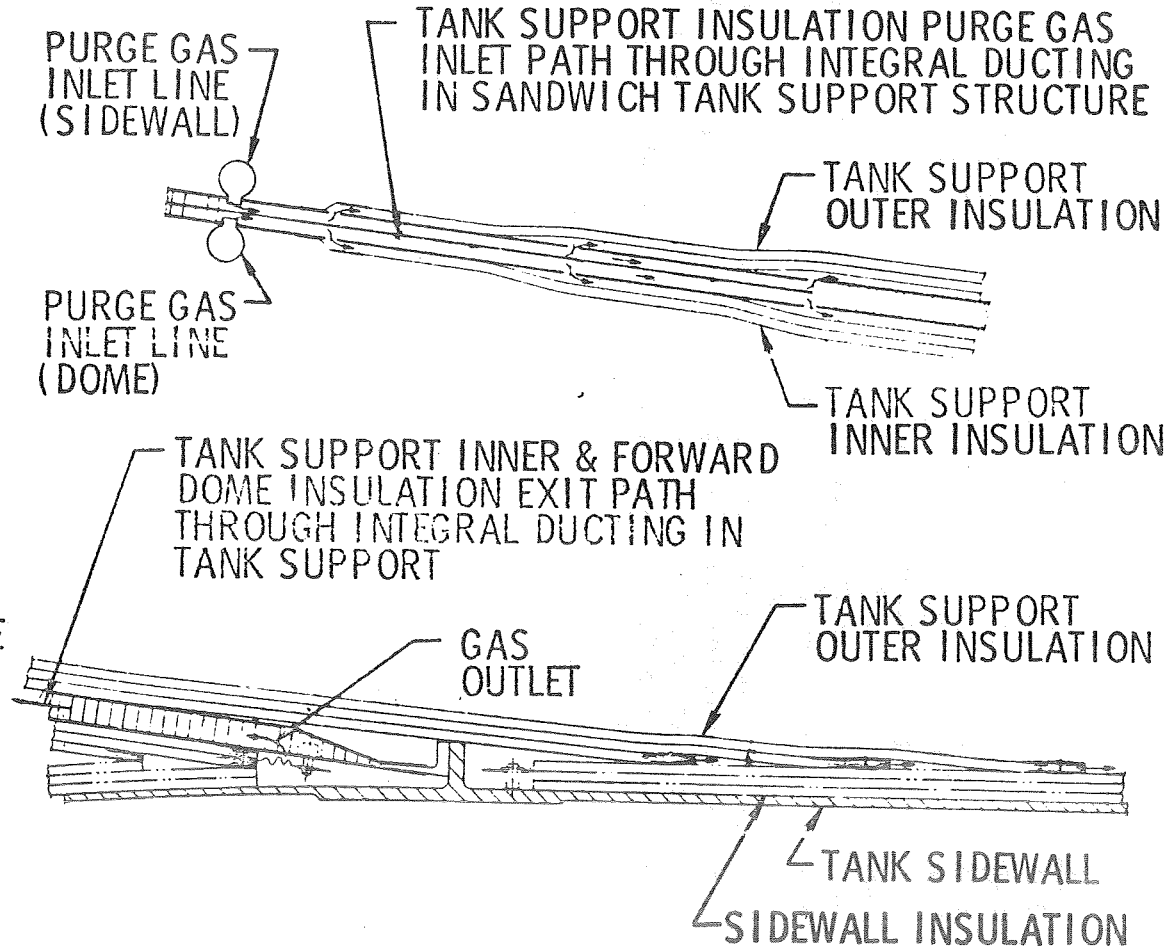

PENETRATIONS

A particularly important and difficult area encountered in purge design is that of penetrations through the insulation, both piping and electrical. The figure shows a conceptual design of insulation applied around a typical pipeline. The insulation is mounted on a fiberglas shell which is attached to the pipe and to the tank. No attempt is made to insulate the pipe directly. This allows for pipe movement which occurs upon tank chilldown due to the thermal contractions. Also, the open volume eliminates the problem of leakage through the line joints and fittings into the insulation, degrading its performance. This open volume as well as the MLI is purged.

The concept eliminates difficulties with attachment of the multi-layer insulation over a complex surface and facilities purging and attachment of the purge bag. This latter item is formed in the shape of a sleeve and clamped to the outer end of the fiberglas insulation support structure.

20395

TYPICAL PIPING PENETRATION

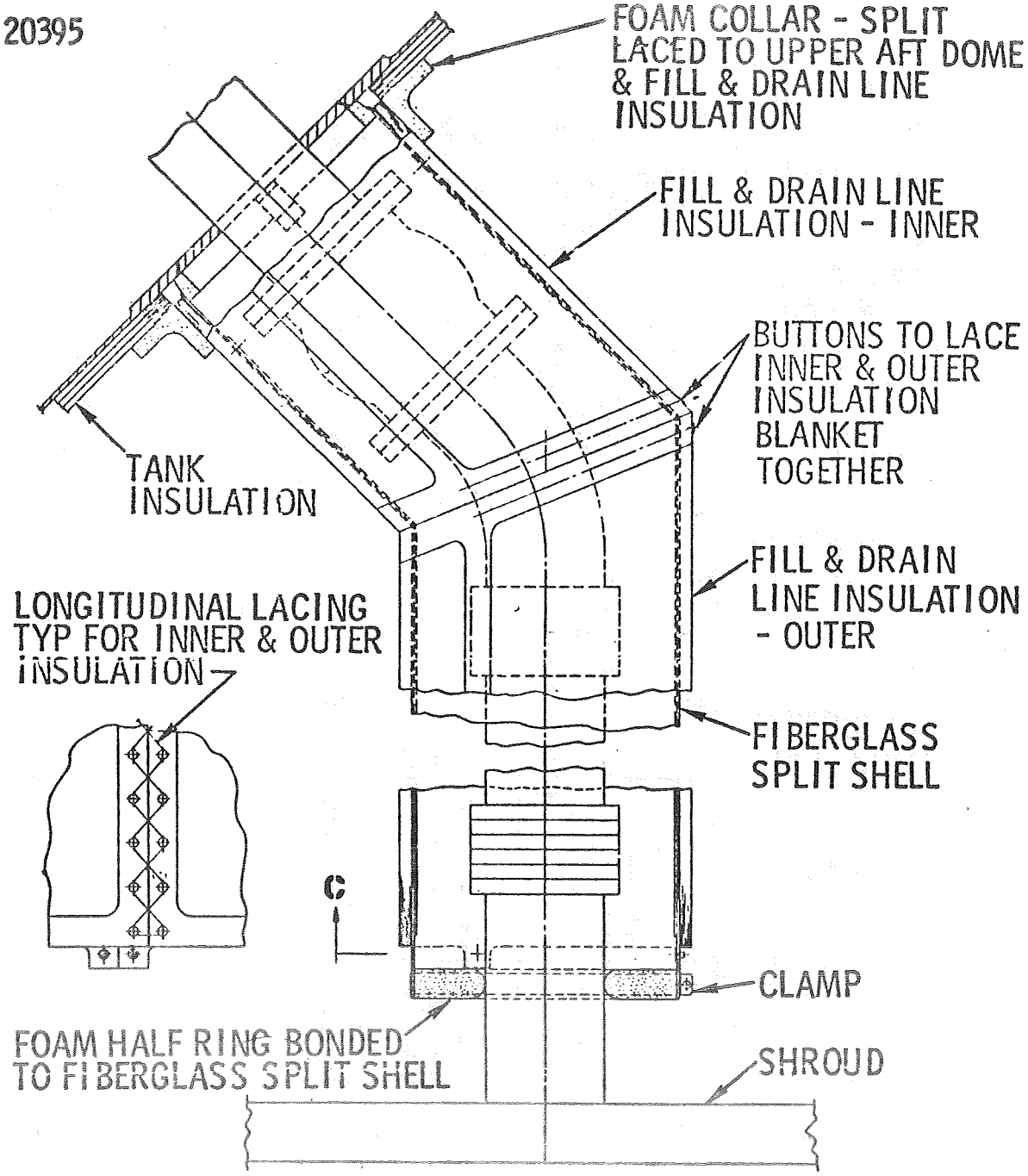

DESIGN FEATURES

- ALLOWS PIPE MOVEMENT
- ELIMINATES LINE LEAKAGE INTO MLI
- FACILITATES MLI ATTACHMENT
- FACILITATES PURGE BAG ATTACHMENT

PURGE GAS EVACUATION CONSIDERATIONS

Up to this point, attention has been given to getting the purge gas into the insulation and getting the condensibles out. However, successful operation of the purged concept requires that the gases entrapped within the insulation be evacuated in as short a time as possible after vehicle launch. Specifically, the interstitial gas pressure must be reduced below approximately 10^{-4} torr before the multi-layer insulation takes on its high performance properties.

Some of the important considerations in design of this evacuation system are shown in the figure. As implied above, the interstitial pressure history is the main design criteria. The protective cover over the insulation (purge bag) should be open during launch but closed during reentry. This is impractical to do; consequently, evacuation valves are required. It may also be necessary to pre-condition the multilayer insulation by running a hot gas through it prior to tank fill. This reduces adhered gases which outgas slowly after launch increasing the pressure within the insulation.

It also appears desirable to perforate the multi-layer insulation (small holes through the reflective layers). These improve gas entrance during repressurization and purging and gas evacuation after launch.

The insulation-to-bag gap appears necessary to ensure adequate evacuation during both the continum and free-molecular flow periods (very low pressure).

CONSIDERATIONS FOR SUCCESSFUL MLI EVACUATION

MLI INTERSTITIAL PRESSURE HISTORY

- PROTECTIVE COVER OPEN AND REENTRY CLOSURE
- EVACUATION PIPING AND VALVE DESIGN
- MLI PRECONDITIONING REQUIREMENTS
- MLI PERFORATION REQUIREMENTS
- INSULATION TO BAG GAP

INSULATION PROTECTION BETWEEN FLIGHTS

In designing the MLI system for protection from the in-atmosphere environmental effects, consideration must also be given to the ground storage or turn-around time period between flights. During this time, it is highly likely that maintenance and refurbishment operations will be undertaken in and around the tankage. This could expose the insulation to the launch site environment for an extended period.

Two protection approaches can be taken. The first, maintaining a desiccant system within the purge bag or an active purge with nitrogen gas. However, this has the disadvantage that the controlled environment is broken when the bag is opened. The second approach is to select an insulation material insensitive to the potential degrading effects of the launch site environment.

The results of a MDAC materials degradation test program are shown in the figure. Here, samples of double goldized kapton and double goldized mylar, both typical insensitive reflector materials, were exposed to a salt-fog environment for 96 hours. This is a very severe test of launch site environment effects. However, it will be noted that no degradation was experienced by the double goldized kapton. The mylar material, on the other hand, showed deterioration. It can be concluded that use of the double goldized kapton should yield an insulation system requiring no special environmental protection during between flight vehicle storage.

MATERIAL DEGRADATION IN LAUNCH SITE MOISTURE ENVIRONMENT

MATERIAL	SALT FOG* 96 HR		
DOUBLE GOLDIZED KAPTON	0%,	0%,	0%
DOUBLE GOLDIZED MYLAR	25%,	10%,	0%

*METAL REMOVAL BY TAPE ADHESION TEST
(3) DIFFERENT SAMPLES

NON DESTRUCTIVE INSPECTION AFTER FLIGHT

For a reusable insulation system, inspection between flights to ensure structural integrity and design thermal performance is a must. A consideration of inspection approaches can be constrained to those of the non-destructive type, preferably one which requires no physical contract or movement of the insulation. Several approaches have been investigated at MDAC. The figure illustrates the most promising concept found; an electromagnetic probe. Shown is a simple setup of an induction coil probe in contact with the multilayer insulation specimen, an approach compatible with a purged configuration. Two-percent corrosion was detected. In addition, compression was detected, a direct measurement of thermal performance. Data repeatability was also obtained. The method has the advantage in that it is usable at random locations anywhere on the MLI installation. A capacitor technique and infrared and microwaves were also studied. A capacitor was found to have limited applicability and the latter two methods were not applicable.

NON-DESTRUCTIVE MLI PREFLIGHT INSPECTION

TEST SET-UP

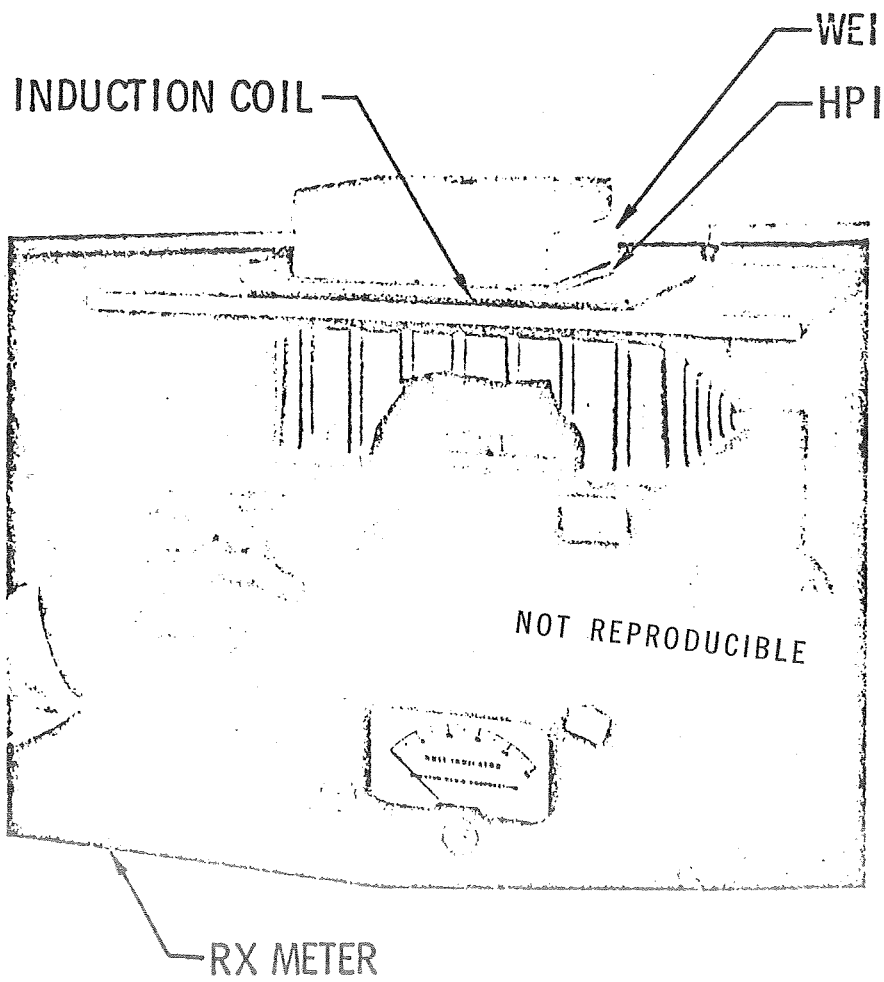

CONCLUSIONS

INDUCTION COIL - PROMISING

- 2% CORROSION DETECTED
- COMPRESSION DETECTED
- OBTAINED DATA REPEATIBILITY
- USEFUL AT RANDOM LOCATIONS

CAPACITOR - VERY LIMITED APPLICABILITY

INFRARED AND MICROWAVE - NOT APPLICABLE

SUMMARY

It can be concluded that protection of the multi-layer insulation is required during the in-atmosphere phases of the shuttle orbiter mission. Three approaches have been suggested: Gaseous purge, self-evacuating and vacuum dewar.

A tradeoff study showed that the purge system merits additional development. Several areas can be identified for this development to evolve a practical working purge-repressurization system:

1. Evacuation and reentry gas distribution requirements and hardware;

2. Preconditioning requirements for the MLI; and,

3. Purge bag material and installation design.

Between flight inspection of the MLI is also mandatory. An electromagnetic probe has been identified as a very promising approach which is compatible with a purged MLI configuration. Additional development is recommended on this item also.

SUMMARY

- MLI ENVIRONMENTAL PROTECTION APPROACHES
  - VACUUM DEWAR
  - GASEOUS PURGE
- TANK SHAPE AFFECTS PROTECTION SYSTEM SELECTION
  - SELF EVACUATING
- GASEOUS PURGE & REPRESS SYSTEM TECHNOLOGY READY FOR FURTHER DEVELOPMENT
- PURGE & REPRESS SYSTEM DEVELOPMENT AREAS
  - EVACUATION/REENTRY REQUIREMENTS AND HARDWARE
  - MLI PRECONDITIONING REQUIREMENTS
  - PURGE BAG MTL AND INSTALLATION DESIGN
- MORE MLI INSPECTION WORK REQUIRED

THIS PAGE INTENTIONALLY LEFT BLANK

PRECEDING PAGE BLANK NOT FILMED

N71-29615

"EFFECT OF ENVIRONMENT ON INSULATION MATERIALS"

R. T. PARMLEY

LOCKHEED

TECHNICAL MANAGER

J. BARBER

LEWIS RESEARCH CENTER

THIS PAGE INTENTIONALLY LEFT BLANK

EFFECT OF ENVIRONMENT
ON
INSULATION MATERIALS

CONTRACT NAS 3-14342

JUNE 1970 - DECEMBER 1971

R. T. PARMLEY

LOCKHEED MISSILES & SPACE COMPANY

J. R. BARBER

NASA/LEWIS PROGRAM MANAGER

PRECEDING PAGE BLANK NOT FILMED

THIS PAGE INTENTIONALLY LEFT BLANK

PRECEDING PAGE BLANK NOT FILMED

PROGRAM SUMMARY

In this program, 20 candidate high performance insulation materials are being subjected to eight conditions that represent possible operational environments. These exposures include ground contaminants, various operational temperatures, space vacuum, space-vented propellants, and tank leakage. The objective of this program is to obtain and evaluate the data from these exposures in order to provide both a quantitative and qualitative description of the degradation to certain physical and thermal properties, and from this, to obtain a better understanding of the environmental effects on the insulation performance.

To satisfy these objectives, Lockheed is conducting an extensive test program on six multilayer radiation shield materials, four multilayer spacer materials, four ground hold insulation materials and six miscellaneous insulation materials. Up to 7318 data points will be obtained, reduced and tabulated in handbook form (up to 1200 property data plots and extensive data tables).

IDENTIFICATION OF RADIATION SHIELD MATERIALS

Test Material		Test Material Source	Applicable Purchase Spec.
Film Coating	No. of Sides Coated		
Mylar-Aluminum	1	National Metallizing Div., Standard Packaging Corp., Cranbury, N.J. 08512	LAC 22-4402
Mylar-Aluminum	2		LAC 22-4402
Kapton-Aluminum	1		LAC 22-4413
Mylar-Gold	1		LAC 22-4402 + Addendum A
Mylar-Gold	2		LAC 22-4402 + Addendum A
Kapton-Gold	1		LAC-4413 + Addendum A

MULTILAYER INSULATION RADIATION SHIELD MATERIALS

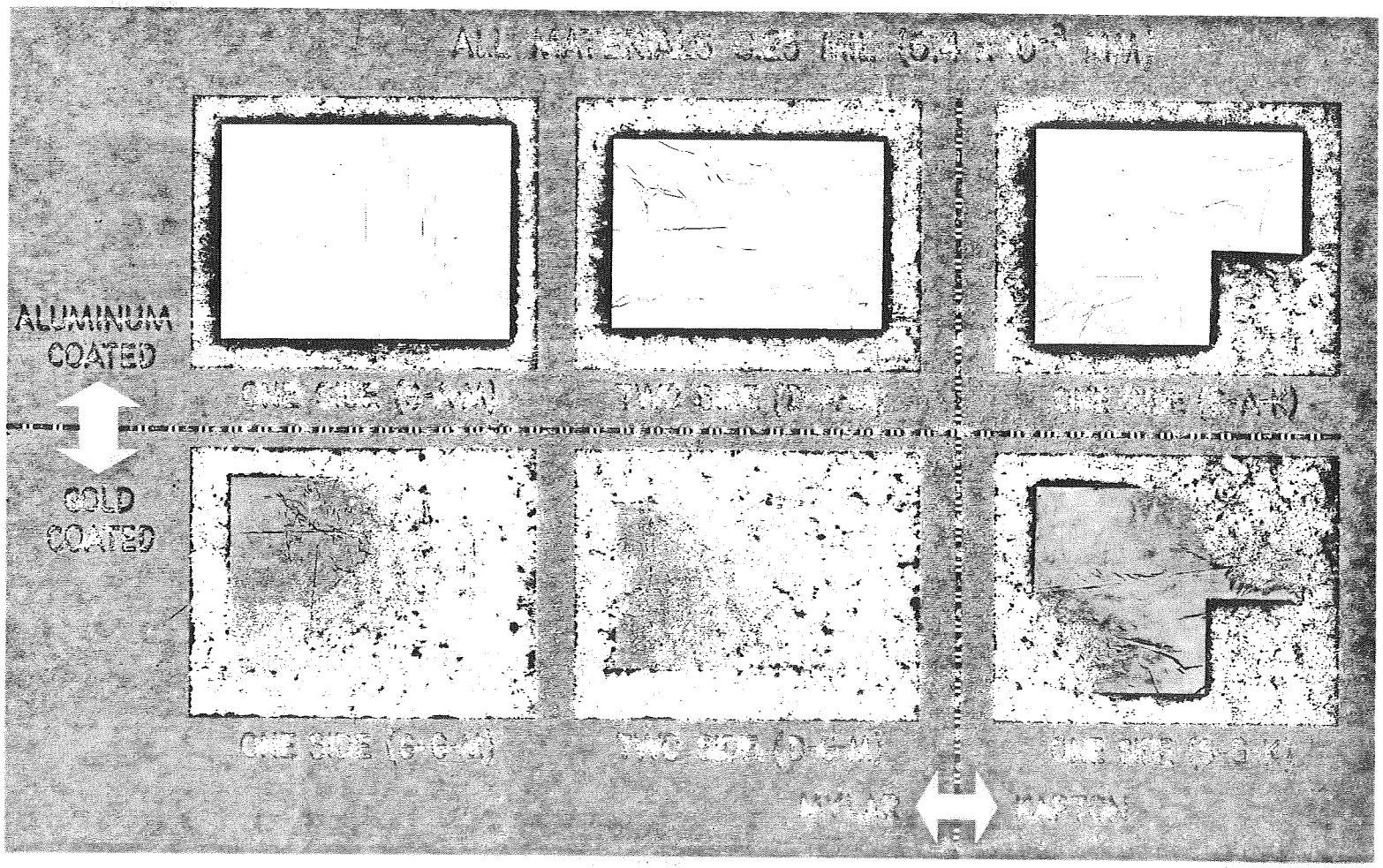

NOT REPRODUCIBLE

IDENTIFICATION OF INSULATION SPACER MATERIALS

Test Material	Test Material Source	Applicable Purchase Spec.	Nominal Thickness mils (mm)
Silk Net "Illusion Silk Net," approx. 1/16 in. Hexagonal Mesh	John Heathcoat Co., New York, New York	None	5 (0.13)
Nylon Net 1/16 × 3/32 in. Hexagonal Mesh	Sears Roebuck & Co.	None	9 (0.23)
Tissuglas Style 60G	Pallflex Products Co.	LAC 26-4382	0.6 (1.52×10^{-2})
Dacron Net (.0024 lb/ft^2) B/2A, 198 meshes/in.^{2}	Apex Mills 49 W. 37th Street New York, New York	None	6.7 (0.12)

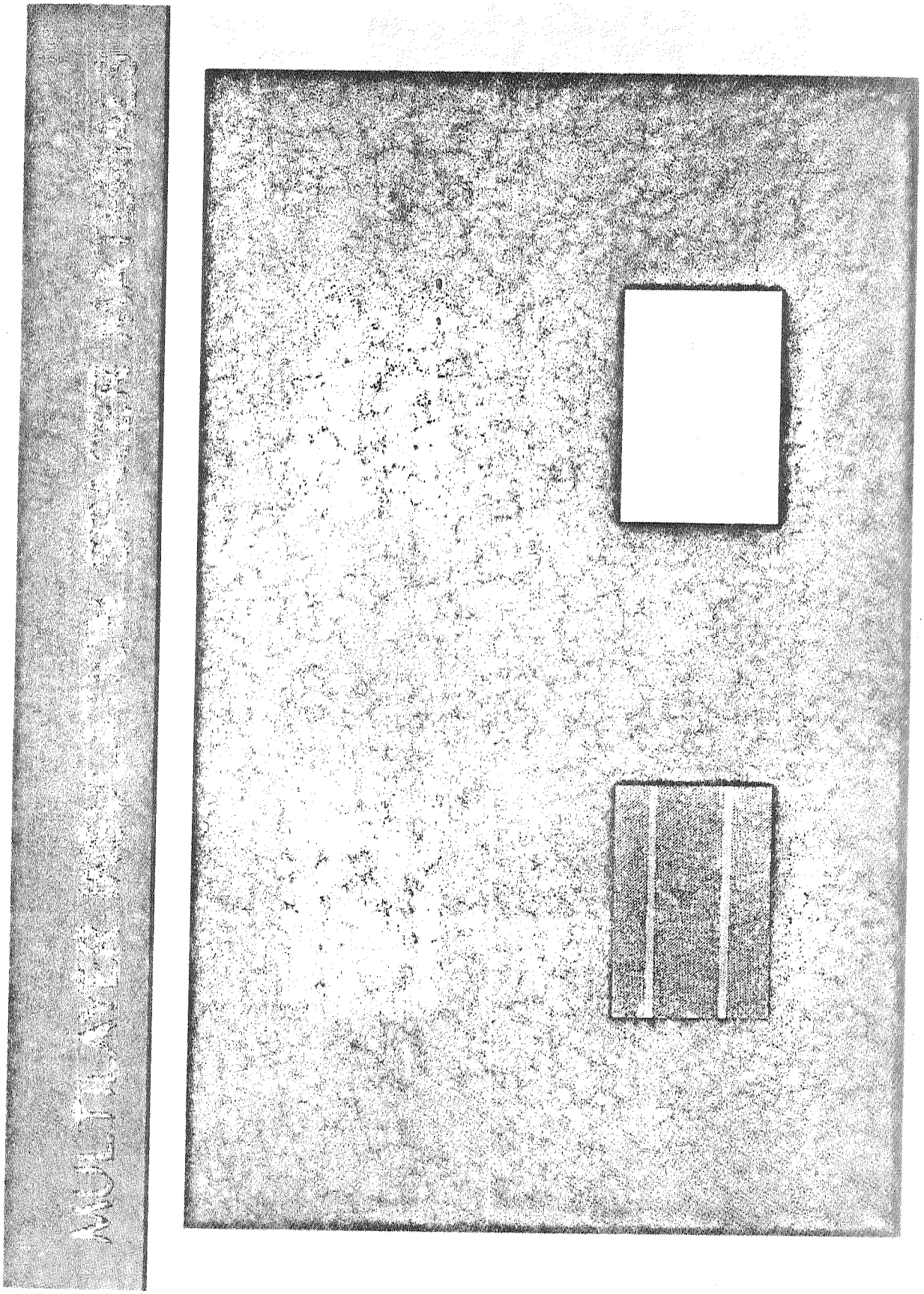

NOT REPRODUCIBLE

IDENTIFICATION OF GROUND HOLD INSULATION MATERIALS

Test Material	Test Material Source
Beta Fiber Fabric (6.3 oz/yd) Style 15035 Finish 9362	J. P. Stevens & Co., Inc. 1460 Broadway New York, New York
Narmco 7343/7139 Adhesive	Narmco Materials Div. Costa Mesa, Calif.
Goodyear Pliobond Adhesive 4001/4004	Goodyear Tire & Rubber Co. Adhesive Dept. 1745 Cottage St. Ashland, Ohio 44805
Polyurethene Foam (2 lb/ft^3), BX-250-A	Nopco Chemical Div. of Diamond Shamrock Corp. 60 Park Place Newark, New Jersey 07101 (Blown foam supplied by North American Rockwell Corp.)

IDENTIFICATION OF MISCELLANEOUS INSULATION MATERIALS

Test Material	Test Material Source	Applicable Purchase Spec.	Nominal Thickness mils (mm)
Velcro Fasteners 100% Polyester 1-in. wide, white HPE-12-1-100 Hook HPE-12-1-100 Loop	The Hartwell Corp. 9035 Venice Blvd Los Angeles, 34, Calif.	None	–
Teflon Film TFE	DuPont	AMS 3651 EPS 22-302	10 (0.25)
Thermatrol Paint (2A-100)	Lockheed Missiles & Space Co. (LMSC)	LAC 37-4294 101 (Lockheed Process Bulletin 55)	–
3M Co. Series 400 Black Paint with primer, DuPont 65-3011, Dark Gray	Reflective Products Div. 3M Co., St. Paul, Minn.	None	–
Paint Substrate			
Epoxy Glass	LMSC	MIL-P-18177C	16 (0.41)
Aluminum, 6061-T6	LMSC		20 (0.51)

EXPOSURE ENVIRONMENTS

The insulation materials are exposed to a series of environments (including a separate control environment for reference) to determine the effect of the environment on specific material properties as a function of exposure time, exposure temperature or in some cases fluorine or oxygen partial pressure. Test equipment used to provide these exposure environments, and in some cases provide in-situ measurements as well such as outgassing, are shown on the opposite page. Other measurements, summarized in later charts, are made prior to and immediately following the exposures. The simulated environments are divided into those occuring at atmospheric pressure and orbital pressure.

Atmospheric Environments (All at ambient pressure.)

- High Temperatures During Ascent at 200°F (93°C) and 40% R.H.
- High Humidity at 95% R.H. and 95°F (35°C)
- Salt Spray Under Humid Conditions at 95% R. H. and 95°F (35°C)
- Water Condensation (Immersion) at 70°F (21°C)
- Fluorine Gas Leakage Under Humid Conditions at 95°F (35°C) and Different Fluorine Partial Pressures

Orbital Environments

- Gaseous Fluorine Leakage at 70°F (21°C) and 10^{-3} Torr Pressure
- Gaseous Oxygen Leakage at 70°F (21°C) and 10^{-3} Torr Pressure
- Prolonged Vacuum Exposure at 10^{-6} Torr, at Different Exposure Temperatures Ranging from 660°R (365°K) to 37°R (21°K)
- Prolonged Vacuum Exposure at 10^{-6} Torr at Different Exposure Temperatures Ranging From 660°R (365°K) to 140°R (78°R) With and Without Prior Exposure to a a GN_2 or GHe Purge Environment at 530°R (294°K) [Outgassing Tests Only]

ENVIRONMENTAL EXPOSURE APPARATUS

SIMULATED ATMOSPHERIC ENVIRONMENTS

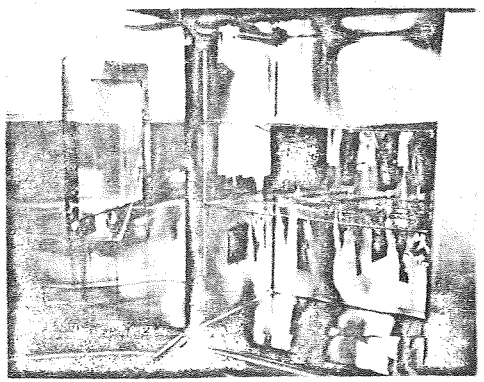

200°F (93°C), 40% RH AND 95% RH AT 95°F (35 °C)

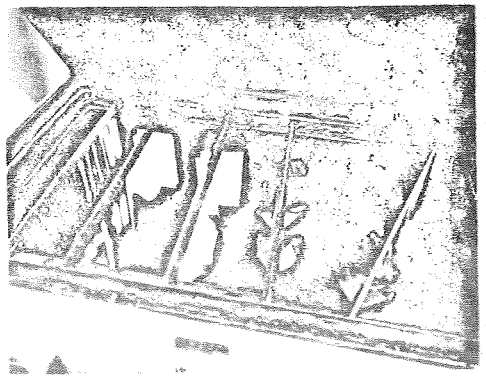

95% RH/SALT AIR AT 95°F (35°C)

SIMULATED ORBIT ENVIRONMENTS

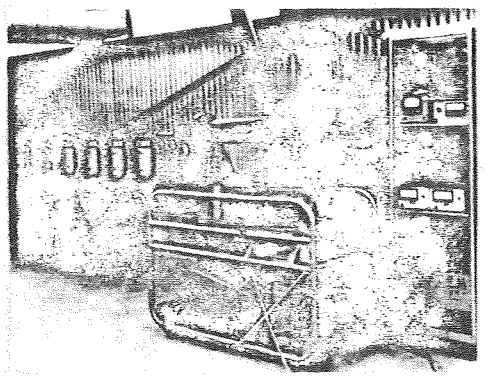

O_2 AND F_2 EXPOSURE[1]

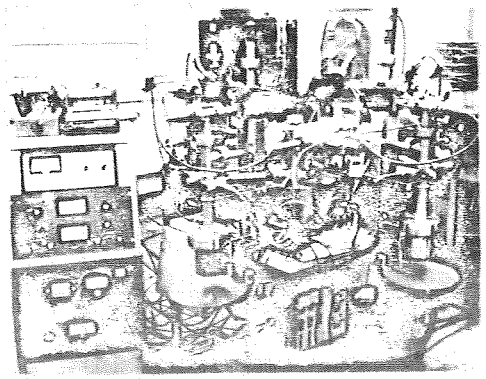

OUTGASSING

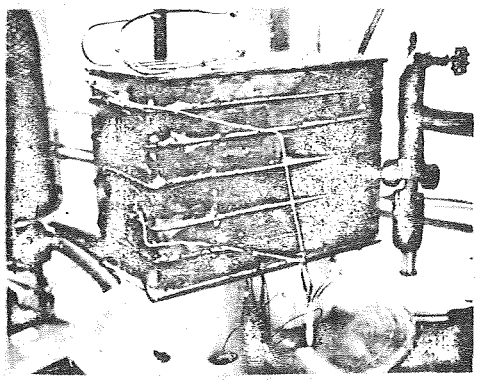

VACUUM, 660°R (365°K), 530°R (295°K

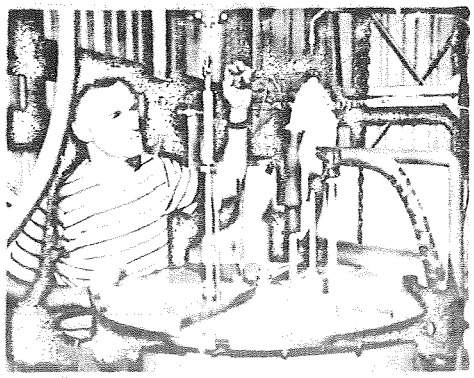

VACUUM, 140°R (78°K), 37°R (21°K)

NOTE: 1. SIMULATED ATMOSPHERIC ENVIRONMENT TESTS ALSO PERFORMED IN THIS APPARATUS
2. WATER IMMERSION TESTS, NOT SHOWN, PERFORMED IN LARGE PYREX BEAKERS

NOT REPRODUCIBLE

NOT REPRODUCIBLE

TYPICAL COMPUTER PLOTS

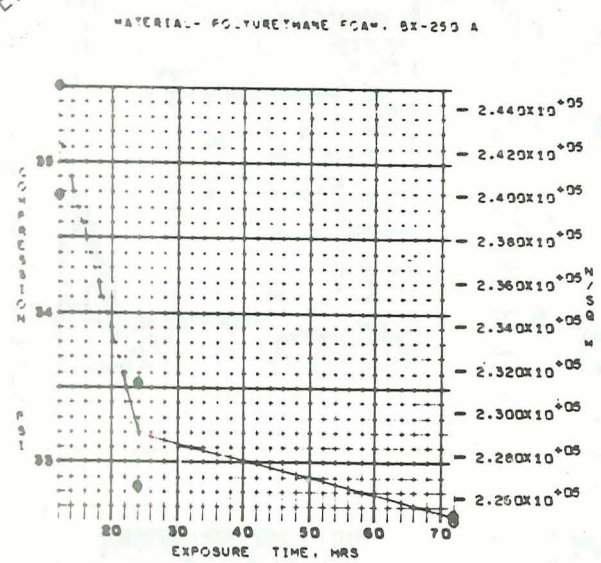

FIG ENVIRONMENT 5
95 PERCENT R.H. 95 DEG F
(35 DEG C)

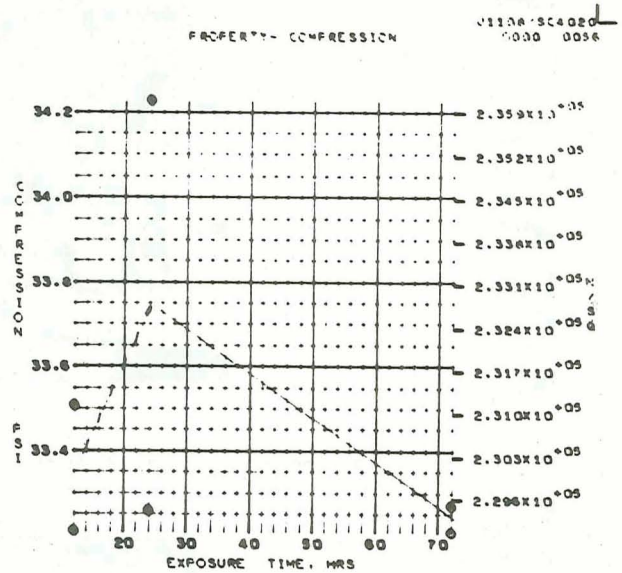

FIG ENVIRONMENT 6
95 PERCENT R.H./SALT AIR
95 DEG F (35 DEG C)

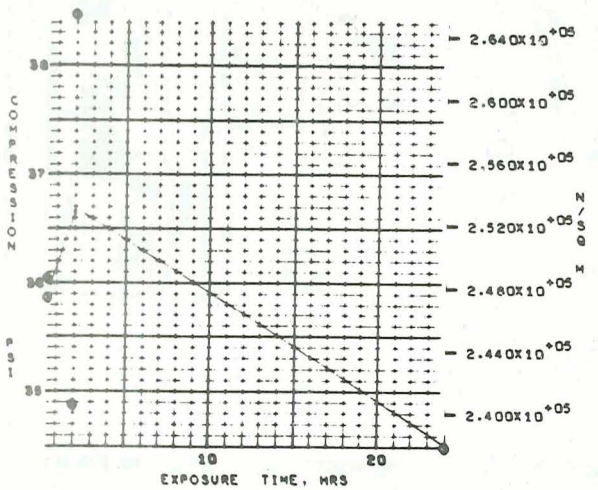

FIG ENVIRONMENT 7
WATER IMMERSION AT 70 DEG F
(21 DEG C)

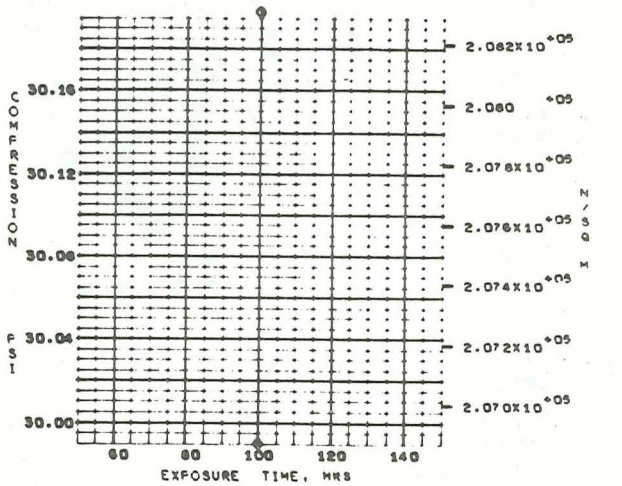

FIG ENVIRONMENT 8
GASEOUS OXYGEN, 70 DEG F
(21 DEG C) 1.E-03 TORR

TYPICAL TABULAR DATA

NOT REPRODUCIBLE

MATERIAL -POLYURETHANE FOAM, BX-250 A
PROPERTY -COMPRESSION

TABLE ENVIRONMENT 5
95 PERCENT R.H. 95 DEG F
(35 DEG C)

F	HOURS	PSI	N/SQ M
	12.0	.348+02	.240+06
	12.0	.355+02	.245+06
	24.0	.335+02	.231+06
	24.0	.328+02	.227+06
	72.0	.327+02	.225+06
	72.0	.326+02	.225+06

TABLE ENVIRONMENT 6
95 PERCENT R.H./SALT AIR
95 DEG F (35 DEG C)

F	HOURS	PSI	N/SQ M
	12.0	.332+02	.229+06
	12.0	.335+02	.231+06
	24.0	.342+02	.236+06
	24.0	.333+02	.229+06
	72.0	.332+02	.229+06
	72.0	.333+02	.230+06

TABLE ENVIRONMENT 7
WATER IMMERSION AT 70 DEG F
(21 DEG C)

F	HOURS	PSI	N/SQ M
	.5	.359+02	.247+06
	.5	.360+02	.249+06
	2.0	.385+02	.265+06
	2.0	.349+02	.241+06
	24.0	.345+02	.238+06
	24.0	.345+02	.238+06

TABLE ENVIRONMENT 8
GASEOUS OXYGEN, 70 DEG F
(21 DEG C) 1.E-03 TORR

F	HOURS	PSI	N/SQ M
	100.0	.300+02	.207+06
	100.0	.302+02	.208+06

NOTE: (1) SEE TABLE FOR IDENTIFICATION OF TEST MATERIALS
(2) ACCURACY OF MEASUREMENTS IS ESTIMATED TO BE +- 4 PERCENT
(3) THE DEPENDENT VARIABLES ARE IN SCIENTIFIC NOTATION
THE E+01 ETC. IS THE EXPONENT OF 10
(4) THE PRE-TEST DATA IS MARKED WITH A ONE IN THE F COLUMN

OUTGASSING CALCULATIONS

For the outgassing apparatus shown previously, mass balance equations can be written for the cases of an empty chamber and chamber plus sample.

$$-\frac{V_c}{RT_c}\left(\frac{dP_{co}}{dt}\right) = S\frac{(P_{co} - P_{do})}{RT_p} - Q_c A_c \qquad \text{(Empty Chamber)}$$

$$-\frac{V_c}{RT_c}\left(\frac{dP_{cs}}{dt}\right) = S\frac{(P_{cs} - P_{ds})}{RT_p} - Q_c A_c - Q_s A_s \qquad \text{(Chamber Plus Sample)}$$

where

V_c	=	sample chamber volume
T_c	=	sample temperature
T_p	=	pumping line temperature
S	=	volumetric pumping speed, volume per unit time
Q_c, Q_s	=	chamber, sample outgassing rates, mass released, per unit time
A_c, A_s	=	chamber, sample area
P_{co}	=	empty chamber gas pressure
P_{cs}	=	chamber pressure with sample in place
P_{do}	=	downstream gas pressure for empty chamber
P_{ds}	=	downstream gas pressure with sample in place

The chamber outgassing value, Q_c, is determined in a preliminary empty chamber experiment. At times of one hour or more after initiation of evacuation, the term $-\frac{V_c}{RT_c}\left(\frac{dP_{cs}}{dt}\right)$ is usually negligible. The sample outgassing rate is then given by:

$$Q_s = \frac{S}{A_s RT_p}\left[P_{cs}(t) - P_{ds}(t)\right] - \frac{Q_c A_c}{A_s}$$

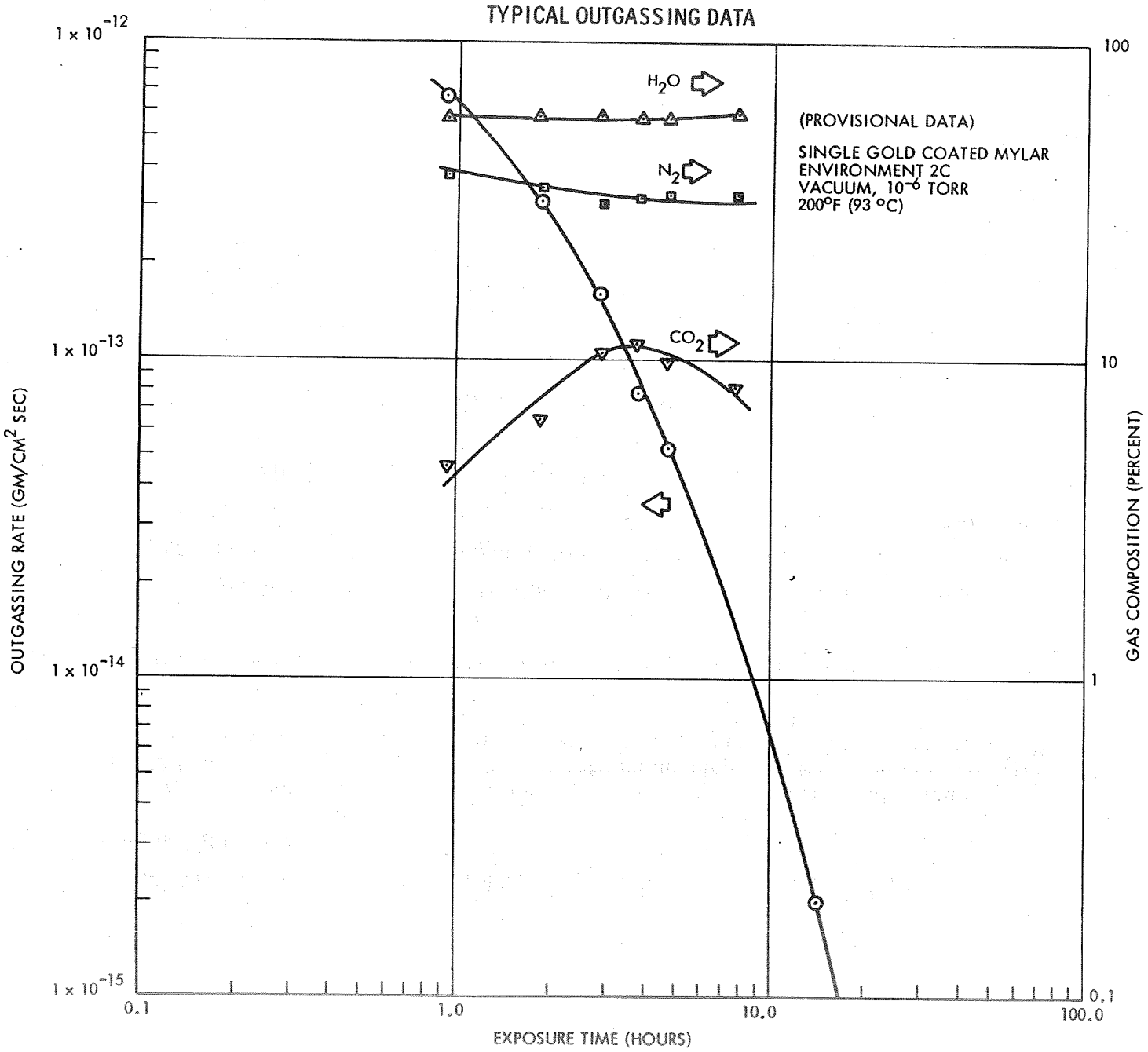
TYPICAL OUTGASSING DATA
(PROVISIONAL DATA)
SINGLE GOLD COATED MYLAR
ENVIRONMENT 2C
VACUUM, 10^{-6} TORR
200°F (93 °C)
H_2O
N_2
CO_2
OUTGASSING RATE (GM/CM^2 SEC)
1×10^{-12}
1×10^{-13}
1×10^{-14}
1×10^{-15}
GAS COMPOSITION (PERCENT)
100
10
1
0.1
EXPOSURE TIME (HOURS)
0.1
1.0
10.0
100.0

TEST TRENDS OF MULTILAYER INSULATION RADIATION SHIELD MATERIALS

Apparent test trends noted to date are as follows:

> Overall, the gold-coated substrates exhibited fewer property changes than the aluminum coated substrates. Following the 72 hour, 95% R. H. exposure, a faint pattern developed in the aluminum coatings. This pattern plus the appearance of pinholes in the aluminum coating became more pronounced in the 95% R. H./salt air environment going from the 12 hour exposure to the 24 hour exposure; the aluminum coating disappeared following the 72 hour exposure. Following the same 72 hour exposure, some minute pinholes were observed on the gold coatings as well. No coating damage was noted in any of the other environments.

The emittance of both of the single, gold coated films (S-G-M and S-G-K) shows the following trends: an increase after exposure to the 95% R. H./salt air environment and the room temperature vacuum environment and a decrease following exposure to the high temperature vacuum environment. The double gold-coated mylar (S -G-M) also shows an increase in emittance following the 95% R. H./salt air exposure.

The adhesion qualities of the gold coatings are apparently adversely affected to a small extent by exposure to the following three environments: 200° F, 40% R. H.; 95% R. H., 95° F; and 95% R. H./salt air.

The tensile strength of mylar coated with aluminum on one side showed decreases following three exposures and no increases; mylar coated with aluminum two sides showed increases in tensile strength following four exposures and no decreases. Overall, the exposures have relatively little effect on the tensile strengths of either mylar or kapton.

PERCENT CHANGE IN PROPERTIES FOR EXPOSED MULTILAYER INSULATION RADIATION SHIELD MATERIALS

[ALL MATERIALS 0.25 MIL (6.4×10^{-3} MM)]

PROPERTY[1] / ENVIRONMENT	EXPOSURE PARAMETERS: O_2 OR F_2 P.P.[2] TORR	TEMP °R (°K)	TIME, HR	ALUMINUM COATED: MYLAR – ONE SIDE (S-A-M) W	AD	F_b	F_t	ϵ	α	MYLAR – TWO SIDES (D-A-M) W	AD	F_b	F_t	ϵ	KAPTION – ONE SIDE (S-A-K) W	AD	F_b	F_t	ϵ	α	GOLD COATED: MYLAR – ONE SIDE (S-G-M) W	AD	F_b	F_t	ϵ	α	MYLAR–TWO SIDES (D-G-M) W	AD	F_b	F_t	ϵ	KAPTION – ONE SIDE (S-G-K) W	AD	F_b	F_t	ϵ	α
SIMULATED ATMOSPHERIC ENVIRONMENTS (AT AMBIENT PRESSURE)																																					
200°F (93°C) 40% R.H.			24		NC	NC	-28	-7																										NC	NC	NC	NC	
			72		NC	NC	-28	-10																										NC	NC	NC	NC	
			240		NC	NC	NC	-7			NC	NC	+16	NC		NC	NC	NC	-12			-5	NC	NC	NC			NC	NC	NC	NC		NC	NC	+12	NC	
95% R.H. AT 95°F (35°C)			12		NC	NC	NC	-10			NC	NC	+8	NC		NC	NC	NC	-7									NC	NC	NC	NC						
			24		NC	NC	NC	-12			NC	NC	NC	NC		NC	NC	NC	-21									NC	NC	NC	NC						
			72		NC	NC	NC	+80			NC	NC	NC	NC		NC	NC	NC	NC			-.8	NC	NC	NC			-.1	NC	NC	NC		-2	NC	NC	NC	
95% R.H./SALT AIR AT 95°F (35°C)			12		NC	NC	NC	NC			NC	NC	NC	+12		NC	NC	NC	NC									NC	NC	NC	NC						
			24		-2.5	NC	NC	+40			NC	NC	NC	+14		-2	NC	-24	NC									-1	NC	NC	NC						
			72		D	NC	NC	D	D		D	NC	NC	D		D	NC	NC	D	D		-26	NC	NC	+41			NC	NC	NC	+32		NC	NC	-14	+30	
WATER IMMERSION AT 70°F (21°C)			0.5		NC	NC	NC	NC			NC	NC	NC	NC		NC	NC	NC	NC			NC	NC	NC	NC			NC	NC	NC	NC		NC	NC	NC	NC	
			2		NC	NC	NC	NC			NC	NC	NC	NC		NC	NC	NC	NC			NC	NC	NC	NC			NC	NC	NC	NC		NC	NC	NC	NC	
			24		NC	NC	NC	NC			NC	NC	NC	+20		NC	NC	NC	NC			NC	NC	NC	NC			NC	NC	NC	NC		NC	NC	-10	NC	
95% R.H./F_2 AT 95°F (35°C)	10^{-3}		4																																		
	760[3]		4																																		
SIMULATED ORBITAL ENVIRONMENTS																																					
GASEOUS FLUORINE AT 70°F (21°C)	10^{-3}		100																																		
	10^{-3}		3600																																		
GASEOUS OXYGEN AT 70°F (21°C)	10^{-3}		100		NC	NC	NC	NC														NC	NC	NC	+28												
	10^{-3}		3600																																		
VACUUM, $\leq 10^{-6}$ TORR		660 (365)	24		NC	NC	-28	NC								NC	NC	NC	+7																		
		660 (365)	240		NC	NC	NC	-8			NC	NC	+17	NC		NC	NC	NC	-19			NC	NC	NC	-24			NC	NC	NC	NC		NC	NC	NC	-16	
		530 (295)	240		NC	NC	NC	-7			NC	NC	+8	NC		NC	NC	NC	NC			NC	NC	NC	+16			NC	NC	NC	NC		NC	NC	NC	+27	
		140 (78)	240		NC	NC	NC	NC			NC	NC	NC	NC		NC	NC	NC	NC									NC	NC	NC	NC						
		37 (21)	240		NC	NC	NC	NC			NC	NC	NC	NC		NC	NC	NC	NC									NC	NC	NC	NC						

1. W = WEIGHT
   AD = COATING ADHESION (% REMOVED)
   F_b = FLEXIBILITY
   F_t = TENSILE ULTIMATE
   ϵ = EMITTANCE
   α = SOLAR TRANSMITTANCE
2. P.P. = PARTIAL PRESSURE
3. TOTAL PRESSURE = 2 ATM (1520 TORR)
4. NC = NO CHANGE WITHIN ACCURACY OF MEASUREMENT ($\pm 2\sigma$)
5. D = SPECIMEN DETERIORATED IN ENVIRONMENT TO EXTENT POST-ENVIRONMENT TESTS COULD NOT BE PERFORMED

TEST TRENDS OF MULTILAYER INSULATION SPACER MATERIALS

Apparent test trends noted to date are as follows:

The tensile strength of dacron net is not affected by the environmental exposures. Nylon net's strength decreases 27% in the high temperature vacuum environment while silk net loses 37% of its strength in the high temperature, 40% R. H. environment. Tissuglas loses strength in all the environmental categories and disintegrates when immersed in water.

The compression tests use 20 layers of each spacer material. For these tests the height of silk net, nylon net and dacron net (T_2/T_1) recovers to approximately ± 10% of the control value (following an environmental exposure and release of the compressive load at $0.5\ T_1$).

(Note: In every case for control specimens or exposed specimens, the absolute height of the layers is less after release of the compressive load than before the load is applied.)

PERCENT CHANGE IN PROPERTIES FOR EXPOSED MULTILAYER INSULATION SPACER MATERIALS

ENVIRONMENT \ PROPERTY[1]	EXPOSURE PARAMETERS: O_2 or F_2 P. P.[2] TORR	TEMP °R(°K)	TIME HR	SILK NET W	SILK NET F_c[6]	SILK NET T_2/T_1	SILK NET F_t	NYLON NET W	NYLON NET F_c[6]	NYLON NET T_2/T_1	NYLON NET F_t	DACRON NET W	DACRON NET F_c[6]	DACRON NET T_2/T_1	DACRON NET F_t	TISSUGLAS W	TISSUGLAS F_c[6]	TISSUGLAS T_2/T_1	TISSUGLAS F_t
SIMULATED ATMOSPHERIC ENVIRONMENTS (AT AMBIENT PRESSURE)																			
200° F (93° C) 40% R. H.			24		-80	+12	NC		-8	-4	NC		-36	-6	NC		+78	-8	-35
			72		-68	+8	NC		-1	NC	NC		+2	+4	NC		+4	NC	-45
			240		-84	+8	-37		-34	-5	+35				NC		+6	-12	NC
95% R. H. AT 95° F (35° C)			12		+14	+12	NC		-9	NC	NC		+2	NC	NC		+60	NC	NC
			24		-15	NC	NC		-38	-5	NC		-48	+7	NC		0	NC	-58
			72				NC		-5	-5	NC		-39	NC	NC		+181	NC	NC
95% R. H. /SALT AIR AT 95° F (35° C)			12				-11		-1	-10	NC		0	-11	NC		+41	+17	-66
			24				-18		-2	-5	NC		+12	NC	NC		-11	NC	-61
			72				-16		+72	-5	NC		+45	-8	NC		-11	+19	-82
WATER IMMERSION AT 70° F (21° C)			0.5		-83	NC	-12		+22	NC	NC		-12	NC	NC		D	D	D
			2		-16	-5	NC		-9	-10	NC		+2	-7	NC		D	D	D
			24		-87	-10	NC		-43	-10	NC		-22	-6	NC		D	D	D
95% R. H. /F_2 AT 95° F (35° C)	10^{-3}		4																
	760[3]		4																
SIMULATED ORBIT ENVIRONMENTS																			
GASEOUS FLUORINE AT 70° F (21° C)	10^{-3}		100																
	10^{-3}		3600																
GASEOUS OXYGEN AT 70° F (21° C)	10^{-3}		100		-50	+16	NC		+23	NC	NC		-15	NC	NC		-14	NC	-32
	10^{-3}		3600																
VACUUM, $\leq 10^{-6}$ TORR		660 (365)	24		-38	+7	NC		+44	NC	NC		-20	-6	NC		+357	-5	NC
		660 (365)	240		-59	+8	-12		-6	NC	-27		-6	-6	NC		-14	-10	-58
		530 (295)	240																
		140 (78)	240		-83	-6	-8		+20	NC	NC		-33	-6	NC		+231	NC	-48
		37 (21)	240		-43	+8	-13		-16	+6	NC		-83	-21	NC		-6	-19	NC

1. W = WEIGHT
   F_c = COMPRESSION ULTIMATE AT $(0.5)T_1$
   T_2/T_1 = COMPRESSION RECOVERY
   F_t = TENSILE ULTIMATE
2. P. P. = PARTIAL PRESSURE
3. TOTAL PRESSURE = 2 ATM (1520 TORR)
4. NC = NO CHANGE WITHIN ACCURACY OF MEASUREMENT ($\pm 2\sigma$)
5. D = SPECIMEN DETERIORATED IN ENVIRONMENT TO EXTENT POST-ENVIRONMENT TESTS COULD NOT BE PERFORMED
6. DUE TO THE VARIABLE PROPERTIES OF SPACERS UNDER A COMPRESSIVE LOAD A 2σ SPREAD WAS FELT TO BE MEANINGLESS FOR DETERMINING WHETHER A CHANGE HAD TAKEN PLACE. THEREFORE ALL DATA RESULTS ARE SHOWN FOR INTERPRETATION.

TEST TRENDS OF GROUND-HOLD INSULATION MATERIALS

Apparent test trends noted to date are as follows:

Both the room temperature cured adhesive, 7343/7139, and the high temperature cured adhesive, 4001/4004, pick up shear strength following the high temperature/vacuum or high temperature/40% R. H. exposures. (The percentage increase is greater for the room temperature cured adhesive as would be expected.) The shear strength of 4001/4004 adhesive apparently decreases following water immersion.

The tensile strength of beta glass cloth apparently increases after exposure to the high temperature, 40% R. H. environment although the reason for this increase is not understood.

The compression strength of polyurethane foams decreases following exposure to all the environments. High temperature plus vacuum has the greatest effect followed by high temperature at 40% R. H.

PERCENT CHANGE IN PROPERTIES FOR EXPOSED GROUND-HOLD INSULATION MATERIALS

ENVIRONMENT \ PROPERTY[1]	EXPOSURE PARAMETERS			BETA GLASS CLOTH		NARMCO 7343/7139 ADHESIVE		GOODYEAR PLIOBOND 4001/4004 ADHESIVE		POLYURETHANE FOAM, 2 PCF		
	O_2 OR F_2 P.P.[2] TORR	TEMP °R (°K)	TIME, HR	W	F_t	W	F_s	W	F_s	W	ρ	F_c
SIMULATED ATMOSPHERIC ENVIRONMENTS (AT AMBIENT PRESSURE)												
200 °F (93°C) 40% R.H.			24		+30		+31		NC			-23
			72		+32		+53		+37			-29
			240		+49		+94		+56			-30
95% R. H. AT 95° F (35°C)			12		NC		NC		NC			-3
			24		NC		NC		-25			-7
			72		NC		NC		-25			-10
95% R. H./SALT AIR AT 95° F (35°C)			12		NC		NC		NC			-5
			24		+35		NC		NC			-8
			72		NC		NC		NC			-6
WATER IMMERSION AT 70° F (21°C)			0.5		-21		NC		-47			NC
			2		NC		NC		-36			NC
			24		NC		NC		-29			-7
95% R.H./F_2 AT 95° F (35°C)	10^{-3}		4									
	760[3]		4									
SIMULATED ORBIT ENVIRONMENTS												
GASEOUS FLUORINE AT 70° F (21°C)	10^{-3}		100									
	10^{-3}		3600									
GASEOUS OXYGEN AT 70° F (21°C)	10^{-3}		100		NC		NC		NC			-16
	10^{-3}		3600									
VACUUM, $\leq 10^{-6}$ TORR		660 (365)	24		NC		+56		+34			-38
		660 (365)	240		NC		+95		+81			-51
		530 (295)	240									
		140 (78)	240		NC		NC		NC			-7
		37 (21)	240		NC		NC		NC			-5

1. W = WEIGHT
   F_s = TENSILE SHEAR
   F_t = TENSILE ULTIMATE
   ρ = DENSITY
   F_c = COMPRESSION ULTIMATE
2. P.P. = PARTIAL PRESSURE
3. TOTAL PRESSURE = 2 ATM (1520 TORR)
4. NC = NO CHANGE WITHIN ACCURACY OF MEASUREMENT ($\pm 2\sigma$)
5. D = SPECIMEN DETERIORATED IN ENVIRONMENT TO EXTENT POST-ENVIRONMENT TESTS COULD NOT BE PERFORMED

TEST TRENDS OF MISCELLANEOUS INSULATION MATERIALS

Apparent test trends noted to date are as follows:

The measured properties of the thermatrol paint and series 400 black paint are relatively insensitive to the environmental exposures.

TFE teflon film apparently decreases slightly in tensile strength following exposure to vacuum at temperature levels ranging from room temperature to liquid hydrogen temperature.

The tensile strength of Velcro fasteners remains comparatively unaffected by the environmental exposure while the peel strength apparently decreases after exposure to some of the environments. This latter trend may be more apparent than real due to the limited number of control specimens run to date. Additional control tests scheduled later may shift the peel test results shown back toward the no change condition.

PERCENT CHANGE IN PROPERTIES FOR EXPOSED MISCELLANEOUS INSULATION MATERIALS

ENVIRONMENT \ PROPERTY[1]	EXPOSURE PARAMETERS: O_2 OR F_2 P.P.[2] TORR	TEMP °R(°K)	TIME, HR	POLYESTER VELCRO FASTENERS: W	F_t	F_s	F_p	TFE-TEFLON FILM: W	F_t	F_b	THERMATROL PAINT ON ALUMINUM: W	AD	ϵ	α	THERMATROL PAINT ON FIBERGLASS: W	AD	ϵ	α	SERIES 400 BLACK PAINT ON ALUMINUM: W	AD	ϵ	α	SERIES 400 BLACK PAINT ON FIBERGLASS: W	AD	ϵ	α
SIMULATED ATMOSPHERIC ENVIRONMENTS (AT AMBIENT PRESSURE)																										
200° F (93° C) 40% R.H.			24		NC	-26	NC		NC	NC		NC	NC			NC	NC			NC	+.4			NC	NC	
			72		NC	NC	NC		NC	NC		NC	NC			NC	+.4			NC	+.5			NC	NC	
			240		+46	NC	+31		NC	NC		NC	NC			NC	+.6			NC	+.3			NC	NC	
95% R.H. AT 95° F (35° C)			12		NC	NC	NC		NC	NC		NC	NC			NC	NC			NC	NC			NC	NC	
			24		NC	-28	NC		NC	NC		NC	NC			NC	NC			NC	NC			NC	NC	
			72		NC	-29	+22		NC	NC		NC	NC			NC	NC			NC	NC			NC	NC	
95% R.H./SALT AIR AT 95° F (35° C)			12		NC	-24	NC		NC	NC		NC	NC			NC	NC			NC	+.7			NC	NC	
			24		NC	-21	NC		NC	NC		NC	NC			NC	NC			NC	NC			NC	NC	
			72		NC	NC	NC		-18	NC		NC	NC			NC	NC			NC	+.4			NC	NC	
WATER IMMERSION AT 70° F (21° C)			0.5		NC	NC	NC		NC	NC		NC	NC			NC	NC			NC	NC			NC	NC	
			2		NC	-23	NC		NC	NC		NC	NC			NC	NC			NC	NC			NC	NC	
			24		NC	-30	NC		NC	NC		NC	NC			NC	NC			NC	NC			NC	NC	
95% R.H./F_2 AT 95° F (35° C)	10^{-3}		4																							
	760[3]		4																							
SIMULATED ORBIT ENVIRONMENTS																										
GASEOUS FLUORINE AT 70° F (21° C)	10^{-3}		100																							
	10^{-3}		3600																							
GASEOUS OXYGEN AT 70° F (21° C)	10^{-3}		100		NC	NC	NC		NC	NC			NC			NC	NC			NC	NC			NC	NC	
	10^{-3}		3600																							
VACUUM, $\leq 10^{-6}$ TORR		660 (365)	24		NC	-29	NC		NC	NC		NC	NC			NC	NC			NC	NC			NC	NC	
		660 (365)	240		NC	NC	+18		NC	NC		NC	NC			NC	NC			NC	NC			NC	NC	
		530 (295)	240		NC	NC	NC		-12	NC		NC	NC			NC	+.4			NC	+.6			NC	NC	
		140 (78)	240		NC	NC	NC		-17	NC		NC	NC			NC	NC			NC	NC			NC	NC	
		37 (21)	240		NC	NC	NC		-15	NC		NC	NC			NC	+.6			-.5	NC			NC	NC	

1. W = WEIGHT
   F_b = FLEXIBILITY
   α = SOLAR ABSORBTANCE
   F_t = TENSILE ULTIMATE
   AD = PAINT ADHESION (% REMOVED)
   F_s = TENSILE SHEAR
   ϵ = TOTAL NORMAL EMITTANCE
   F_p = T-PEEL STRENGTH
2. P.P. = PARTIAL PRESSURE
3. TOTAL PRESSURE = 2 ATM (1520 TORR)
4. NC = NO CHANGE WITHIN ACCURACY OF MEASUREMENT ($\pm 2\sigma$)
5. D = SPECIMEN DETERIORATED IN ENVIRONMENT TO EXTENT POST-ENVIRONMENT TESTS COULD NOT BE PERFORMED

THIS PAGE INTENTIONALLY LEFT BLANK

PRECEDING PAGE BLANK NOT FILMED

N71-29616

"PPO FOAM INTERNAL INSULATION"

G. B. YATES

R. E. TATRO

GENERAL DYNAMICS

THIS PAGE INTENTIONALLY LEFT BLANK

PRECEDING PAGE BLANK NOT FILMED

PPO FOAM INTERNAL INSULATION

by

G. B. Yates and R. E. Tatro

INTRODUCTION

The reusable mission and life cycle requirements of the space shuttle vehicle have resulted in a reassessment of currently available cryogenic insulation systems, most of which were designed for the launch phase of a mission of an expendable vehicle. The various phases of the multiple mission cycle impose new loads and thermal cycling requirements on the insulation materials. Both external and internal insulation systems have been used on existing space launch vehicles. An internal insulation concept has been selected for the space shuttle vehicle. Installation inside the tank minimizes exposure of the material to potentially harmful external environments and keeps the tank skin and insulation bond line warm minimizing thermal stresses.

INTRODUCTION

COMPARISON OF PPO FOAM & OTHER LH_2 INSULATIONS

MATERIALS DEVELOPMENT: PPO FOAM & ADHESIVES

MANUFACTURING

THERMAL PERFORMANCE

CONCLUSIONS

CANDIDATE LH_2 TANK INSULATION SYSTEMS

Candidate insulation systems for application to space shuttle liquid hydrogen tanks are shown below. The values listed for density and thermal conductivity, though based on limited R&D information, are considered to be representative for the various systems. PPO foam was selected by Convair Aerospace for comprehensive development because it is open-celled and therefore not subjected to cyclic pressure fatigue, it is a simple, single-component insulation material, it has the potential for maximum reliability and reusability, it is a tough material with good cryogenic properties, and it has a competitive $k \times \rho$ product.

CANDIDATE LH_2 TANK INSULATION SYSTEMS

MATERIAL	k W/M°K (BTU/HR.FT.°R)	ρ KG/M^3 (LB./CU.FT.)	$k \times \rho$
1. POLYURETHANE RIGID CLOSED-CELL FOAM EXTERNAL, SPRAY-ON, SII	.026 (.015)	32 (2.0)	.83 (.030)
2. FIBERGLASS-FILLED HONEYCOMB, PERFORATED FACE SHEET INTERNAL, SST CONCEPT	.0865 (.050)	40 (2.5)	3.46 (.125)
3. POLYIMIDE OPEN-CELL FOAM-FILLED HONEYCOMB INTERNAL	.0865 (.050)	40 (2.5)	3.46 (.125)
4. PPO FOAM INTERNAL	.108 (.0625)	40 (2.5)	4.32 (.~~188~~)
5. POLYURETHANE OPEN-CELL FOAM-FILLED HONEYCOMB INTERNAL	.0865 (.050)	64 (4.0)	5.53 (.200)
6. POLYURETHANE RIGID CLOSED -CELL FOAM INTERNAL, 3D REINFORCED, S-IVB	.0865 (.050)	88 (5.5)	7.61 (.275)
7. FIBERGLASS BLANKET, HELIUM PURGED EXTERNAL	.173 (.100)	64 (4.0)	11.06 (.400)

*2.0 LB./CU.FT. MATERIAL CAN BE PRODUCED

PPO FOAM PHYSICAL CHARACTERISTICS

PPO foam is an anisotropic, elongated open-cell material which has physical and mechanical characteristics similar to those of honeycomb. The foam is manufactured by placing rigid sheets of powdered resin and catalyst between paper-covered, steam-heated plates and drawing the plates apart rapidly to produce the elongated cells. PPO foam thicknesses of up to 80 mm (3.1 in) and densities from 30 to 180 kg/m^3 (1.9 to 12 pcf) have been produced. When used as an internal insulation system, surface tension prevents liquid entry into the open cells and causes an insulating layer of gaseous hydrogen to form at the tank wall. The cell diameters range in size up to 760 μm (0.030 in).

PHYSICAL CHARACTERISTICS OF PPO FOAM

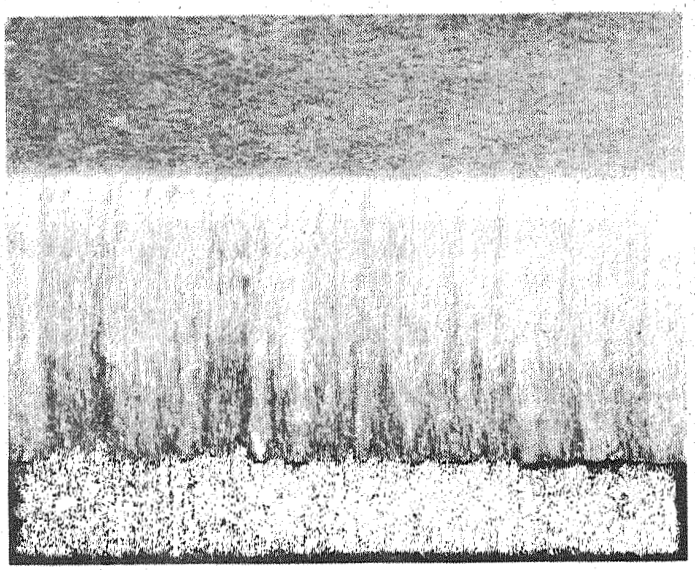

CELL SIDE VIEW 40 CM (1.5 IN.) THICK SHEET (2X)

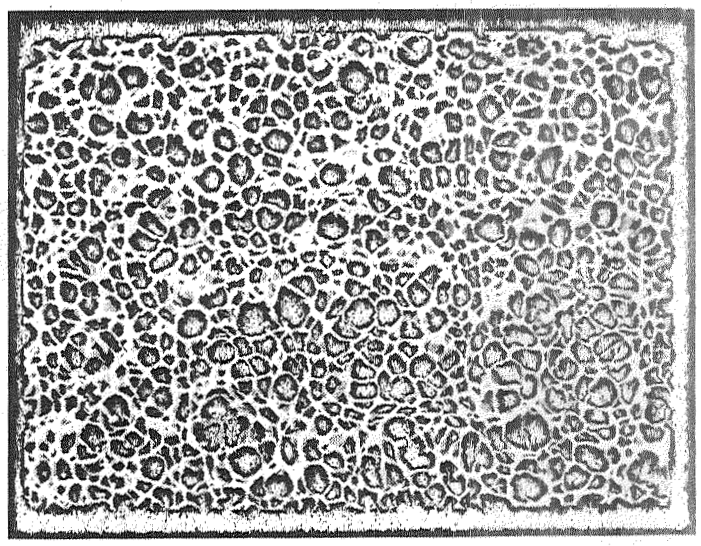

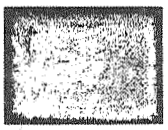

CELL END VIEW
0.076 MM (0.003 IN.) THICK SLICE (ACTUAL SIZE & 10X)

LATERAL GAS FLOW DEMONSTRATION

The manufacturing technique results in a density gradient parallel to the fiber direction in the material. In a 50 mm (2 inch) sheet with an overall density of 37.3 kg/m^3 (2.33 lb/ft^3) the local densities when cut in 1/3 slices were 40.3, 30.9 and 40.8 kg/m^3 (2.52, 1.93 and 2.55 lb/ft^3). This 27 percent density gradient through the material is typical of the panels received to date. The lateral porosity (perpendicular to the fiber direction) of PPO foam was evaluated by flowing helium gas through a funnel bonded to the face of a 15-cm (6-inch) diameter foam specimen. When submerged in water, gas was observed exiting the sides of the specimen indicating a reduced resistance to lateral gas movements between the cells inside the foam. This does not, however, appear to have an appreciable effect on the thermal performance of the foam.

PPO FOAM GAS FLOW DEMONSTRATION

FOAM DENSITY

UPPER THIRD: 40.5 KG/M^3 (2.52 PCF) MIDDLE THIRD: 30.9 KG/M^3 (1.93 PCF) LOWER THIRD: 40.8 KG/M (2.55 PCF)

OVERALL: 37.3 KG/M^3 (2.33 PCF)

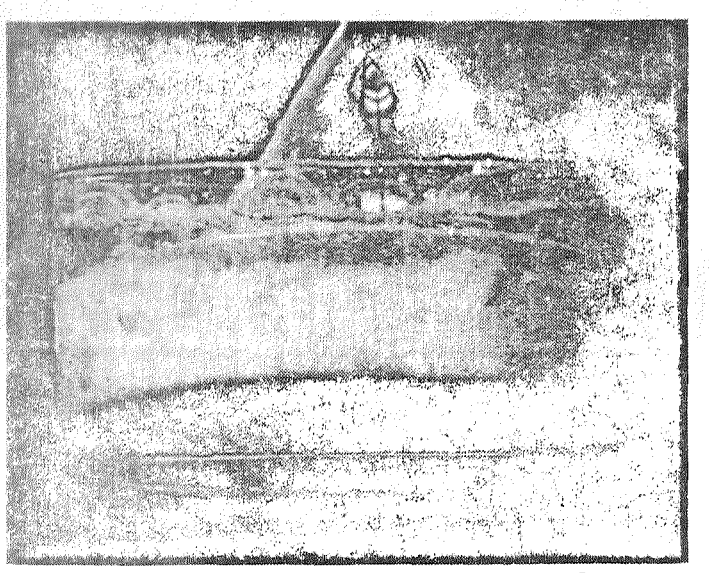

HELIUM FLOW RATE = 102μM^3/SEC (13CFH)

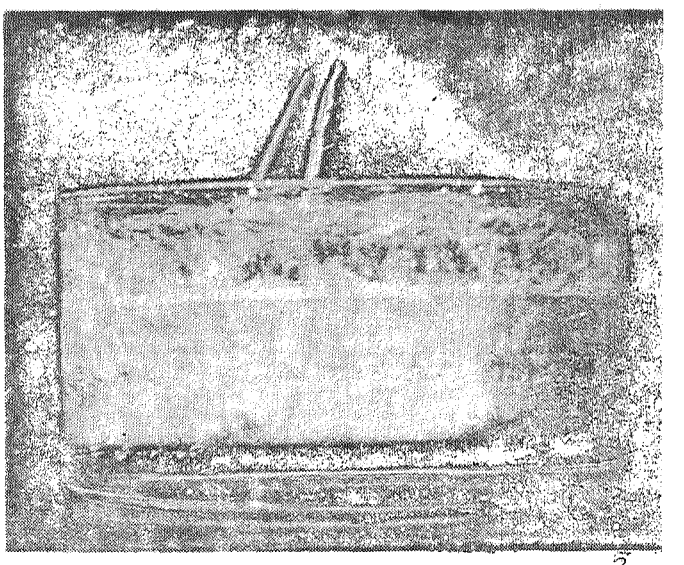

HELIUM FLOW RATE = 275 μM^3/S (35CFH)

X RAY INSPECTION

X ray techniques have been successfully used to inspect the foam panels for internal porosity and high density areas. An example of the identification of voids in early batches of PPO foam using X ray exposures is shown below. It is anticipated that by properly controlling X ray and photo development parameters, relative to the nominal material specific weight (kg/m^2), it will be possible to evaluate foam panel density variations using X ray techniques. Other inspection techniques used, following removal of the paper cover sheets, include visual inspection on a light table, magnification and measurement of surface cell sizes, and bulk density calculations and comparison with X ray data.

X-RAY INSPECTION OF FIVE-CENTIMETER PPO FOAM MATERIAL

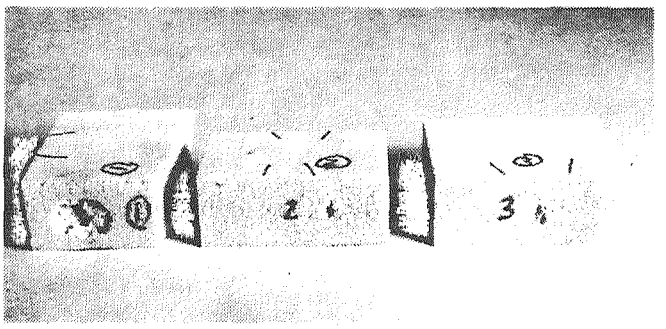

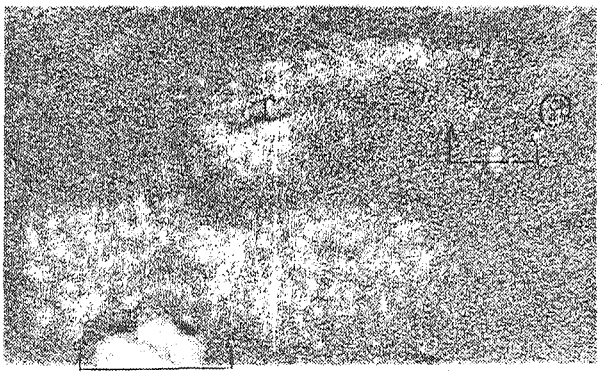

NOT REPRODUCIBLE

FOAM MECHANICAL PROPERTIES

Polyphenylene oxide resin has a heat deflection temperature of 464 K @ 1.82 MN/m^2 (375 F @ 264 psi) and the foam remains flexible at cryogenic temperatures exhibiting 2% elongation and 2% elastic compression parallel to the fiber direction and 12% elongation perpendicular to the fiber direction at LH_2 temperature. The PPO foam mechanical properties have been measured over the temperature range of 20 to 422 K (-423 to 300 F). The properties measured were face tension, compression, core shear, and climbing drum peel. All failures during the mechanical property tests occurred in the foam indicating good bond strength with 7343Z (Crest 7343 modified with 1% Silane), Epon 934, and HT424 adhesives. The foam was found to have sufficient strength for its intended use over the temperature range tested. No indication of incompatibility between the foam and these adhesives was found.

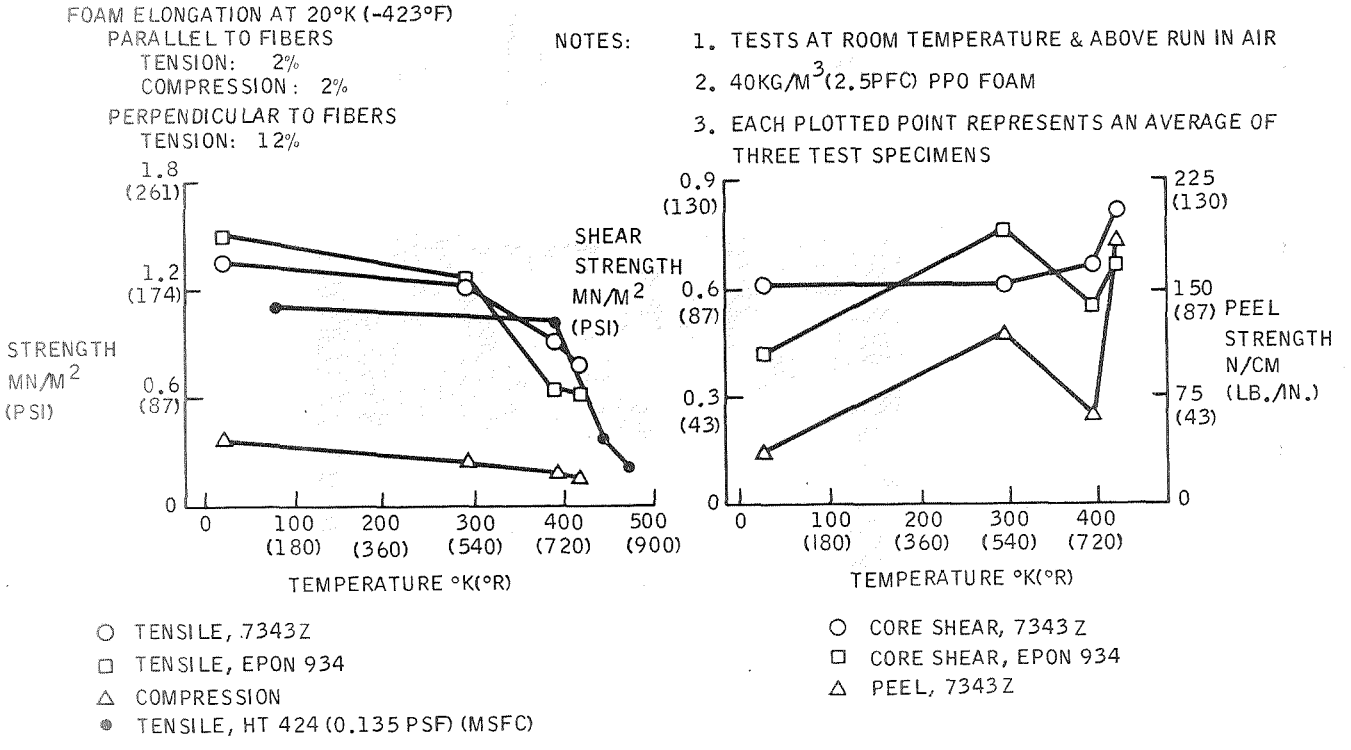

STRUCTURAL INTEGRITY TESTING

Room temperature cure polyurethane and epoxy adhesives for use with PPO foam have been evaluated over the temperature range of 20 to 422 K (-423 to 300F). Polyurethane is tough and exhibits approximately 2% elongation at cryogenic temperature, but it has not generally been accepted for use above 366 K (200F). Epoxy is comparatively brittle at cryogenic temperature (~0.5% elongation) but has better strength at high temperature. Based on lap shear tests, Crest 7343 polyurethane modified with 1% Dow-Corning Silane coupling agent (7343Z), and Epon 934 epoxy were selected for bonding PPO foam specimens for mechanical property testing. The 7343Z lap shear strengths were 26.7 and 1.6 MN/m^2 (3870 and 243 psi), and the Epon 934 strengths were 14.0 and 5.2 MN/m^2 (2027 and 760 psi), at 20 and 422 K (-423 and 300F), respectively. Structural integrity tests have been run on dog bone specimens with 5 × 30 × 4.6 cm (2 × 12 × 1.8 inch) PPO foam specimens bonded to 32-mm (1/8-in) thick 2219 (T81) aluminum. Four hundred load-cycles were run at 20, 294, and 394 K (-423, 70 and 250F) with strains in the aluminum of 0.0035, 0.004, and 0.002 cm/cm, respectively. A total of three specimens were tested with no observable failures, cracks or deterioration.

PPO FOAM BOND STRUCTURAL INTEGRITY TEST SPECIMENS

MATERIALS

- .32 CM (.125 IN.) 2219 (T81) ALUMINUM
- 4.6 CM (1.8 IN.) PPO FOAM, TEST SECTION AREA, 5.1 X 18.4 CM (2 X 7.25 IN.)
- CREST 7343 POLYURETHANE ADHESIVE MODIFIED WITH 1% DOW-CORNING 6040Z SILANE

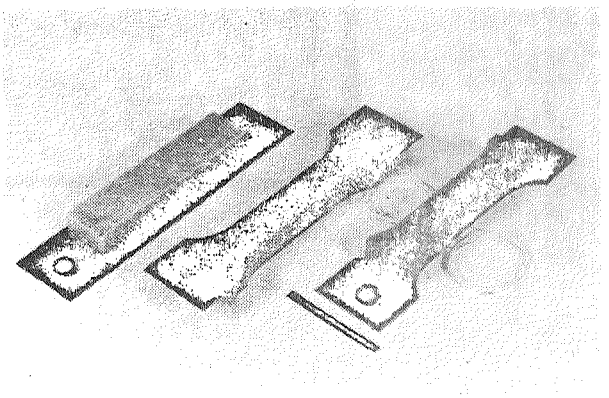

TEST CONDITIONS

TEMPERATURE °K°(F)	STRAIN CM/CM	NO. LOAD CYCLES
20 (-423)	.0035	400
294 (70)	.0040	400
394 (250)	.0020	400

SMALL RADIUS FORMING

PPO foam panels can be accurately formed to nearly any desired shape. Examples of pieces of PPO formed to extremely small radii are shown below. A 20-mm (0.8-in) thick PPO foam panel has been formed in a 46-cm (18-in) diameter elliptical bulkhead. Larger PPO foam panels 46 × 71 × 4.5 cm (18 × 24 × 1.8 in) have been formed on 91-cm (3-ft) radius, single curvature surfaces and on compound curvature Centaur bulkhead tooling. The panels are vacuum bagged and hot formed in an oven.

SMALL-RADIUS PPO FOAM FORMED PARTS

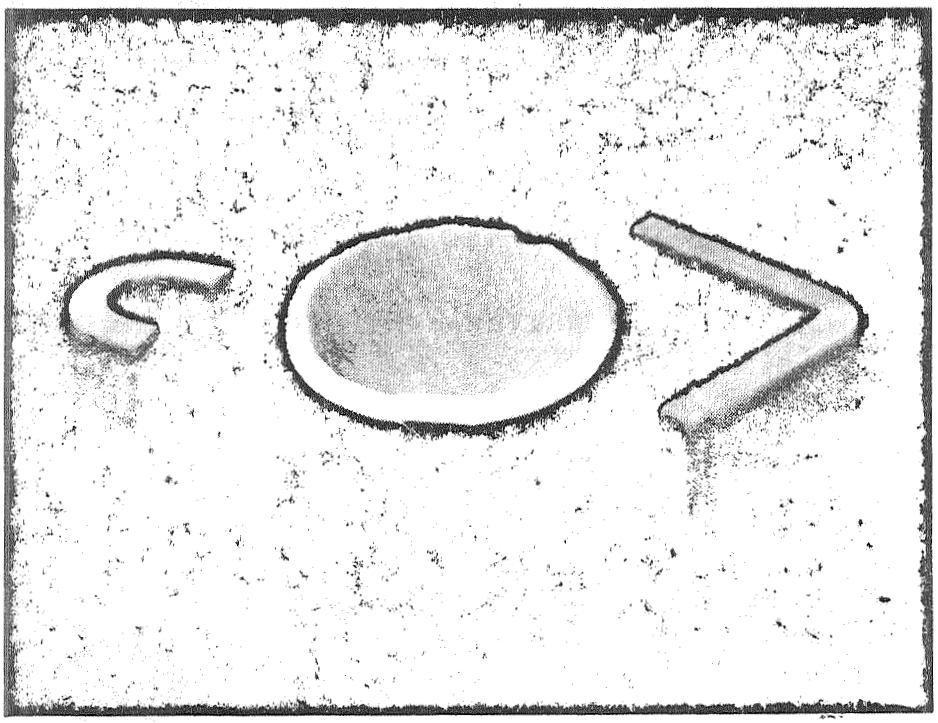

PPO FOAM FEASIBILITY TEST APPARATUS

Tests have been performed to determine the concept feasibility of several open-cell insulation materials. Small-scale LH_2 tests were performed using 15.2 cm (6-in) diameter Lexan polycarbonate beakers. A heater was bonded to the bottom of the beaker, with instrumented insulation sample bonded inside, and the apparatus tested in a vented and insulated cryostat. Insulation performance was determined by measuring the hydrogen boiloff rate and temperature profiles in the material. A larger 61-cm (24-in) rectangular aluminum tank was used to evaluate materials in the tank sidewall, bottom, and top orientations. Different open-cell configurations were mounted on the flat surfaces, and low density balsa wood was bonded into the corners to prevent overlapping of the insulation materials. Temperatures, pressure, and boiloff flow rate were measured to evaluate material performance.

PPO FOAM FEASIBILITY TEST APPARATUS

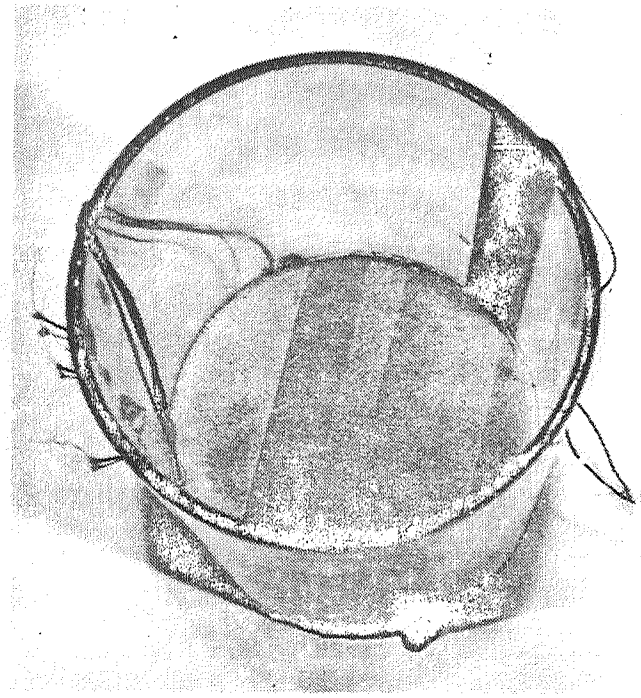

15.2-CM (6-IN.) BEAKER

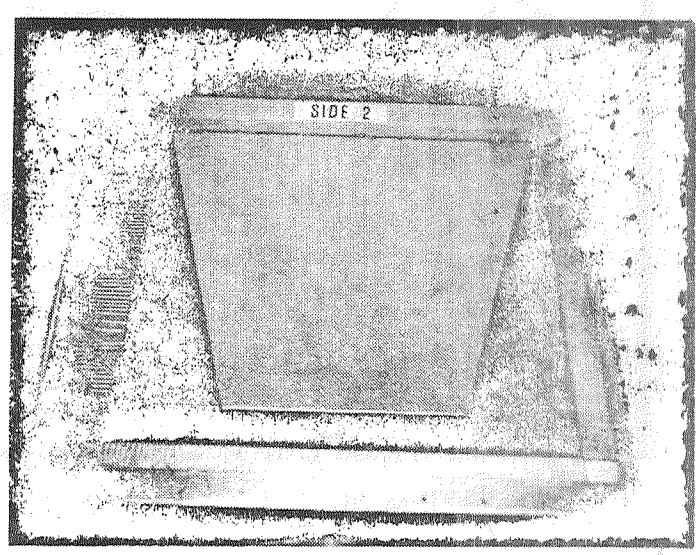

61-CM (24-IN.) TANK

DOUBLE-CURVATURE PANEL WITH A BONDED BUTT JOINT

Techniques are being developed for cutting, forming and bonding full-size PPO foam panels. Large, accurate surface cuts are required to remove the brown cover paper from delivered material. Both mechanical and hot wire cutting techniques have been investigated. Hot wire is the most desirable method because it minimizes debris; however, a considerable amount of new tooling is needed to successfully develop an accurate cut. A rotary knife also makes a clean cut but is time consuming because of the large number of passes required and the hold down tooling which must be moved after each pass. A horizontal band saw, 4 teeth per inch, run in reverse, was found to be the most successful and accurate cutting technique. Flat and preformed curved panels have been bonded to aluminum plate with 7343Z adhesive. Double-curvature forming and bonding of a full-size PPO foam panel is shown below. The panel being formed is a 4.6 × 46.0 × 62.2 cm (1.8 × 18.1 × 24.5 in) part on a section of Centaur bulkhead tooling. The edges of the panel are supported to prevent crushing during the vacuum hot-forming process. The vacuum is applied, the panel is heated and formed, and air cooled to room temperature. The panel was cut in half and then bonded with a bonded butt joint to a stretch formed piece of 2024-0 aluminum sheet.

BONDED PPO FOAM DOUBLE-CURVATURE PANEL, BONDED BUTT JOINT

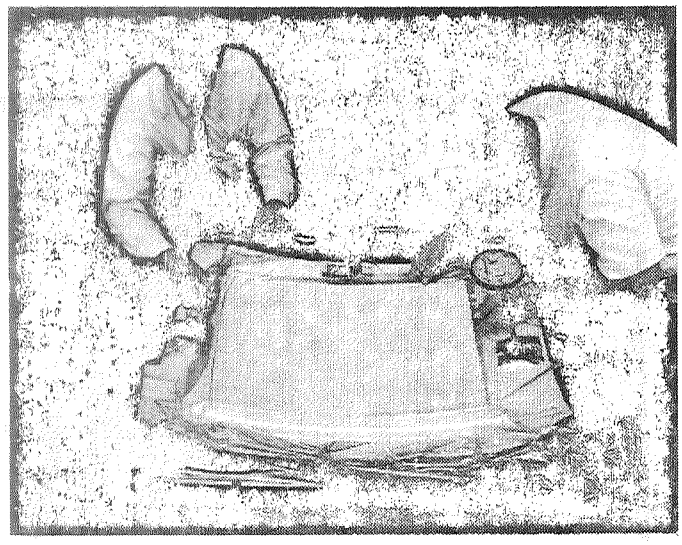

FORMING SETUP

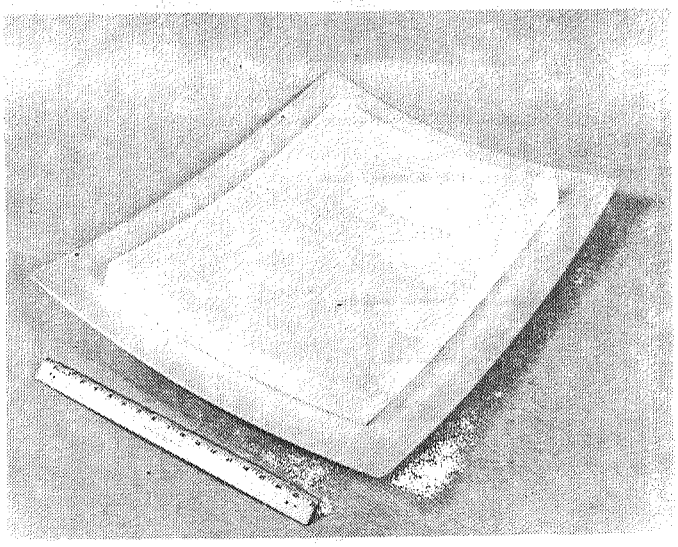

FORMED PPO

THERMAL CONDUCTIVITY TESTING

The thermal conductivity of PPO foam was measured in liquid hydrogen on a guarded hot plate test apparatus. The design employed a 25 cm (10-in) circular test section heater with a 7.8 cm (3-in) annular guard section heater sandwiched between two circular pieces of a solid reference material, 3M Scotchply type 1157 glass reinforced epoxy resin. Identical PPO foam test specimens were bonded to the epoxy surfaces. The symmetrical design permitted determination of the proportional heat flow through the two faces of the specimen by measuring the temperature differences across the two 1.6 cm (0.625-in) thick epoxy disks. A 3.8 cm (1.5-in) polyurethane foam edge guard maintained the specimen edges well above 20 K (-423F). A total of 25 Cr-Cn thermocouples were used to monitor specimen temperatures. The specimen was tested at PPO warm face temperatures of 222, 278, 344, and 400 K (-60, 40, 160, and 260F). The ratio of the thermal conductivity of PPO foam to that of gaseous parahydrogen ranges from 1.10 to 1.25 for the temperature range tested.

PPO FOAM THERMAL CONDUCTIVITY IN LIQUID HYDROGEN

APPARATUS

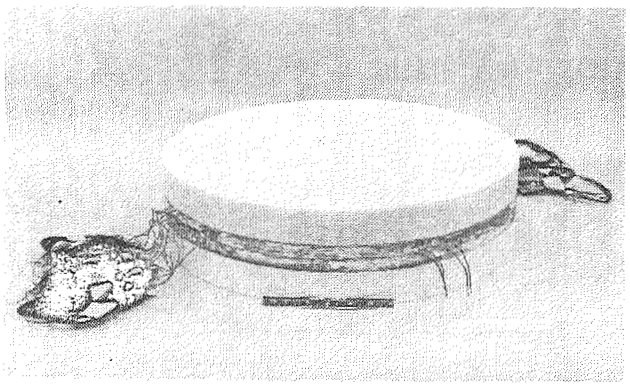

DATA (BOTTOM ORIENTATION)

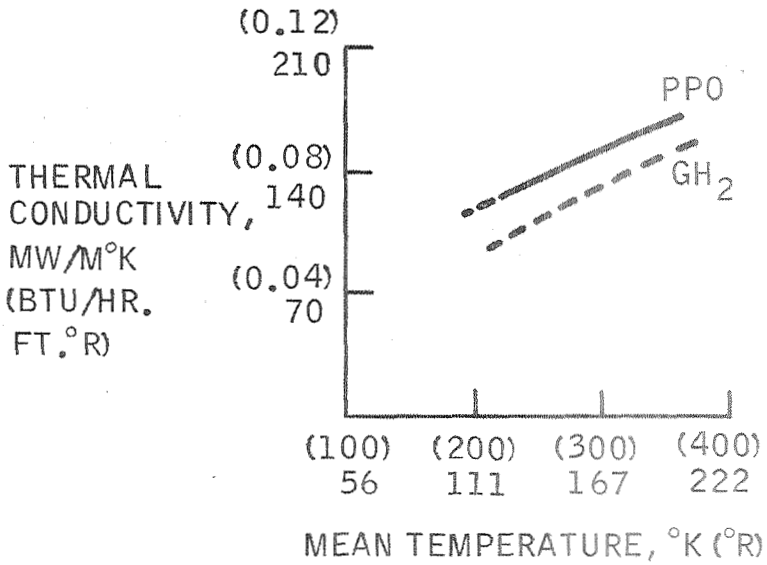

CONCLUSIONS

The feasibility of using PPO foam as an internal open-cell LH_2 tank insulation has been demonstrated. It has a competitive $k \times \rho$ product among the candidate shuttle tankage insulations. It is a tough material with good cryogenic properties and can be easily cut, formed and bonded. It is a simple single component insulation system which does not require seals or reinforcement. Thus, it has a maximum potential for reusability.

CONCLUSIONS

- PPO FOAM FEASIBILITY DEMONSTRATED FOR LH_2 TANKS
- COMPETITIVE $k \times \rho$ PRODUCT
- TOUGH MATERIAL, GOOD CRYOGENIC PROPERTIES, EASILY FABRICATED
- SIMPLE SINGLE COMPONENT INSULATION - MAXIMUM POTENTIAL FOR REUSABILITY

N71-29617

"INTERNAL INSULATION SYSTEMS FOR LH_2 TANKS" AND "GAS LAYER AND REINFORCED FOAM"

H. H. BARKER

McDONNELL DOUGLAS

J. L. McGREW

D. L. BUSKIRK

J. P. GILLE

MARTIN MARIETTA

TECHNICAL MANAGER

J. M. STUCKEY

MARSHALL SPACE FLIGHT CENTER

THIS PAGE INTENTIONALLY LEFT BLANK

PRECEDING PAGE BLANK NOT FILMED

INTERNAL INSULATION SYSTEMS FOR LH_2 TANKS - GAS LAYER AND REINFORCED FOAM

H. H. Barker, Jr.
McDonnell Douglas Astronautics Company,
Western Division

Dr. J. L. McGrew, Dr. D. L. Buskirk and
John P. Gille
Martin Marietta Corporation, Denver Division

Dr. J. M. Stuckey
Marshall Space Flight Center, Alabama

SUMMARY

Two internal insulation systems which may meet the reusability, maximum temperature, and other requirements for the Shuttle booster liquid hydrogen propellant tank insulation are briefly described. Post service experience, method of fabrication, thermal performance, and the contribution of glass thread reinforcement to strength properties of the current 3-D foam insulation are summarized. Progress made toward upgrading the reinforced foam insulation for Shuttle use is outlined. Heat conditioned polyurethane foam appears to have adequate thermal and dimensional stability at the maximum temperature, and two new adhesives under test combine the needed high temperature properties with processing requirements that appear realistic for Shuttle type vehicles.

The materials selection for the gas layer or capillary insulation, potentially usable on the Shuttle, and another version intended for higher temperature service in a cryogenically fueled aircraft, are described. Tests proving the system feasibility, reusability, and low stressed characteristics (essentially free of pressure induced forces) are summarized. The thermal conductivity obtained is essentially equal to that of the interstitial gas trapped between the tank wall and the cryogenic fuel.

THIS PAGE INTENTIONALLY LEFT BLANK

PRECEDING PAGE BLANK NOT FILMED

INTRODUCTION

With the advent of the Space Shuttle Program, the requirement for reusability was introduced as a prime requisite of cryogenic insulation systems for booster type LH_2 propellant tanks. Based primarily on proposed propellant tank configurations and other considerations, internal insulation seems to afford the best potential of meeting the reusability, reliability, and other requirements. On this basis, efforts have been concentrated on developing and qualifying to Shuttle requirements the following three internal insulation systems: Gas layer or capillary insulation (Martin Marietta Corporation), reinforced (3-D) foam (McDonnell Douglas Astronautics Company), and Polyphenylene oxide (PPO) foam (General Dynamics Corporation). A maximum use temperature of 177°C was placed on the Shuttle insulation. This prevents the Shuttle insulation from requiring additional thermal protection as long as aluminum is the primary metal of construction. The 177°C requirement provides for a 28°C cushion capability above MSFC's accepted use temperature (149°C) for the aluminum alloys. Reinforced foam insulation for the Shuttle differs from the 3-D foam insulation used on the Apollo program primarily in reusability and maximum use temperature requirements. The initial effort on the gas layer insulation system was to develop an insulation for liquid methane aircraft tanks. In this case the Shuttle insulation requirement differs in having both a lower minimum and lower maximum use temperature. In this paper the 3-D foam and gas layer insulation are briefly described; progress to date on developing and qualifying materials and insulation systems to Shuttle requirements are summarized; and future plans are outlined.

EXPERIMENTAL

A. 3-D Foam Program for Shuttle

1. Present 3-D Foam Insulation

The 3-D foam insulation system was developed by the Douglas Aircraft Company for use on internal insulation system for LH_2 tanks of the Saturn S-IV and S-IVB stages. This insulation evolved because no single material was found which would adequately satisfy all the design requirements. Due to the favorable past experience with this insulation system, a program was initiated to upgrade it for use on the Shuttle.

a. Description of 3-D Foam Insulation

The components of this composite insulation are shown in figure 1. It consists of a core of 3-D foam which must have adequate structural integrity while serving as the primary thermal barrier. In the 3-D foam, the polyurethane foam is reinforced in three mutually perpendicular directions with S-glass threads. The liner physically ties the individual segments of the foam together, prevents the formation of cracks in the surface of the foam, and acts as a base for the seal coat. For the S-IV stage insulation, a 181 glass cloth impregnated with an epoxy resin was used. As a weight reduction measure for the S-IVB stage, the liner was changed to 116 glass cloth impregnated with a polyurethane resin. The sealer acts as a barrier to retard hydrogen permeation, inhibit moisture penetration, and provides a cleanable surface. For the S-IV stage, six spray coats of polyurethane resin were used. These were changed for the S-IVB stage to a lighter wipe-on coat of the same polyurethane resin used to impregnate the glass cloth. The 3-D foam is bonded to the tank wall with an epoxy adhesive.

b. 3-D Foam Insulation Experience

A summary of 3-D insulation service experience is presented in figure 2. Each of two battleship vehicles have survived over 100 cryogenic loadings; the all-systems vehicle 30 loadings, and each flight stage a minimum of 2 and maximum of 6 loadings. Except for the delamination of the seal coat on the first battleship vehicle, no significant degradation has been encountered. This composite insulation system has been proven for ground hold operation and has functioned for both the boost phase and orbital flight on the Saturn program. The insulation system has been demonstrated to be highly reliable and efficient for repeated cryogenic exposures and a variety of environmental conditions.

c. Fabrication of 3-D Foam

The 3-D foam insulation is fabricated by McDonnell Douglas Astronautics Company at Huntington Beach, California. Figure 3 shows the glass reinforcement in the 3-D foam. The frame of the hand strung 3-D glass thread matrix is placed over a cavity containing machine-mixed polyurethane foam components. The expanding foam rises through the glass fibers. The foam blocks are cut and contoured into tile thickness of approximately one inch. The tiles are post cured for one-hour at 190°F.

d. Mechanical Properties

The effects of the 3-D reinforcement on mechanical properties are clearly shown in figure 4. When compared to an unreinforced foam of eassentially the same density, both the tensile and compressive strengths of the reinforced foams are increased. Reinforcement has little or no effect on shear properties. The elongation and compressibility of the foam are also decreased by reinforcement.

e. Thermal Effectiveness

The thermal effectiveness of the 3-D foam insulation as calculated for Saturn S-IV and S-IVB stages is presented in figure 5. These data show that the thermal conductivity appears to be approaching that of helium gas. Due to the use of a helium purge, the 3-D foam is probably nearly saturated with a combination of helium and hydrogen gas, and accordingly should have a conductivity greater than pure helium. On longer exposure it is expected that the thermal performance would tend to more nearly approach that of the gases.

2. Development of Shuttle 3-D Foam

Since previous experience has shown that the present 3-D foam insulation system is highly reliable and reusable, tests were run to determine the maximum usable temperature of the present 3-D system. These tests showed that the present system is limited to a maximum use temperature of around 93 to 107°C (200 to 225°F) which is well below the 177°C goal for the Shuttle.

a. Materials Investigation

To upgrade the high temperature capabilities of this system, maximum use is being made of the experience gained over the past 10 years from working with this composite. The apparent key problem areas for developing the insulation for the Shuttle are reusability and a maximum service temperature of 177°C. These constraints formed the baseline for the materials development program. Accordingly, each element of the composite is being separately investigated.

(1) Foams:

A survey was conducted of commercially available foams and foamable materials including polyurethanes, phenolics, epoxies, polyimides, and polybinzimidazoles. The first foam materials investigated were the polyurethanes, which were used extensively in the Saturn program. The materials were evaluated by thermogravimetric analyses, thermomechanical analyses, differential scanning calorimeter, isothermal oven tests, thermal expansion tests and multiple and continuous high temperature exposures. Unreinforced foams have been used during most of the testing with no compromise of technical results to avoid the expense of fabricating 3-D foam.

Figure 6 shows typical weight loss data during isothermal heating of the various polyurethane foams. The lower curve shows that most of the new so-called high temperature polyurethane foams tended toward a continuous decomposition with time during isothermal exposure. The tendency of two new foams to exhibit a stabilization in weight loss is indicated by the middle curve. The present 3-D foam insulation also tends toward weight stabilization as shown in the upper curve. Excessive weight loss in the foam is undesirable due to attendant degradation of the strength and thermal properties. It is also possible that the expelled gases may contribute to pressure build-up which may tend to cause either debonding of the foam to the tank wall or the liner to the foam. Most of the foams tend to expand or grow when exposed to heat. Those foams exhibiting a trend toward weight stabilization during heating also exhibited a dimensional stabilization after a prolonged heating cycle. The expansion of the current Saturn S-IVB stage 3-D foam after heat treatment or conditioning is shown in figure 7. Heat conditioned current Saturn S-IVB stage 3-D foam appeared to be usable to about 150°C. Figure 8 shows the expansion characteristics of a new polyurethane foam both initially and after heat conditioning at 177°C. This heat conditioned foam obviously is more stable, has better high temperature properties than heat conditioned current 3-D foam, and should be usable at 177°C.

The significance of the expansion of the foams on heating is that the expansion forces may be sufficient to cause structural failure of the composite (debonding of foam to wall or liner to foam or both). The weight and dimensional stability of conditioned foam offers an interesting and promising application for Shuttle. The effect of conditioning on thermal conductivity is being evaluated along with the capabilities of the composite to survive thermal shock and cryogenic temperatures.

(2) Adhesives

The following target properties governed the selection of adhesives for this study:

(a) Tensile bond strength of at least 6.89×10^5 N/m^2 (100 psi) over the temperature range -253 to 177°C (-423 to 350°F).

(b) Initial set temperature at 49°C (120°F) or below

(c) Post cure temperature not to exceed 149°C (300°F)

(d) Working life of approximately 5 hours in the temperature range of -1.0 to 15.5°C (30 to 60°F).

The 100 psi tensile bond strength requirement is a baseline derived from Saturn program experience. The other items will provide a reasonable installation processing requirement.

The strength characteristics, thermal stability, and softening point of various adhesives were evaluated using thermochemical analyses, lapshear tests, zero load heating tests and tensile bond tests. Some effort has been expended in studying the affects of primers, additives, and new catalysts. Latest testing has concentrated on the 177°C tensile bond strength requirement. In figure 9 the results obtained with 2 promising candidate adhesives with heat treated 3-D foam are shown. Also included are typical data obtained over the temperature range with the present S-IVB 3-D foam insulation system (adhesive, 3-D foam and liner). This shows that the current 3-D foam is unacceptable and one of the new adhesives appears marginal at 177°C. The two new adhesives also generally meet all the other previously listed requirements for initial set, post cure, and working life. Verification of cryogenic strength properties are in progress. Additional effort will be conducted to study the effects of aging upon repeated cycling from cryogenic temperature to 177°C.

(3) Weight Reduction

All the foams being evaluated are nominal 2 lb/cu. ft. density. The foam used in producing the current 3-D foam has a nominal 3 lb/ft^3 density. By using a low density foam, the weight of the installed insulation should decrease by approximately 20-25%, assuming no changes in the combined weights of the adhesive and liner occurs.

b. Future Plans

In the development and qualification of materials and the insulation system, maximum use will be made of previous experience using the 3-D system in the Saturn-Apollo program. Future plans are as follows:

(1) Finalize materials for 177°C Shuttle insulation
(2) Develop fabrication and installation processes
(3) Perform structural and thermal verification tests
(4) Qualify service and repair procedures
(5) Define tank surface preparation requirements
(6) Medium scale tank test to demonstrate installation processes and to show that the installed insulation system is effective, reliable and reusable when exposed to Shuttle environments.

B. Gas Layer Insulation Program

Another insulation system having certain potential advantages for use on the Shuttle is the gas layer or capillary insulation. This system, called MARCAP by the Martin Marietta Corporation, is a unique, lightweight, unevacuated, internal insulation concept for cryogenic fuels. This novel approach utilizes capillary forces to position a gas layer between the contained liquid cryogen and the tank wall.

Some of the potential advantages are: low stressed system, lightweight, reusable, and usable over a wider temperature range than other similar insulations. In addition to this Shuttle effort, the NASA-Lewis Research Center has funded a program (NAS3-12425) to develop a similar insulation for cryogenically fueled aircraft.

1. Description of the Gas Layer or Capilliary Internal Insulation System

a. Basic Concept

The basic concept is illustrated in figure 10. It consists of a cellular material forming discrete and separate cells (such as honeycomb) attached to the tank wall, and a capilliary cover membrane attached to the liquid side of the cellular material. This membrane is perforated with one or more openings per cell. A structurally stable liquid/gas interface forms at each of the openings, preventing the entry of liquid into the cell and thereby positioning a layer of gas between the liquid and the tank wall. Because pressure is equalized across this interface (except for a very small capilliary pressure difference), the system is essentially free of pressure induced structural loading.

b. Thermodynamic Consideration

Figure 11 shows another veiw of the gas layer insulation. When a quantity of cryogen is added to the tank, the liquid contacts the capillary cover shown in the figure on the right side. The gas in the cell cools and contracts, and some liquid enters the cell through the hole, where it boils. The gas, produced by boiling cryogens, pressurizes the cell and liquid is held out of the cell. Probably an excess of liquid intake occurs. In the initial cooldown, the gas bubbles flow from the cell until all the liquid is evaporated. Equilibrium is then established with a liquid/gas interface at each opening. This equilibrium is shown more clearly in the expanded view on the lower left of figure 11. When the pressure in the tank is decreased after equilibrium interfaces have been established, gas will bubble from the insulation cells to obtain a new state of equilibrium. Repressurization results in a sequence of events similar to the initial cooldown of the system.

c. Heat Transfer

When a gas layer is established between the liquid and the tank wall, liquid conductive and convective heat transfer is eliminated in the insulated region. Gas convection can be minimized by use of a very small honeycomb cell size or by filling the cells with a material to restrict gas flow. Experience shows that reduction of cell size to control free convection is impractical, but that a low density opaque batting material is a convenient means for reducing convective and radiant heat transfer. With convective and radiative heat transfer minimized, and because of the small solid cross sectional area of the honeycomb material, gas conduction is the primary mode of heat transfer. Tests have indicated that a thermal conductivity equal to that of the interstitial gas can be closely approximated.

d. Structural Considerations

Since only a small static pressure difference can exist across the capillary interface, the loading across the membrane due to pressure changes depends on the area of the openings and the cell volume. Rapid pressure cycle tests that have been conducted, as well as analytical predictions, indicate that this pressure loading condition is not severe. In addition to these two sources of pressure loading on the structure, there is a bouyancy effect for cells mounted on the tank wall. In come cases, slosh forces may also constitute one of the significant loadings on the insulation structure. However, under no circumstances is the insulation system called on to withstand the tank operating pressure. Because these loads are small, a very light cellular structure can be used. Thermally induced stresses are minimized by providing flexible members (honeycomb) and excess material in the capillary cover. Dimpling of the cover film is required for each cell, thus, making it possible to accommodate thermally induced contraction and expansion without inducing significant stress.

2. Insulation Test Program For Shuttle

Many materials were evaluated and numerous tests designed to establish the adequacy of gas layer insulation under expected environmental and load conditions. Since structural integrity and material compatibility are the primary considerations for long term reliability, effort has been concentrated in these areas.

a. Materials Selection

In figure 12 the materials under study for both the aircraft and Shuttle insulation systems are listed. To determine the suitability of materials to the expected environment, all materials were first subjected to thermogravimetric analysis and differential scanning calorimeter tests to determine the threshold of chemical changes. Materials which showed indications of chemical changes at or below their intended service temperatures were disqualified. Film materials which passed these tests were subjected to thermal expansion and tensile tests over the anticipated service temperature range. These tests were run both before and after they were subjected to extended thermal cycle tests in their intended environments. The adhesives were subjected to the same tests except lapshear tests were substituted for tensile tests.

The 177°C temperature requirement for the Shuttle allowed a much wider consideration of materials than that of the aircraft with a 371°C maximum temperature requirement. Kapton is the preferred honeycomb material for both insulation systems based on its low and high temperature characteristics. Kapton is also the best cover film material based on strength, coefficient of expansion, and chemical compatibility. However, it is very difficult to dimple and

dimpling of the cover film is required to minimize thermal contraction and expansion stresses. Therefore, Kapton core material and Teflon capillary cover film were selected for the Shuttle insulation system.

All room temperature curing adhesives tested were found to be inadequate at 177°C. Several adhesives with elevated cure temperatures were satisfactory, e.g., epoxy phenolic and some epoxies. An adhesive for the 177°C Shuttle insulation system has not yet been found that meets all processing targets. Some of the more promising adhesives being investigated for 3-D foam insulation are under consideration. The high temperature cures and post cures required for the polyimide adhesives employed in the aircraft insulation version eliminate them from the Shuttle insulation.

The materials used in the aircraft insulation can also be used as a higher temperature version of the insulation for potential use on advanced Shuttle vehicles not limited to aluminum alloy. For the aircraft insulation there are about 35 cells/foot in the core. For the Shuttle it is planned to use only 9 cells/foot in the core. However, recent tests have indicated that it may be advantageous to use a smaller cell size core for the Shuttle to insure an adequate bond of the capillary cover to the core.

2. Structural and Thermal Verification Test

Practically all structural and thermal verification tests to date have been performed under the NASA-Lewis Research Center contract using the aircraft insulation, pending final selection of an adhesive for the Shuttle insulation. Pressure cycle tests have been run on 19-inch diameter domes insulated with the aircraft version of the insulation. One of the insulated domes that has been tested is shown in figure 13. The insulated dome is installed on the bottom of an insulated double-walled pressure chamber of the test apparatus illustrated in figure 14. Either LN_2 or LH_2 can be used in the test chamber, although most of the testing has been done with LN_2. External heat is applied to the insulated dome, and for the aircraft insulation the maximum test temperature is 371°C. Chamber pressure is cycled from one atmosphere to 30 psig (2.07×10^5 N/m^2 gage) at a rate of pressure change of 50 psi (3.50×10^5 N/m^2) per minute. Repeated pressure cycle tests have shown no thermal performance degradation and no debonding of the insulation.

Insulated domes have been subjected to 140 - decibel accoustical vibrations both before and after several pressure cycle tests without encountering damage or change in thermal conductivity.

Insulation specimens have been subjected to thermal shock tests using the test equipment shown in figure 15. The skin for the aircraft insulation is heated to 371°C, and is then lowered into liquid nitrogen. When the skin cools to approximately room temperature the test sample is withdrawn and the cycle is repeated. The time required for one complete cycle is approximately three minutes. Specimens have undergone 5000 cycles without failure.

c. Future Plans

Future plans are as follows:

(1) Finalize materials selection for 177°C Shuttle insulation

(2) Develop fabrication and installation processes

(3) Complete structural and thermal verification tests

(4) Develop servicing and repair techniques

(5) Define procedures for tank surface preparation

(6) Conduct medium scale tank tests with LH_2 simulating pressure cycling and aerodynamic heating

(7) Minor effort on developing 343°C insulation for advanced Shuttle vehicles.

CONCLUSIONS

A. 3-D Foam Insulation

1. Use on Shuttle appears feasible

2. Development of an improved version usable at 177°C seems likely

3. Procedures for fabrication and installation of the insulation are already available from the Saturn program and are directly applicable to Shuttle.

B. Gas Layer Insulation

1. Results to date show concept feasibility and indicate the system is reusable and reliable

2. Gas layer insulation appears somewhat lighter than 3-D foam and will probably have a thermal conductivity only slightly greater than that of the gaseous cryogen

3. This general insulation approach appears usable at temperatures up to 343-371°C with current available materials.

20296

INTERNAL INSULATION COMPOSITE CONCEPT

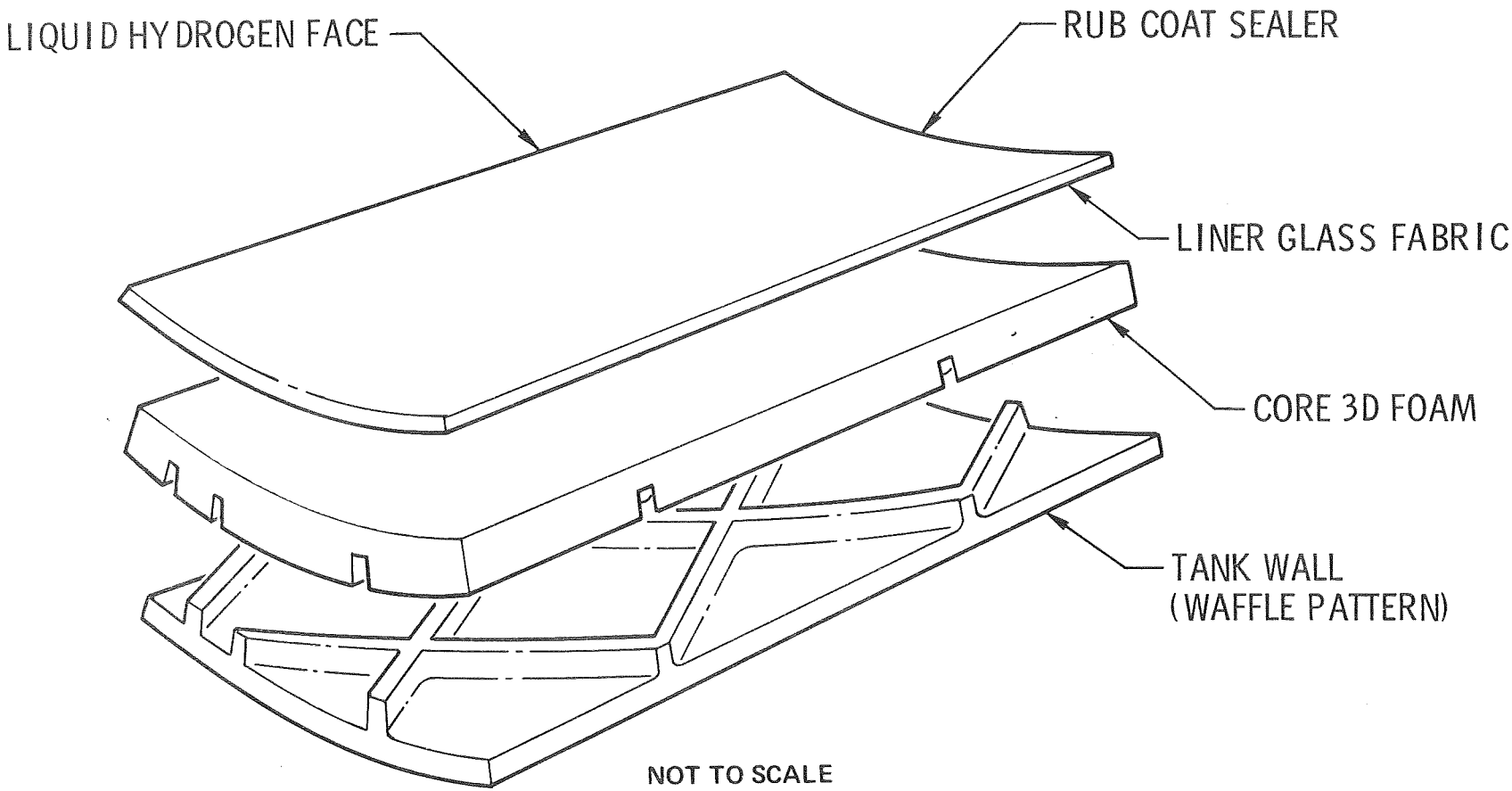

FIGURE 1

SUMMARY OF 3-D INSULATION SERVICE EXPERIENCE

VEHICLE	INSULATION DESCRIPTION	APPROXIMATE NUMBER OF LOADINGS	APPROXIMATE NUMBER OF FIRINGS	INSULATION DEGRADATION
FIRST BATTLESHIP VEHICLE	181 FIBERGLAS LINER 70% BY WEIGHT EPOXY RESIN	60 AT SACRAMENTO 100 AT TULLAHOMA	15 AT SACRAMENTO 350 AT TULLAHOMA	SEALER COATING PEELED OFF AT DELIVERY TO TULLAHOMA. REPAIRED. SAME CONDITION AFTER 100 LOADINGS AT TULLAHOMA
SECOND BATTLESHIP VEHICLE	181 FIBERGLAS LINER, 50% BY WEIGHT EPOXY RESIN	135 AT MSFC	120 AT MSFC	NO SIGNIFICANT DEGRADATION
ALL SYSTEMS VEHICLE	116 FIBERGLAS LINER, 50% BY WEIGHT POLYURETHANE RESIN	30	15	NO SIGNIFICANT DEGRADATION
PRODUCTION SATURN S-IVB STAGE	116 FIBERGLAS LINER, 50% BY WEIGHT POLYURETHANE RESIN	MAXIMUM OF 6 PER STAGE	MAXIMUM OF 2 PER STAGE	NO SIGNIFICANT DEGRADATION OF STAGES FLOWN TO DATE

FIGURE 2

NOT REPRODUCIBLE

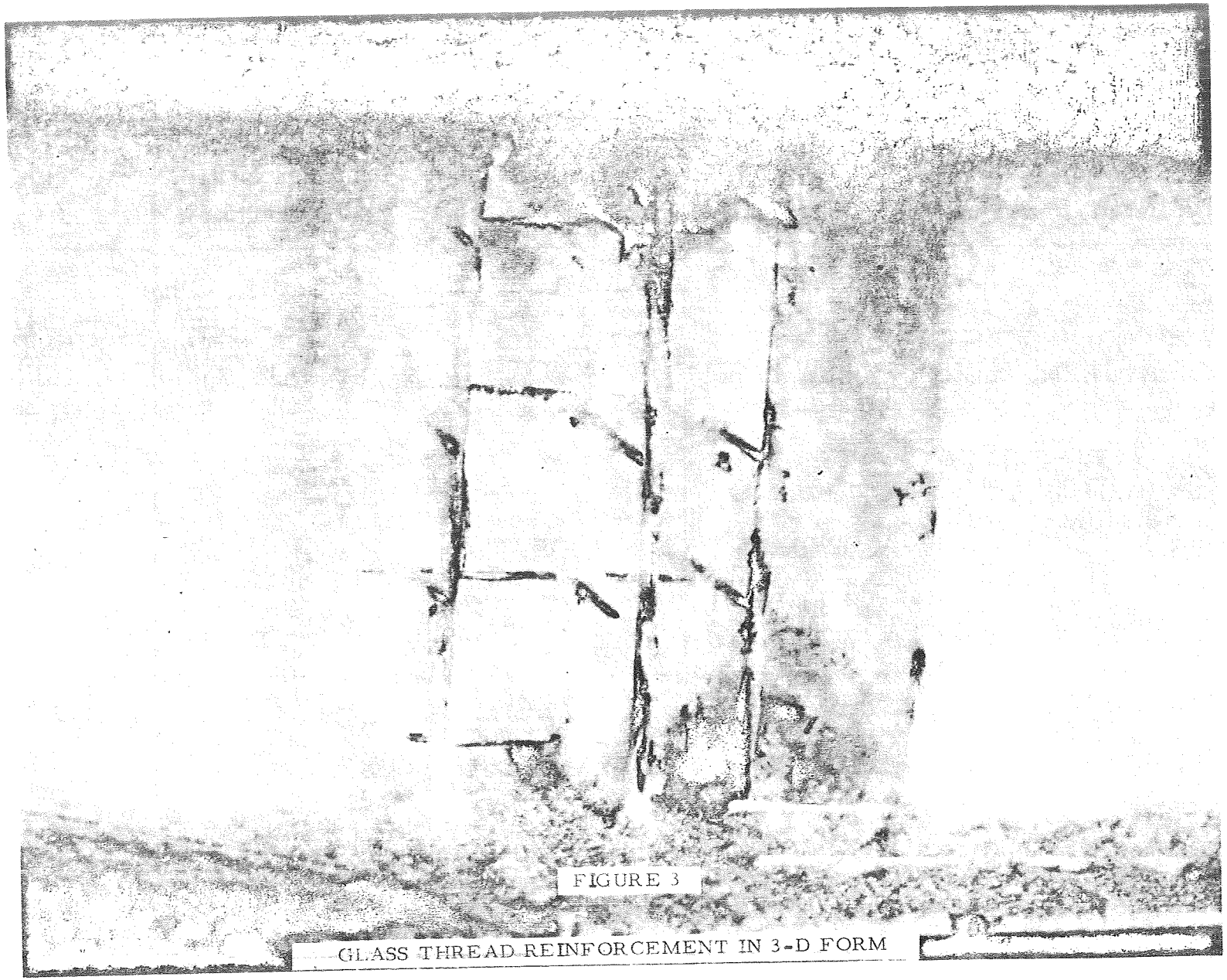

FIGURE 3

GLASS THREAD REINFORCEMENT IN 3-D FORM

3-D FOAM PROPERTIES

PROPERTY	UNREINFORCED FOAM	3-D FOAM
	$6.4\text{-}8.0 \times 10^1$ K/m^3	8.32×10^1 K/m^3
	(4-5 Lb/Ft^3)	(5.2 Lb/Ft^3)
TENSILE STRENGTH N/m^2	5.17×10^5 (75 PSI)	6.89×10^5 (100 PSI) Min. (250 PSI) Avg. $>$ (500 PSI) Max.
	10% Elongation	2% Elongation
COMPRESSION STRENGTH N/m^2	5.17×10^5 (75 PSI)	6.89×10^5 (100 PSI) Min. (180 PSI) Avg. $>$ (220 PSI) Max.
	10% Deformation	$<$ 2% Deformation
SHEAR STRENGTH N/m^2	3.5×10^5 (50 PSI)	$\geq 3.5 \times 10^5$ (50 PSI)

FIGURE 4

20301

POLYURETHANE 3-D FOAM MAXIMUM THERMAL CONDUCTIVITY

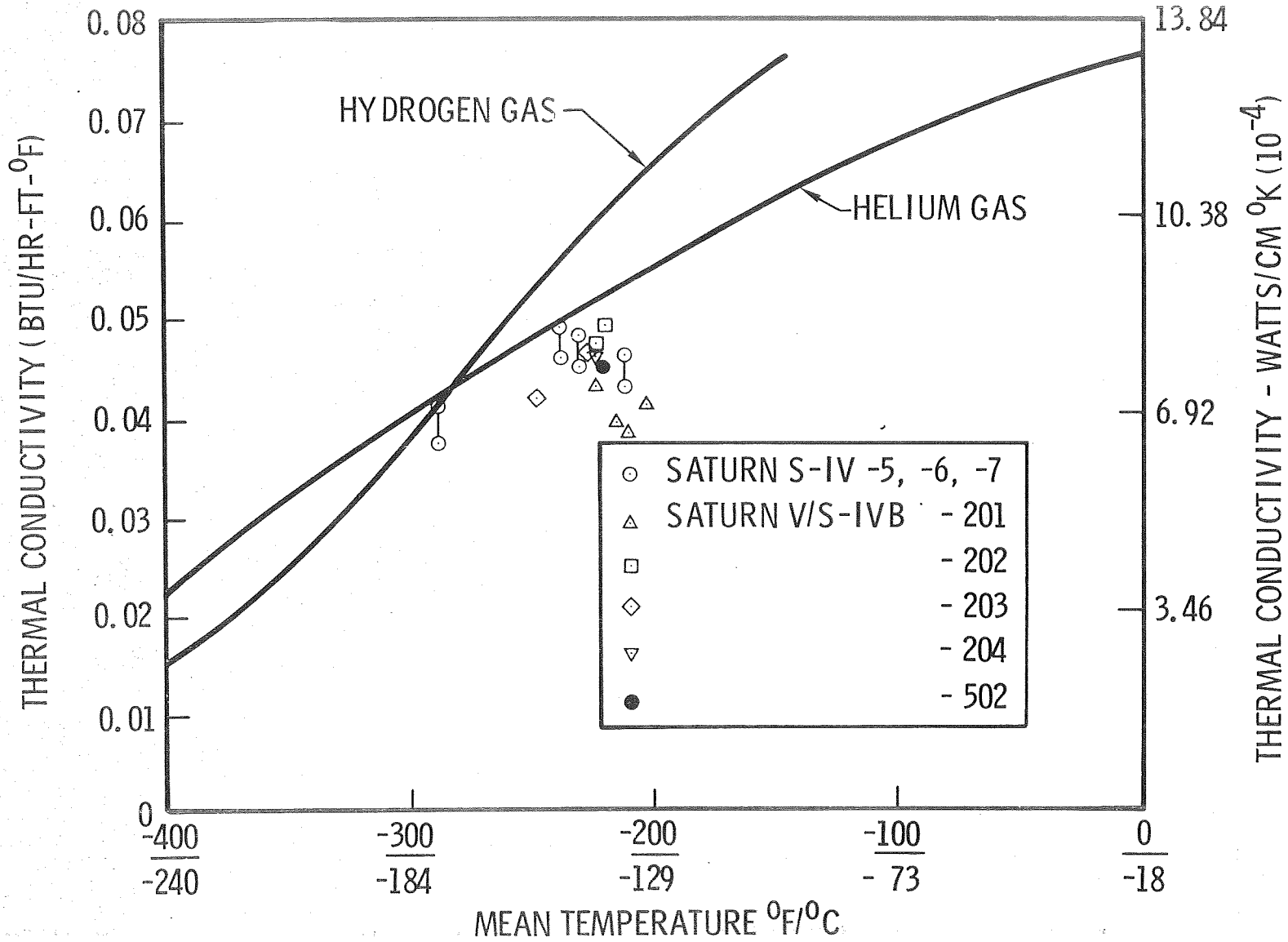

20299

350°F (177°C) ISOTHERMAL TESTS-POLYURETHANE FOAM

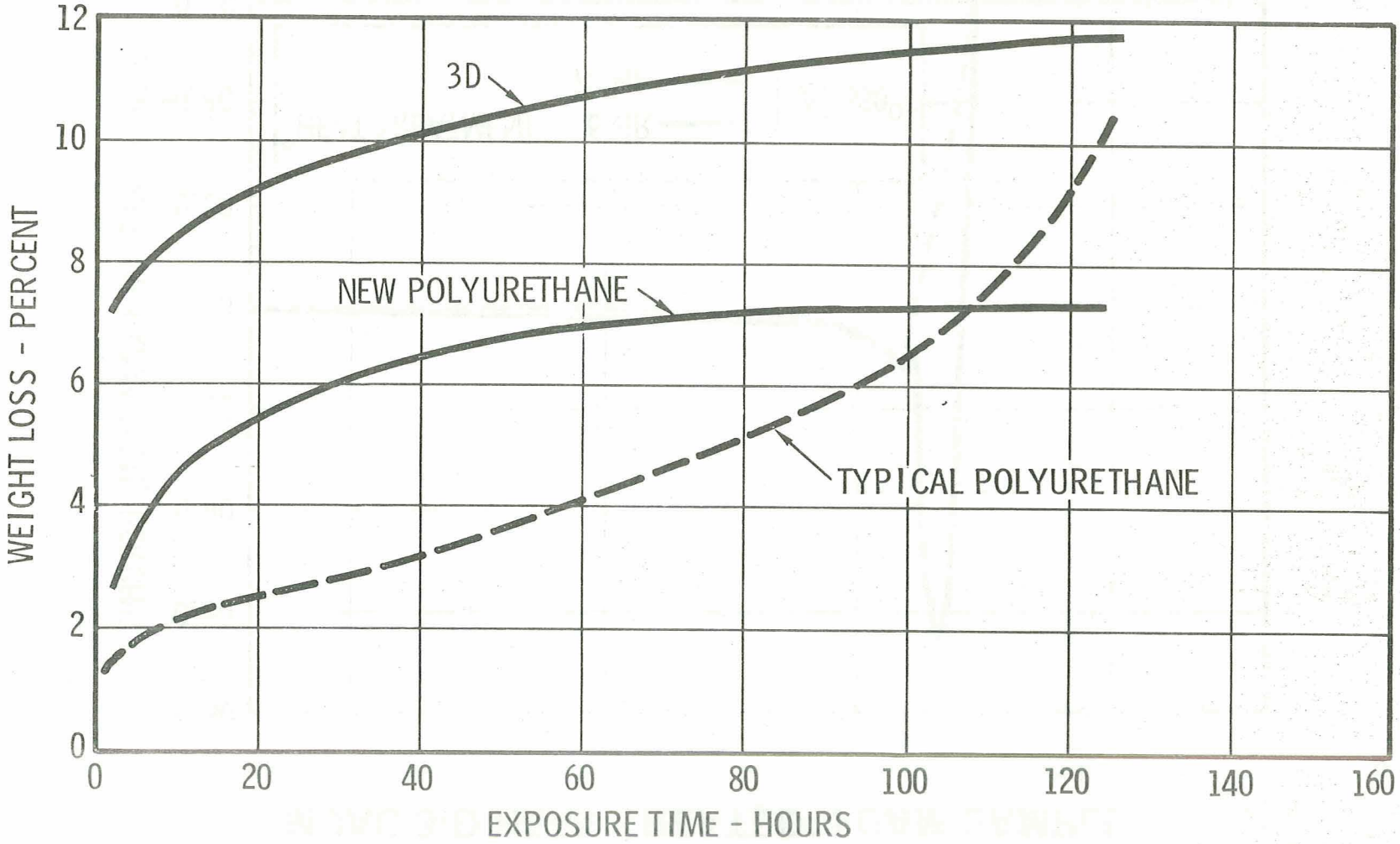

FIGURE 6

20297

LINEAR THERMAL EXPANSION OF MDAC 3-D HEAT TREATED* FOAM SAMPLE

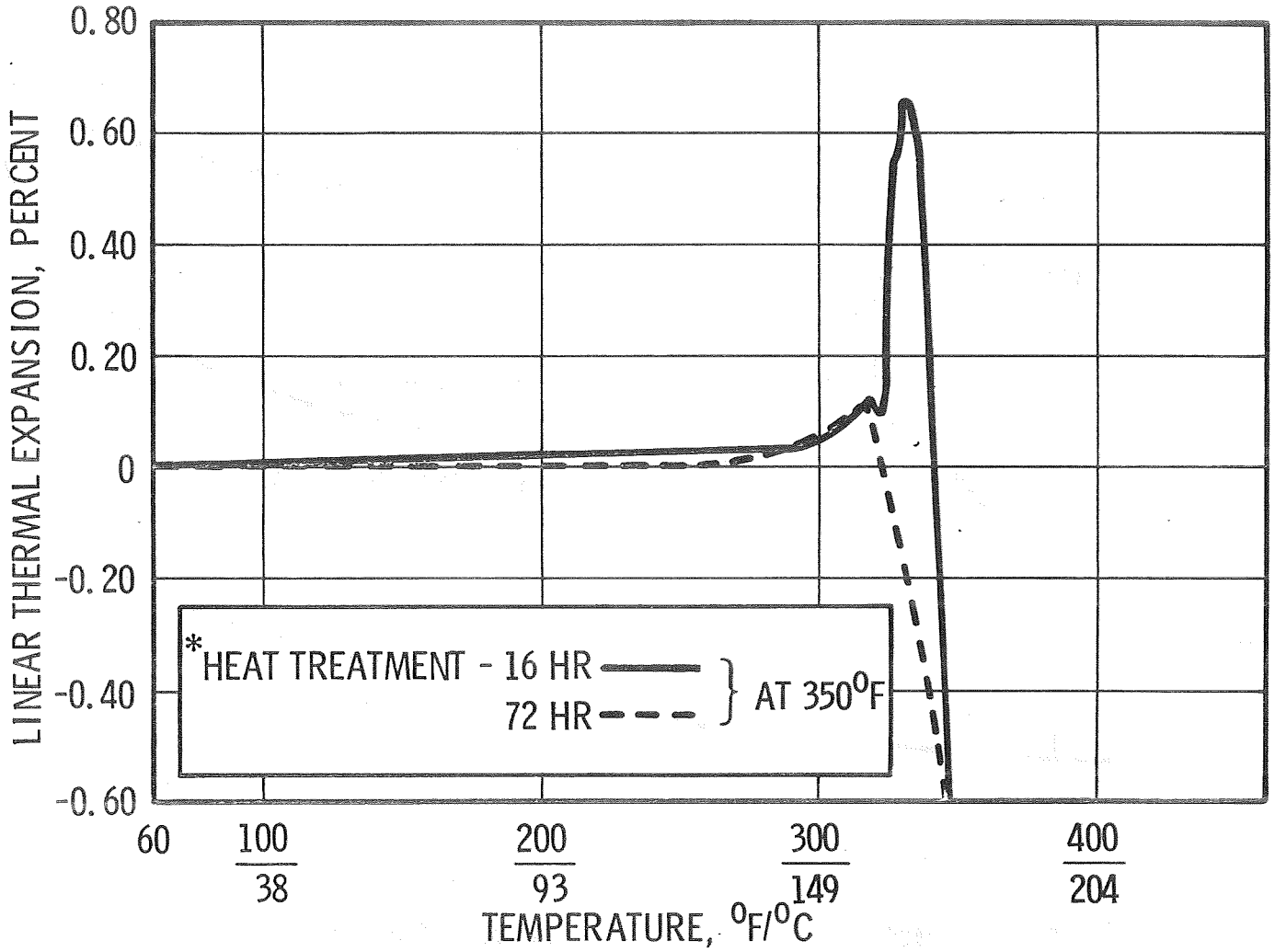

FIGURE 7

LINEAR THERMAL EXPANSION OF NEW POLYURETHANE

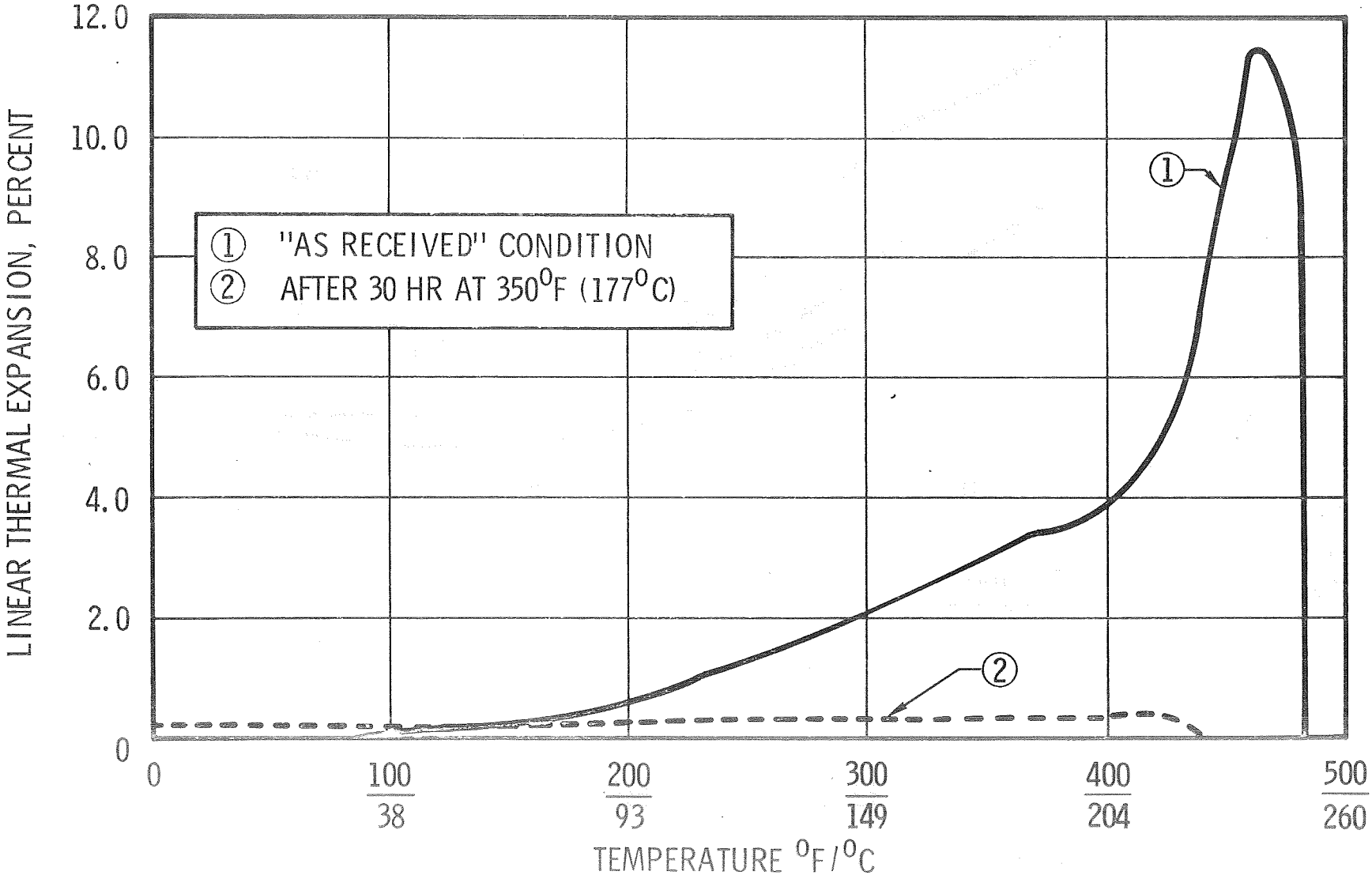

FIGURE 8

20299

TENSILE BOND STRENGTH

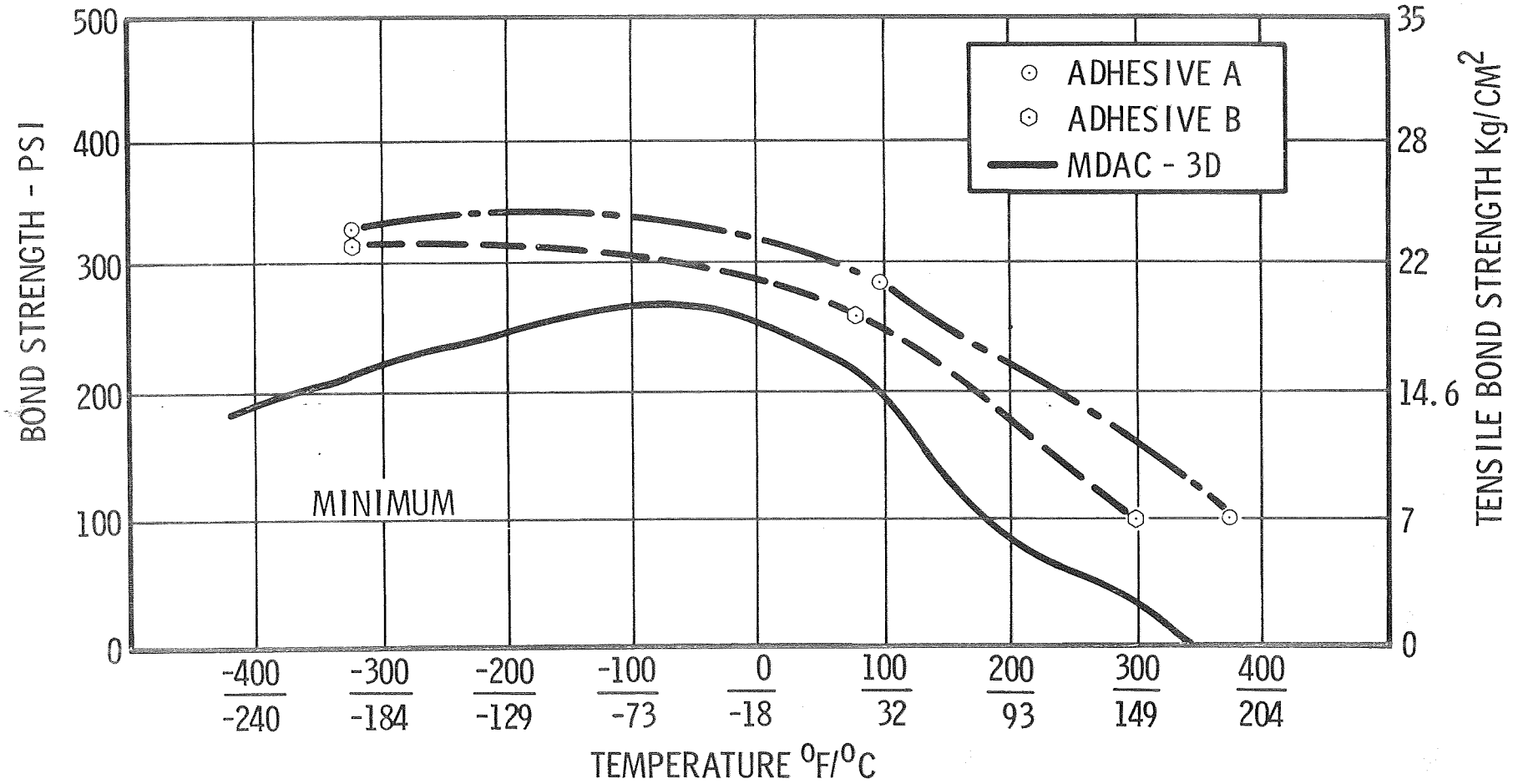

FIGURE 9

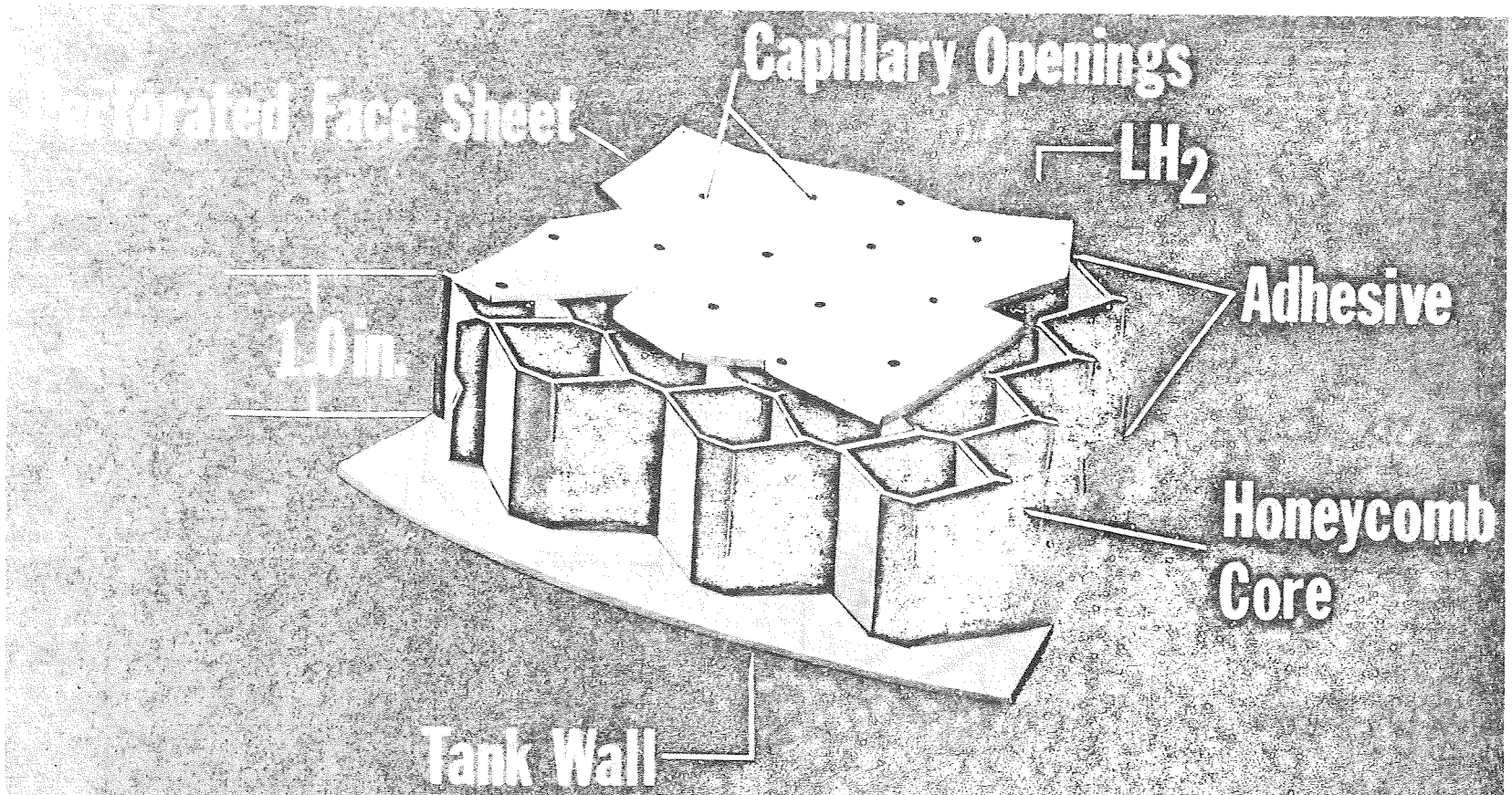

FIGURE 10

GAS LAYER INSULATION

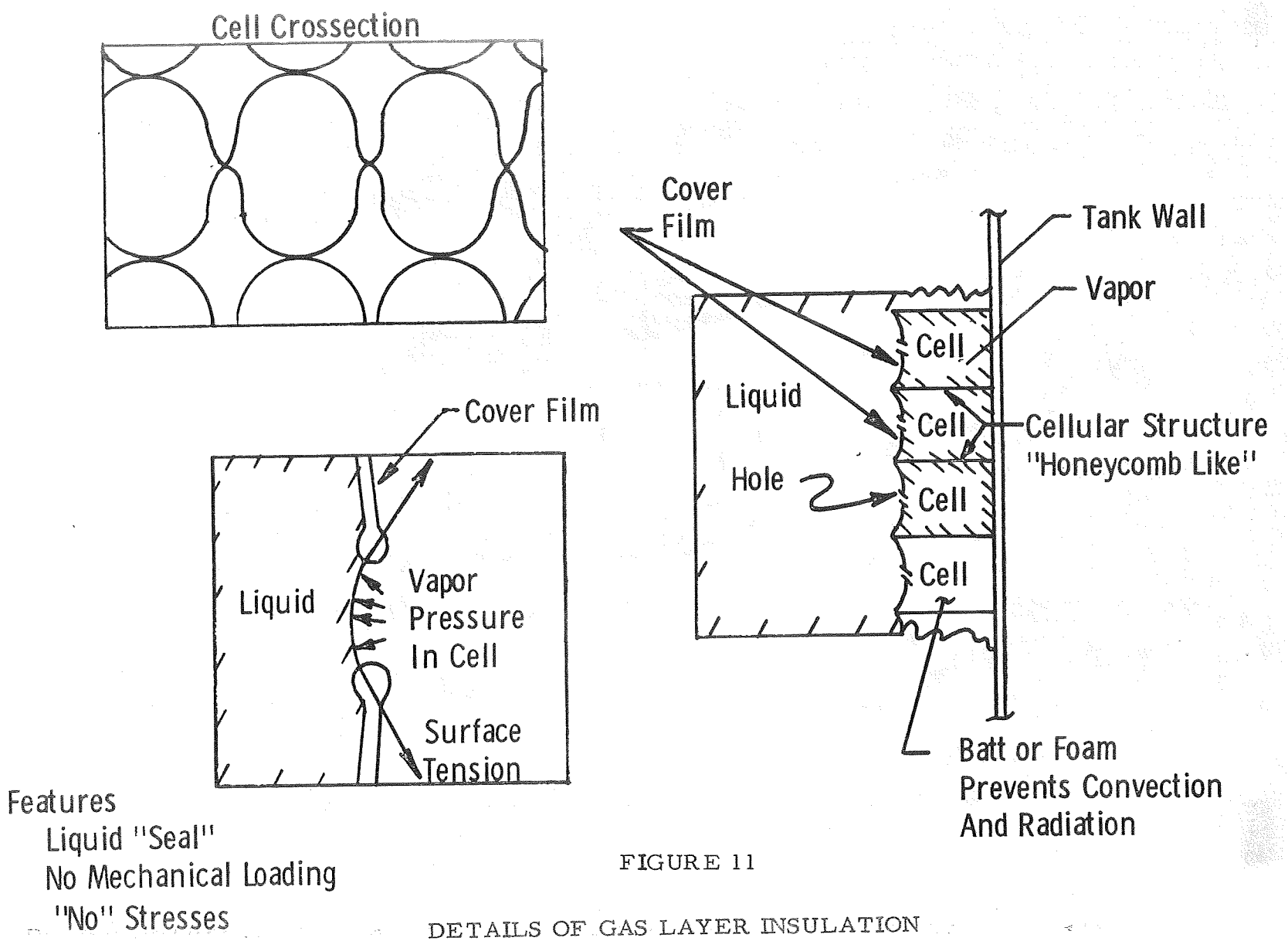

FIGURE 11

DETAILS OF GAS LAYER INSULATION

MATERIALS FOR GAS LAYER INSULATION CONCEPTS

	AIRCRAFT CONCEPT 371°C MAX TEMP	SHUTTLE CONCEPT 177°C MAX TEMP
CORE	KAPTON	KAPTON
ADHESIVE (CORE TO TANK)	POLYIMIDE	NOT FINALIZED
CAPILLARY COVER	KAPTON FILM	TEFLON FILM
ADHESIVE (COVER-TO-CORE)	POLYIMIDE	NOT FINALIZED
CORE FILLER	OPACIFIED BATTING	OPACIFIED BATTING

FIGURE 12

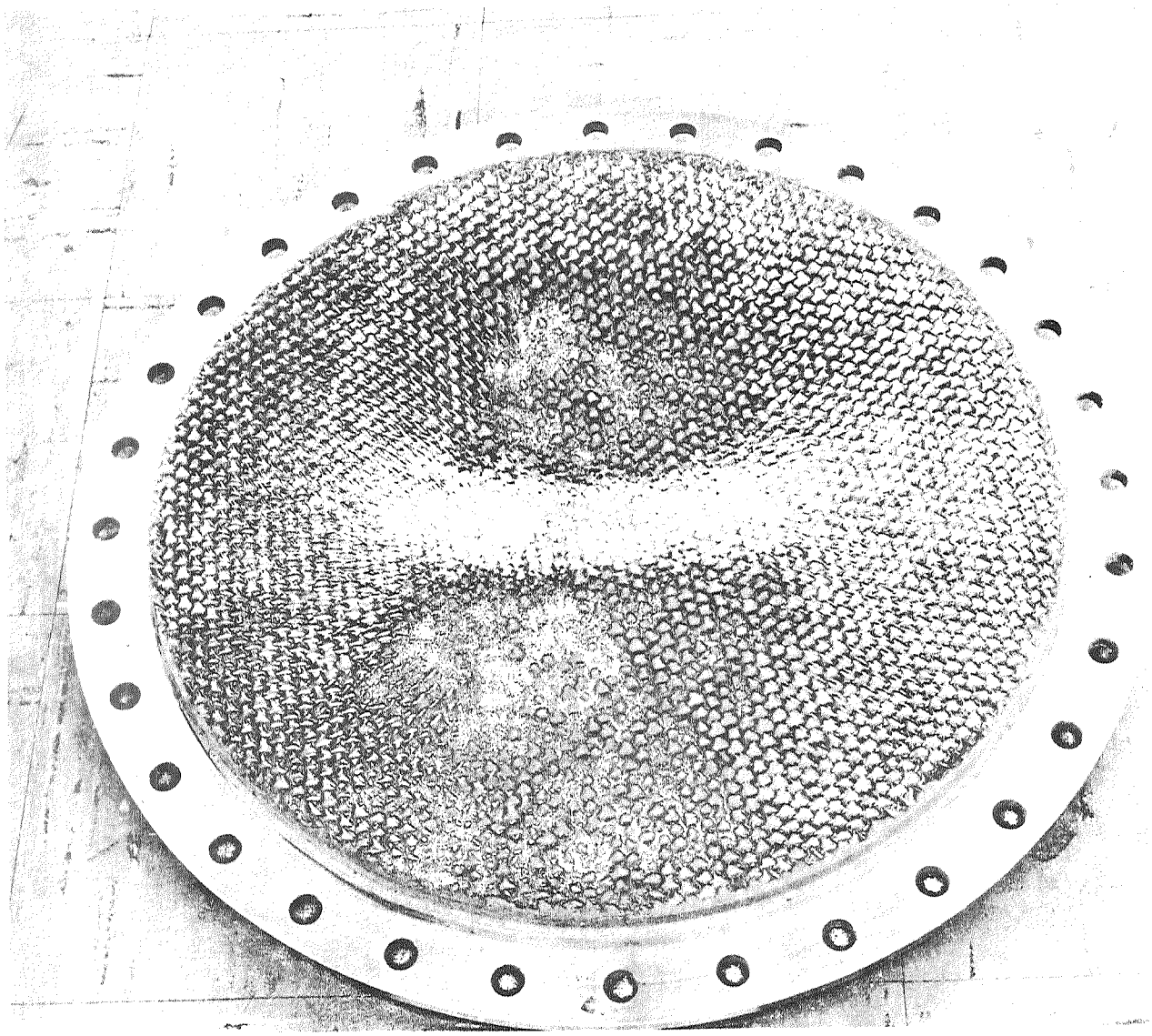

½-in. Polyimide Honeycomb
Polyimide Film
PF105-700 Insulation
(Opacified)

Biaxial Test - LN_2
10-29-69

FIGURE 13

INSULATED DOME SPECIMEN

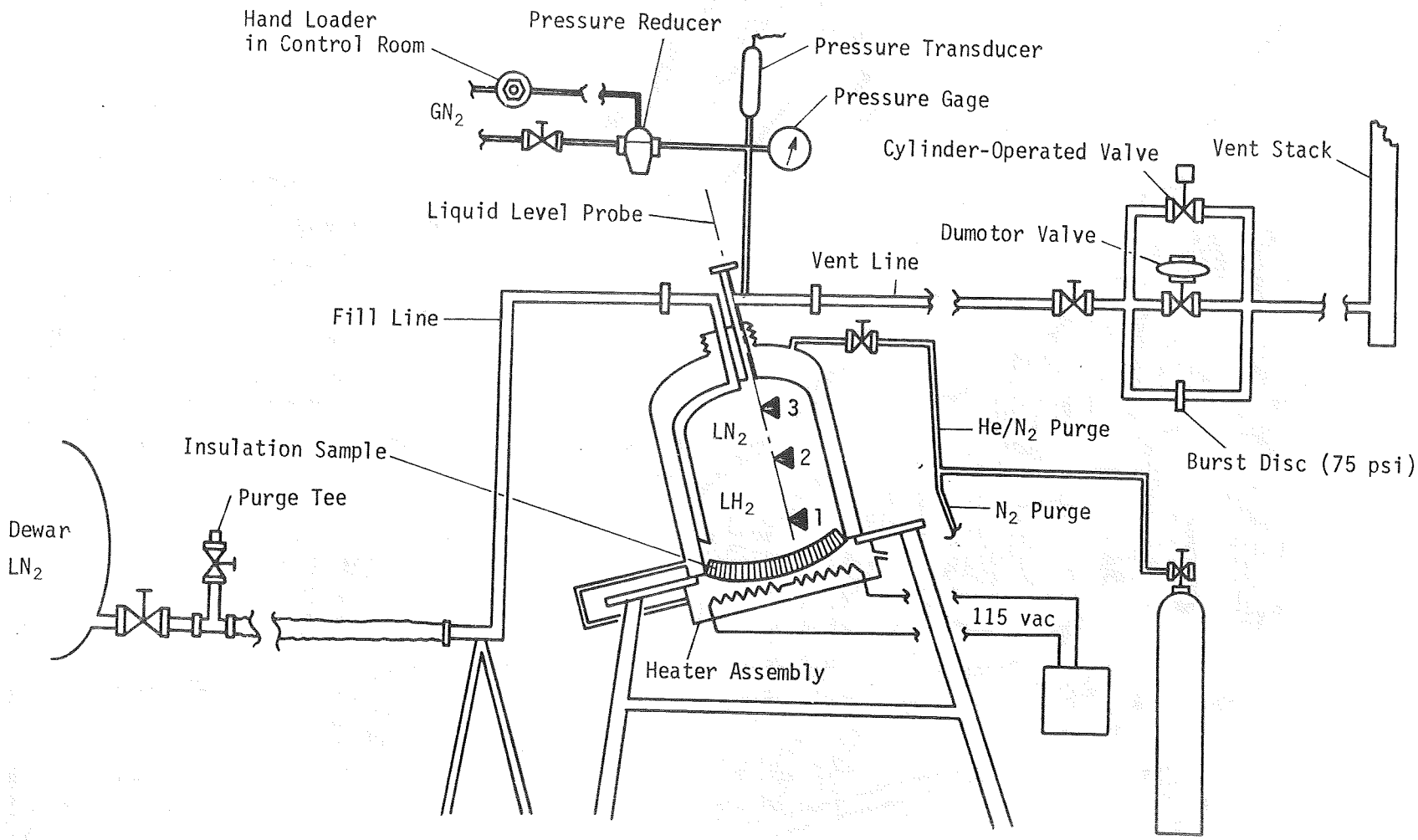

FIGURE 14

PRESSURE CYCLING TEST APPARATUS

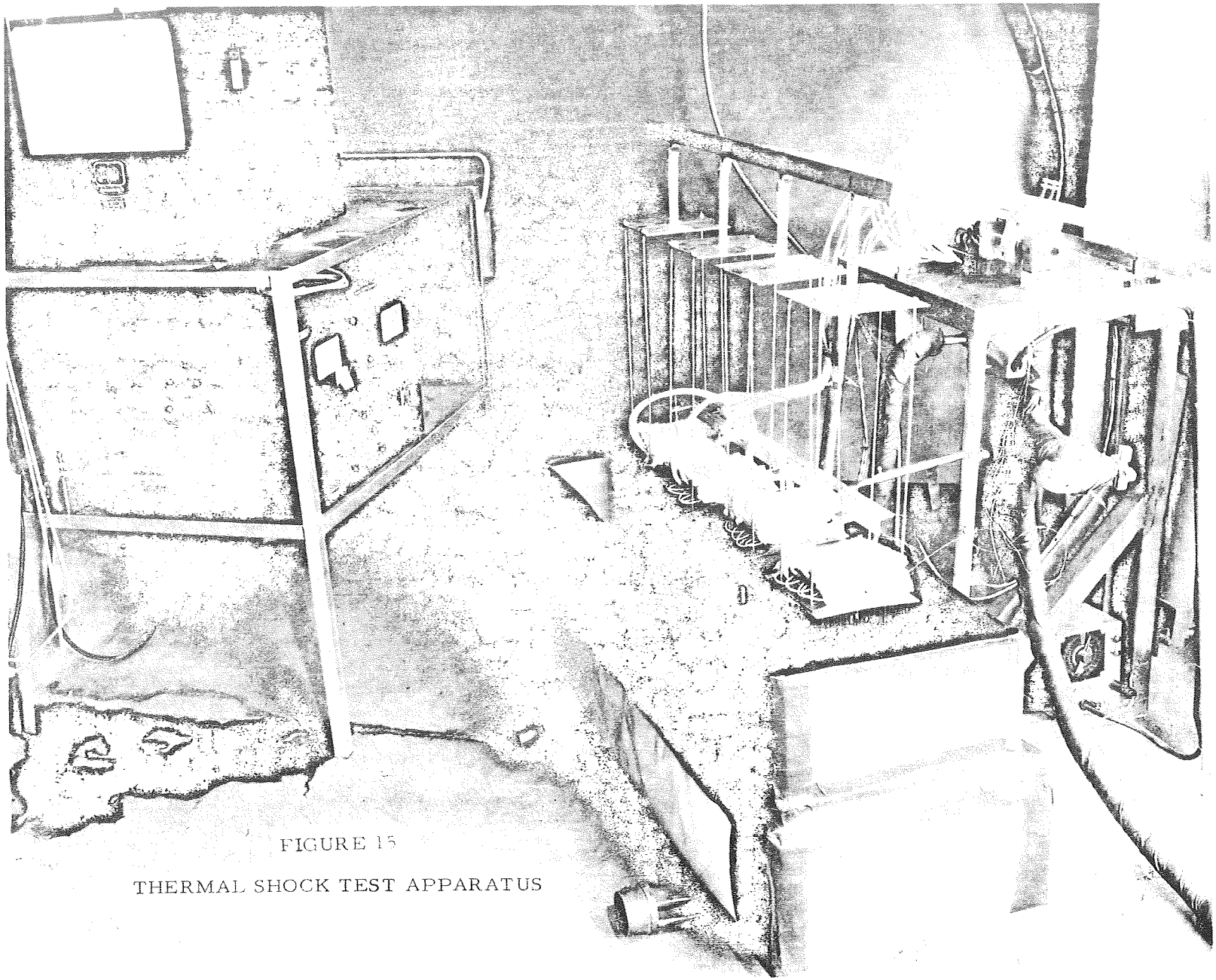

FIGURE 15

THERMAL SHOCK TEST APPARATUS

N71-29618

"SHUTTLE CRYOGEN TECHNOLOGY PROGRAM"

C. C. WOOD

MARSHALL SPACE FLIGHT CENTER

THIS PAGE INTENTIONALLY LEFT BLANK

SHUTTLE CRYOGEN TECHNOLOGY PROGRAM

Charles C. Wood

NASA/Marshall Space Flight Center
Huntsville, Alabama

THE TOTAL SPECTRUM OF ACTIVITY HAS NOT BEEN ADDRESSED IN THE EIGHT PRECEDING PAPERS. THIS PAPER WILL IDENTIFY OTHER AREAS OF TECHNOLOGY WHICH ARE IN PROCESS WHICH WILL BE ADDRESSED LATER AS TANGIBLE RESULTS BECOME MORE PLENTIFUL.

PRECEDING PAGE BLANK NOT FILMED

SHUTTLE CRYOGEN PROGRAM

THE TECHNOLOGY PLAN IS SHOWN. THE MANY AREAS OF INVOLVEMENT ARE CONSOLIDATED FOR CONVENIENCE INTO THE FIVE CATEGORIES SHOWN. THE SHUTTLE TECHNOLOGY REQUIREMENTS SHOULD BE MET BY EARLY 1973 WHICH IS COMPATIBLE WITH THE SHUTTLE DEVELOPMENT SCHEDULE. THE TECHNOLOGY POSTURE IS MORE FAVORABLE IN SOME AREAS DUE TO FUNDAMENTAL TECHNOLOGY PROGRAMS IN PROGRESS AT SHUTTLE INCEPTION AND/OR EARLIER FUNDING FROM THE SHUTTLE TECHNOLOGY PROGRAM.

MARSHALL SPACE FLIGHT CENTER

SCIENCE & ENGINEERING

SHUTTLE CRYOGEN PROGRAM

LAB: S&E-ASTN-P

NAME: C. C. Wood

DATE: 4-7-71

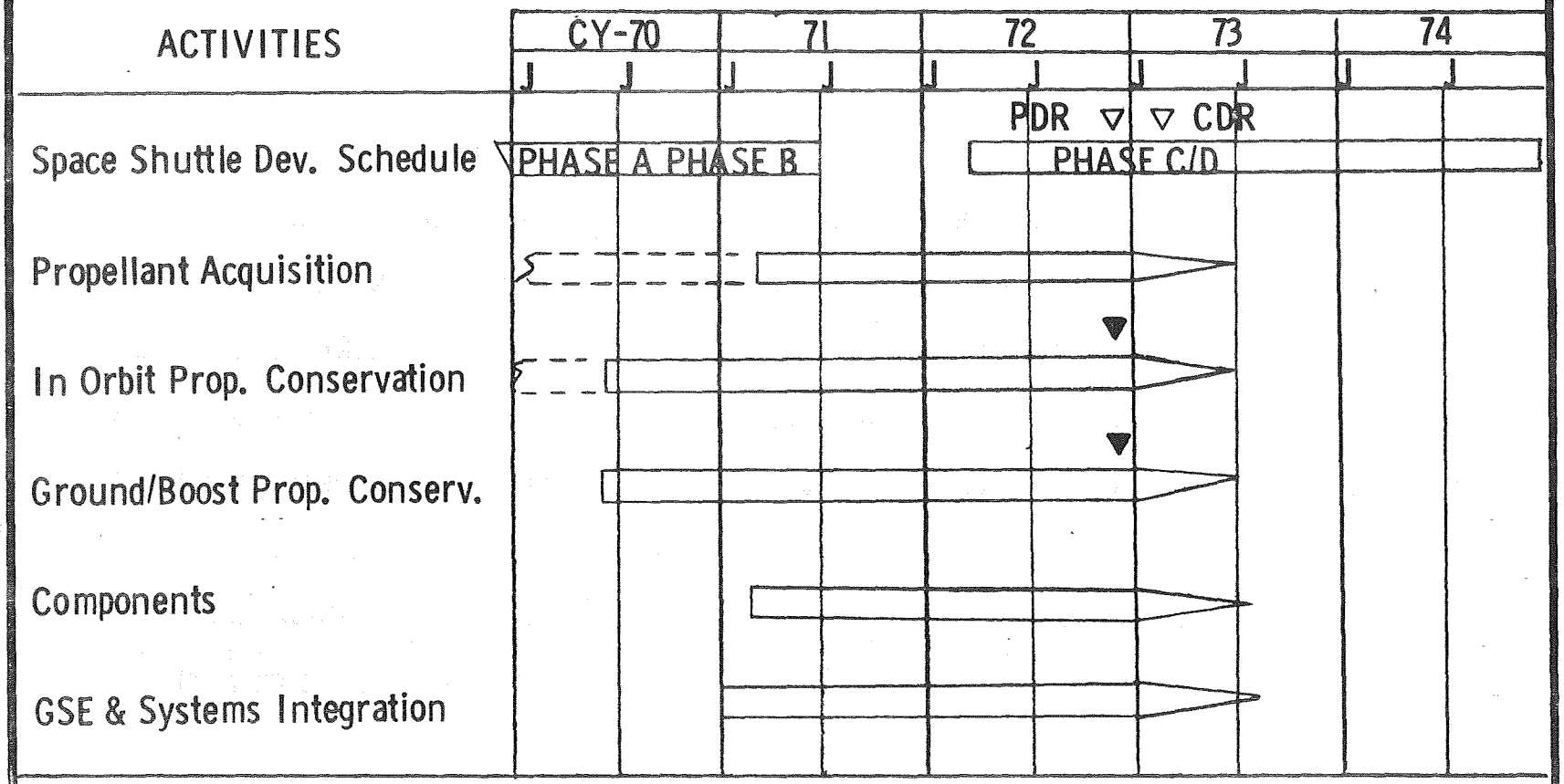

PRE-SHUTTLE EFFORT

SYSTEM DEMONSTRATION

MSFC - Form 3369 (Rev June 1970)

CHART No. _____

CRYOGENIC COMPONENTS

TECHNOLOGY PROGRAMS IN SIX AREAS ARE IN PROGRESS OR PLANNED. THE AREAS OF EMPHASIS AND THE BROAD WORK SCHEDULES ARE SHOWN ON CHART 3. ONLY LIMITED TECHNOLOGY PROGRAMS IN THE COMPONENTS AREA HAVE BEEN CONDUCTED SINCE THE APOLLO PROGRAM AND THE REQUIREMENTS FOR THE APOLLO PROGRAM ARE CONSIDERABLY DIFFERENT FROM SHUTTLE REQUIREMENTS, THUS A SUBSTANTIAL TECHNOLOGY ADVANCEMENT IS NECESSARY. MORE SPECIFICS CONCERNING THE NEEDS AND THE TECHNOLOGY PROGRAMS FOR THE FIRST TWO ITEMS, VACUUM JACKETED DUCTING AND LIFE TEST METHODOLOGY, ARE SHOWN ON THE FOLLOWING TWO CHARTS.

MARSHALL SPACE FLIGHT CENTER

SCIENCE & ENGINEERING

CRYOGENIC COMPONENTS

LAB: S&E-ASTN-P

NAME: C. C. Wood

DATE: 4-7-71

SHUTTLE IMPACT ON REQ.

PRE-SHUTTLE

- SHORT LIFE
- NO RE-USE
- NO MAINTENANCE

SHUTTLE

- LONG LIFE
- LOW LEAKAGE
- MAINTENANCE
- REPAIR

COMPONENTS

- VACUUM JACKETED DUCTING
  - REQUIREMENTS DEFINITION
  - DESIGN, FABRICATE & TEST
- LIFE TEST METHODOLOGY
  - REQUIREMENTS DEFINITION
  - TEST AND EVALUATION
- TANK VENT
  - REQUIREMENTS DEFINITION
  - DESIGN, FABRICATE & TEST
- COMPOSITE FEEDLINES WITH & WITHOUT VACUUM JACKET
  - REQUIREMENTS DEFINITION
  - DESIGN, FABRICATE & TEST
- LONG LIFE VALVE DESIGN
  - REQUIREMENTS DEFINITION
  - DESIGN, FABRICATE & TEST
- REDUCED SEAL LEAKAGE DEV.
  - REQUIREMENTS DEFINITION
  - DESIGN, FABRICATE & TEST

PROGRAM SCHEDULE

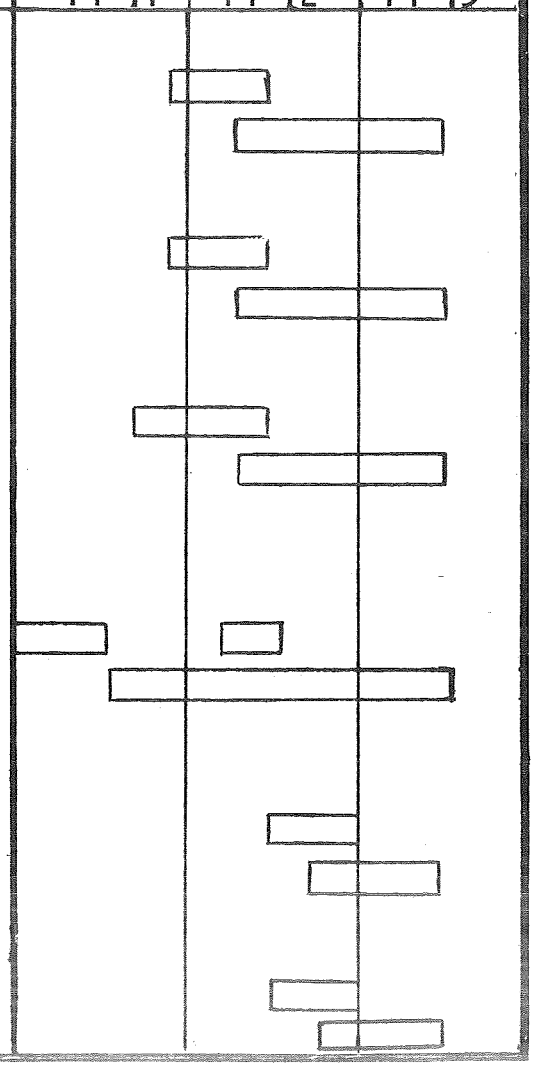

MSFC - Form 3369 (Rev June 1970)

CHART No. _____

THIS PAGE INTENTIONALLY LEFT BLANK

MARSHALL SPACE FLIGHT CENTER SCIENCE & ENGINEERING	VACUUM JACKETED DUCTING	LAB: S&E-ASTN-P NAME: C. C. Wood DATE: 4-7-71

- TECHNOLOGY PROBLEMS
  - HIGH FAILURE RATES EXPERIENCED IN APOLLO PROGRAM NOT ACCEPTABLE TO SHUTTLE
  - MANY APOLLO STAGES REQUIRED VACUUM LINE REPLACEMENT AFTER STATIC FIRING AND AFTER STORAGE
  - RESULTING MAINTENANCE PROBLEMS TOO SEVERE FOR SHUTTLE PROGRAM
- TECHNOLOGY OBJECTIVES
  - DEVELOP DESIGN FEATURES AND FABRICATION TECHNIQUES
    - -- IMPROVE LIFE
    - -- SIMPLIFY MAINTENANCE
    - -- IMPROVE RELIABILITY
- PROGRAM PLAN

	FY 71	FY 72
- MILESTONES		
-- ENVIRONMENT REQ.	●	
-- OPTIMIZE DESIGN OF FLANGES, GIMBALS, SUPPORTS	●	
-- SYSTEM DESIGN	●	
-- CRYOGENIC TEST OF 14" DUCT SEGMENT		●

MSFC - Form 3369 (Rev June 1970)

CHART No. _____

PRECEDING PAGE BLANK NOT FILMED

THIS PAGE INTENTIONALLY LEFT BLANK

MARSHALL SPACE FLIGHT CENTER SCIENCE & ENGINEERING	LIFE TEST METHODOLOGY	LAB: S&E-ASTN-P NAME: C. C. Wood DATE: 4-7-71

- TECHNOLOGY PROBLEMS
  - CURRENT LIFE TESTING PHILOSOPHY IMPRACTICAL FOR SHUTTLE
    - -- LONG LIFE REQUIREMENTS
    - -- EFFECTS OF AGING IN VARIOUS ENVIRONMENTS CANNOT BE RELIABLY ACCELERATED
- TECHNOLOGY OBJECTIVES
  - ESTABLISH PARAMETERS THAT INDICATE ULTIMATE LIFE WITHOUT FULL LIFE TESTING
  - DETERMINE TEST METHODS THAT INDUCE AND/OR SIMULATE RAPID AGING
- PROGRAM PLAN

	FY-71	FY-72
- MILESTONES		
-- ESTABLISH REQ.	●	
-- COMPILE INFORMATION ON AGING OF VARIOUS MATERIALS	●	
-- DEVELOP TEST PLANS AND PROCEDURES		●
-- TEST AND EVALUATION		●

MSFC - Form 3369 (Rev June 1970)

CHART No. _____

PRECEDING PAGE BLANK NOT FILMED

IN-ORBIT INSULATION

THREE DIFFERENT APPROACHES ARE UNDERWAY TO IDENTIFY POTENTIAL CANDIDATES FOR IN-ORBIT LIQUID HYDROGEN AND OXYGEN STORAGE CONTAINERS - THE GAS PURGED CONCEPT OF MULTI-LAYER INSULATION WHICH HAS BEEN DISCUSSED EXTENSIVELY IN ONE EARLIER PAPER; THE HARD OUTER SHELL MULTI-INSULATION (DEWAR TYPE) CONCEPT WHICH IS ALWAYS EVACUATED AND DOES NOT REQUIRE PURGING DURING REENTRY AND GROUND HOLD; THE SELF EVACUATED MULTI-LAYER INSULATION CONCEPT WHICH ALSO DOES NOT REQUIRE PURGING AND WHICH HAS A FLEXIBLE OUTER SHELL AND UTILIZES CRYO PUMPING OF CARBON DIOXIDE WITHIN THE INSULATION FOR ESTABLISHING THE REQUIRED VACUUM. SUBSTANTIAL INSULATION TECHNOLOGY EFFORT PRECEDED THE SHUTTLE PROGRAM; HOWEVER, THE SHUTTLE PROGRAM INTRODUCED ADDITIONAL REQUIREMENTS. THE SHUTTLE IMPACT ON REQUIREMENTS AND THE SCHEDULE FOR THESE PROGRAMS ARE SHOWN ON CHART 6. MORE DETAILS ON THE HARD SHELL INSULATION AND SELF EVACUATED PANEL PROGRAMS ARE SHOWN ON CHARTS 7 AND 8, RESPECTIVELY.

MARSHALL SPACE FLIGHT CENTER

SCIENCE & ENGINEERING

IN ORBIT INSULATION

LAB: S&E-ASTN-P

NAME: C. C. Wood

DATE: 4-7-71

SHUTTLE IMPACT ON REQ.	TECHNOLOGY PROGRAMS	PROGRAM SCHEDULE FY-71	FY-72	FY-73
PRE SHUTTLE	• PURGED MLI			
SHORT LIFE NO REUSE LOW SURFACE TEMP NO REPRESSURIZATION ONE TIME PURGE	REQUIREMENTS DEFINITION DESIGN FABRICATION & TEST			
	• HARD SHELL INSULATION			
	DESIGN DEFINITION FABRICATION & TEST	*		
SHUTTLE	• SELF EVACUATED PANELS			
LONG LIFE REUSE HIGH SURFACE TEMP REPRESSURIZATION MULTIPLE PURGE	EVALUATE EXISTING SCHEMES DESIGN, FABRICATE & TEST			

* Start of MSC LH_2 Program

Start of LeRC Program

MSFC - Form 3369 (Rev June 1970)

CHART No. _____

HARD SHELL INSULATION

THIS CHART PRIMARILY ADDRESSES THE MSC SPONSORED PROGRAM FOR BOTH LIQUID OXYGEN AND HYDROGEN. A COMPLEMENTARY PROGRAM SPONSORED BY LERC DEALS MORE SPECIFICALLY WITH ESTABLISHMENT OF DESIGN PRINCIPLES AND MANUFACTURING METHODS FOR THE HARD OUTER SHELL AS DISTINGUISHED FROM THE TOTAL TANKAGE SYSTEM.

MARSHALL SPACE FLIGHT CENTER SCIENCE & ENGINEERING	HARD SHELL INSULATION	LAB: S&E-ASTN-P NAME: C. C. Wood DATE: 4-7-71

- TECHNOLOGY PROBLEMS
  - LEAK DETECTION & REPAIR DIFFICULT
  - WEIGHT PENALTY OF HARD SHELL SYSTEMS
  - LIMITED CYCLE LIFE AND THERMAL PERFORMANCE
  - PROPELLANT LEAKAGE EFFECTS AND PERFORMANCE
- TECHNOLOGY OBJECTIVES
  - DEVELOP LIGHT WEIGHT HARD SHELL* USING NOMAX/ALUMINUM SANDWICH
  - BUILD UP PROTOTYPE SYSTEMS AND TEST
- PROGRAM PLAN - MILESTONES

	FY-70	FY-71	FY-72
- DEVELOPING ANALYTICAL TECHNIQUES	●		
- BUILD REMOVABLE HONEY COMB JACKET & TEST CANDIDATE INSULATIONS		●	
- TEST LOX PROTOTYPE INSULATION SYSTEM		●	
- TEST LH_2 PROTOTYPE INSULATION SYSTEM			●

* LeRC EMPHASIS ON HARD SHELL DEVELOPMENT

MSFC - Form 3369 (Rev June 1970)

CHART No. _____

THIS PAGE INTENTIONALLY LEFT BLANK

MARSHALL SPACE FLIGHT CENTER SCIENCE & ENGINEERING	SELF EVACUATED PANELS	LAB: S&E-ASTN-P NAME: C. C. Wood DATE: 4-7-71

- TECHNOLOGY PROBLEMS
  - LEAKAGE CONTROL IN REUSABLE PANELS/INSPECTION TECHNIQUES
  - ATMOSPHERE LEAKAGE THROUGH PANEL CONNECTORS
  - HIGH TEMPERATURE MATERIALS
  - STRUCTURAL INTEGRITY (SHUTTLE "G" LOADS)
  - REPAIR & GAS RECHARGE TECHNIQUES
- TECHNOLOGY OBJECTIVES
  - REDUCE LEAKAGE & DEVELOP INSPECTION METHODS
  - DEMONSTRATION OF FABRICATION TECHNIQUES
  - DEMONSTRATE SYSTEM PERFORMANCE [SCALE TANK TESTS (4 ft)]
- PROGRAM PLAN — FY-71
  - ACCESS PREVIOUS DESIGN PROBLEMS ●
  - DEVELOP DESIGNS & MATERIALS ●
  - BUILD & TEST A SUB SCALE SYSTEM ●

MSFC - Form 3369 (Rev June 1970)

CHART No. _____

PRECEDING PAGE BLANK NOT FILMED

THIS PAGE INTENTIONALLY LEFT BLANK

MARSHALL SPACE FLIGHT CENTER SCIENCE & ENGINEERING	STAGE/GSE SYSTEMS ANALYSIS	LAB: S&E-ASTN-P NAME: C. C. Wood DATE: 4-7-71

SHUTTLE IMPACT ON REQUIREMENTS	TECHNOLOGY PROGRAMS	FY-71	FY-72	FY-73
PRE-SHUTTLE	• LAUNCH SITE PROPELLANT HANDLING			
LONG PREPARATION TIME	FAST CRYOGENIC LOADING			
	SYSTEM PURGE STUDY			
SINGLE CRYOGENIC SYSTEMS	LOX GEYSERING SUPPRESSION (VERTICAL/HORIZONTAL)	Vert.	Horizon.	
	FUEL LEVEL INSTRUMENT			
	• STRATIFICATION			
SHUTTLE EMPHASIS	THERMAL ANALYSIS			
	SUBSCALE TEST			
SHORT PREPARATION TIME	• PROPELLANT PREPRESSURIZATION			
	SYSTEM DESIGN			
OPTIMIZATION OF SEVERAL CRYOGENIC SYSTEMS	SUBSCALE TEST ON			
	• INTEGRATION OF ORBITER CRYO SYSTEMS			
	DEV. OF MODELS FOR EACH SYSTEM			
	DEV. MODEL FOR TOTAL SYSTEM			
	OVERALL SYSTEM ANALYSIS			

MSFC - Form 3869 (Rev June 1970)

CHART No. _____

PRECEDING PAGE BLANK NOT FILMED

MARSHALL SPACE FLIGHT CENTER SCIENCE & ENGINEERING	CRYOGEN TECHNOLOGY CONCLUSIONS	LAB: S&E-ASTN-P NAME: C. C. WOOD DATE: 4/7/71

- THE SATURN V, CENTAUR AND TECHNOLOGY PROGRAMS CONDUCTED DURING THE PAST SEVERAL YEARS HAVE PROVIDED AN EXCELLENT BASE FOR SPACE SHUTTLE CRYOGEN SYSTEM DESIGN.

- ALTHOUGH SUBSTANTIAL TECHNOLOGY ADVANCEMENTS ARE REQUIRED TO SUPPORT THE SPACE SHUTTLE DEVELOPMENT, NO MAJOR TECHNOLOGY BREAKTHROUGHS ARE REQUIRED. HOWEVER, LIMITED OR IMMATURE BACKGROUND DATA PRECLUDE BASELINING AT THIS TIME THE MOST DESIRABLE APPROACHES IN THE AREAS OF PROPELLANT ACQUISITION, PROPELLANT TRANSFER, PROPELLANT MASS GAUGING IN ORBIT, INSULATION AND VARIOUS HARDWARE ASPECTS.

- TECHNOLOGY PROGRAMS IN PROGRESS, AND IN PLANNING ARE EXPECTED TO PROVIDE THE REQUIRED MATURITY IN THE SPACE SHUTTLE CRYOGEN TECHNOLOGY AREAS.

- FOR SEVERAL IMPORTANT AREAS THE TECHNOLOGY PROGRAM IMPLEMENTATION IS JUST COMMENCING.